

populations. Sustainability efforts to increase oysters in the Chesapeake Bay are of particular interest because oysters provide ecosystem services that may be applied as best management practices (BMPs) to reduce nitrogen inputs, which are the primary cause of eutrophication and its consequences. Although observations show that denitrification associated with oysters effectively removes nitrogen, methodologies vary widely, and mechanisms that control denitrification remain poorly understood. First, I determined the role of oysters relative to sediments on oyster reef biogeochemical fluxes. Next, I compared *in situ* and *ex situ* methods for the determination of biogeochemical fluxes associated with oysters. Finally, I conducted field sampling and experiments to characterize how on-bottom oyster aquaculture impacts nitrogen biogeochemistry.

In situ approaches for measuring oyster denitrification and other biogeochemical fluxes are logistically challenging, but incubations must include oysters if the goal of the research is to accurately quantify oyster reef biogeochemical fluxes. Regression of oyster clump fluxes against the oyster tissue biomass indicates significant positive relationships for O_2 and NH_4^+ , marginally significant and positive relationships for dissolved inorganic carbon (DIC) and N_2 , and no significant relationship for NO_x or soluble reactive phosphorus (SRP). Above a restored oyster reef, time series and ensemble-averaged normalized profiles from *in situ* methods reveal that oxygen was removed, whereas DIC, NH_4^+ , N_2 , and SRP were produced at the sediment-water interface. Besides NO_x , N_2 , and SRP, all *in situ* derived fluxes measured over the oyster reef were in the same direction as benthic chamber flux estimates. In addition, fluxes measured across an oyster aquaculture lease show that denitrification was stimulated at the harvested sites during sampling in May and September. Although harvested sites exhibited higher rates of denitrification,

seasonal differences in rates were likely dependent on ambient NO_x concentrations and availability of labile organic matter. Furthermore, seasonal shifts in oyster biomass for a given oyster length from the lease mirrored changes in average oyster-associated denitrification rates from May to September. Oyster biomass was associated with changes in denitrification rates, but the relationships changed depending on the sampling month. This work provided an opportunity to investigate whether sediment-based biogeochemical concepts hold true for oysters and learn about the influence of oysters and associated activities on overall biogeochemistry. Therefore, provided that oysters are grown in favorable denitrification environmental conditions, this work adds to the growing consensus that oysters can play an important role in mitigating nitrogen in coastal areas.

CHARACTERIZATION OF OYSTER-ASSOCIATED BIOGEOCHEMICAL
PROCESSES IN OYSTER RESTORATION AND AQUACULTURE

by

Melanie Jackson

Dissertation submitted to the Faculty of the Graduate School of the
University of Maryland, College Park, and the University of Maryland
Center for Environmental Science, in partial fulfillment
of the requirements for the degree of
Doctor of Philosophy
2019

Advisory Committee:
Jeffrey C. Cornwell, Chair
Lawrence P. Sanford
Jeremy M. Testa
Sairah Y. Malkin
Jennifer L. Bowen, Northeastern University
Alba Torrents, Dean's Representative

© Copyright by
Melanie Jackson
2019

Acknowledgments

It is bittersweet to know that my dissertation and time at Horn Point Laboratory (HPL) is coming to an end...and tears start forming just after one sentence. The support I have received from the HPL community has made all of my experiments and time invested possible. Looking back, I am amazed that during times of weakness, faculty, staff, and students intuitively jumped in to help me combat any doubts and imposter syndrome. I am so grateful to know that there is a support team at HPL cheering me on and pushing me to challenge myself. Other than a broad scientific knowledge, the Ph.D. journey has taught me that I can learn how to do anything if I put in enough effort and that I have leadership skills that were previously untapped.

First, I would like to thank my dissertation examining committee: Jeffrey C. Cornwell, Lawrence P. Sanford, Jeremy M. Testa, Sairah Y. Malkin, Jennifer L. Bowen, and Alba Torrents. Each of you have supported me individually and words cannot express my gratitude enough. I am beyond thankful for my advisor, Jeff Cornwell, for being my champion and providing advice whenever I needed it. His willingness to let me be independent and positivity have ultimately provided me with a mentor and a friend. I offer a special thanks to Larry Sanford for his patience and for teaching me that bottom boundary layer physics isn't as scary as it may first appear. I am grateful to Sairah Malkin for her biogeochemical and non-biogeochemical advice, and for her guidance while slicing cores and profiling. I would also like to thank Jeremy Testa for providing constructive suggestions during committee meetings, and Jennifer Bowen for challenging me with valuable materials and questions during my comprehensive exams. Thanks also goes to Alba Torrents for participating in my defense as my committee's dean's representative. Patricia M. Glibert also deserves a big "thank you" for her support, bringing me to HPL, and helping me strive to become a better writer.

Another thanks to Jeff, for providing me with my "second advisor", Mike Owens. Together, Jeff and Mike have taught me how to master sampling from pumps connected to over 40 ft of tubing, cores, medium chambers, reef ball-chambers, and *in situ* and *ex situ* incubations. Because of you, I can safely say that I can run an efficient and precise incubation experiment in my sleep, and figure out how to make it more innovative and improved for the next go-around. I would especially like to thank Mike for always lending a hand during experiments and for his guidance while I learned new analyses or how to wire pumps. A special thank you goes to the sediment core cake-master and water-sampling device decorator extraordinaire, Kabrena Owens. I thank you for always providing laughs and crafting your way through the lab.

Thank you also to everyone who provided guidance and assistance with data collection, especially Eric Wisner for taking me out on his aquaculture lease to collect cores and oysters, and Jack Seabrease for teaching me how to machine my own incubation chambers. I would also like to thank Lisa Kellogg for all of her time coordinating field work and editing that went into my Chapter 2. Todd Kana for providing guidance on the

interpretation of results and guidance on how to use the MIMS. Emma Green for her support and assistance in the lab. Shannon Hood and everyone in the HPL hatchery for teaching me how to extract polychaetes. Meg Maddox and Erica Kiss for teaching me different measurement techniques. Ralph Kimes and Gordy Dawson for providing assistance with environmental chambers and tanks.

None of this would have been possible without the financial support for this dissertation. Thank you to the NSF Coastal SEES project and NOAA for providing funding for my research and education. Thank you to Shore Rivers, Horn Point education committee, Morrin-Nordlund family, and the Saba family for supporting my professional development and expanding my research network. Special thank you to Maryland Sea Grant for helping me take the next step in my Knauss Fellowship.

A special thank you to Cassie Gurbisz for guiding me through data analysis, all things R, and friendship. Thanks to Katie McFarland for providing advice on oyster physiology resources. Thanks to my cohort-mate Sarah Laperriere for struggling through our initial graduate school years together. Thanks to Anna Priester for passing your obsessive love of oysters onto me. Pinky Liao, Lexy McCarty, and Megan Munkacsy for being such supportive friends and for building each other up.

My family and friends! The biggest thank you of all goes to Adam and the Jackson's: Mom, Dad, Sister, Nanny, Grandpa, Grandma, Grandpa, Harvey, and to my new family the Osborn's. Special thank you to my Mom for always picking up the phone when I needed a good cry or to shout cheers of joy. Thanks to my Dad for providing calming advice that helped me get through the tough days and for taking me on my very first body surfing ride that started it all. Finally, thank you to my calming manatee and husband, Adam. Thank you for taking a chance by following me to Cambridge and being so supportive from the very start.

Table of Contents

Acknowledgments	ii
Table of Contents	iv
List of Tables	vi
List of Figures	viii
Chapter 1: Introduction and overview	1
Chapter 2: Confirmation that live oyster clusters perform the majority of denitrification and nutrient fluxes on restored oyster reefs	11
Abstract	11
Introduction	12
Materials and methods	16
Study area and field sampling	16
Oyster abundance and biomass	18
Biogeochemical flux measurement	18
Statistical Analyses	19
Results	20
Biogeochemical fluxes	20
Discussion	23
Implications	26
Chapter 3: Application of an in situ gradient approach to determining oyster reef concentration gradients and biogeochemical fluxes	34
Abstract	34
Introduction	35
Methods	39
Study Site	39
Materials and Procedures	39
Gradient approach	39
Reef segment incubation approach	42
Assessment	44
Physical conditions	44
Environmental conditions and concentration boundary layers	46
Comparisons of biogeochemical fluxes from the oyster reef	49

Discussion	53
Chapter 4: Impact of oyster aquaculture dredging on sediment biogeochemistry	67
Abstract	67
Introduction	68
Methods	72
Study Site	72
Core collection and incubation	73
Statistical Analysis	77
Results	78
Environmental Conditions	78
Biogeochemical fluxes	81
Discussion	83
Implications	87
Chapter 5: The effect of oyster year-class on biogeochemistry	96
Abstract	96
Introduction	97
Methods	100
Study area and field sampling	100
Oyster and polychaete characteristics	102
Biogeochemical flux measurement	102
Statistical analyses	104
Results	104
Discussion	110
Implications	114
Chapter 6: Conclusions	131
References	137

List of Tables

Table 3.1 Boundary layer profile fitting parameters for June observations.

Table 3.2 Boundary layer profile fitting parameters for August observations.

Table 3.3 Comparison of average nutrient and gas fluxes ($\mu\text{mol m}^{-2} \text{hr}^{-1} \pm \text{SD}$) estimated using the gradient and reef segment incubation approach in June on the restored oyster reef.

Table 3.4 Comparison of average nutrient and gas fluxes ($\mu\text{mol m}^{-2} \text{hr}^{-1} \pm \text{SD}$) estimated using the gradient and reef segment incubation approach in August. The gradient approach was conducted just outside of the reef, whereas the reef segments were acclimated within the same reef as June sampling.

Table 4.1 Physical properties of the location of sediment core collection on the aquaculture lease.

Table 4.2 Chemical properties from the surface (0.5 m) and bottom water (3 m) from Station ET6.2 (<http://data.chesapeakebay.net/WaterQuality>) measured from May to October.

Table 4.3 Sediment characteristics from the control, non-harvested, and harvest sites during May and July. Data are recorded as means \pm SE.

Table 4.4 Water column respiration measured during May, July, and September. Rates were determined based on regression.

Table 4.5 Benthic fluxes statistical results based on two-way and one-way ANOVAs.

Table 5.1 Dates of collection and environmental conditions during collection. Average size of oysters for small, medium, and large size-class chambers (mean \pm SE).

Table 5.2 Biogeochemical fluxes normalized by oyster with statistical results based on two-way and one-way ANOVAs.

Table 5.3 Biogeochemical fluxes normalized by grams of oyster tissue dry weight with statistical results based on two-way and one-way ANOVAs.

Table 6.1 Summary of previous research on oyster-associated denitrification. Standard deviations are provided for denitrification rates if they were stated in the text. ~ denotes rates that were estimated from figures. SH stands for Shell Height. The units from the data for chapter 5 are $\mu\text{mol m}^{-2} \text{h}^{-1}$ per gram DW.

List of Figures

Figure 1.1 Adapted from FAO 2018. Aquaculture contribution to total fish production (excluding aquatic plants). The arrow on the right-hand side denotes the portion of aquaculture made up of molluscs.

Figure 1.2 Number of new papers per year on “oyster restoration” from a Web of Science search on August 31, 2018.

Figure 1.3 Denitrification rates from acclimated restored oyster reef trays versus oyster dry weight biomass (Cornwell et al. unpublished). Data is from restored oyster reef in Harris Creek following methods from Kellogg et al. (2013).

Figure 2.1 Map of study area showing (a) the Choptank River a major tributary to the Chesapeake Bay and (b) the location of the study site (○) within Harris Creek.

Figure 2.2 Diagram of (a) acclimated oysters and sediment for dark and light incubations and (b) oyster clumps alone for dark incubations.

Figure 2.3 Regressions of fluxes from oyster clumps against those from reef segments. Regressions of (a) oxygen demand (b) DIC (c) NH_4^+ (d) $\text{NO}_{2/3}^-$ (e) N_2 (f) and SRP fluxes.

Figure 2.4 Regressions of fluxes from oyster clumps against oyster biomass. Regressions of (a) oxygen demand (b) DIC (c) NH_4^+ (d) $\text{NO}_{2/3}^-$ (e) N_2 (f) and SRP fluxes.

Figure 2.5 Regression of oyster dry weight biomass against denitrification rates for oyster clumps (circles) and total trays (triangles).

Figure 2.6 Stoichiometric plots using O_2 , DIC, and ΣN (sum of NH_4^+ , $\text{NO}_{2/3}^-$, and $\text{N}_2\text{-N}$) from individual fluxes of oysters alone. We assume that $\text{CO}_2:\text{O}_2$ is a 1:1 in the plot of (a) total N flux versus O_2 demand and get a $\text{CO}_2:\Sigma\text{N}$ ratio of 7.4. This is compared to an actual plot of (b) total N flux versus DIC flux, which had a $\text{CO}_2:\Sigma\text{N}$ ratio of 10.8. Both ratios are similar to the Redfield elemental ratio for marine algae (106:16).

Figure 3.1 Map of study area showing (a) the Choptank River a major tributary to the Chesapeake Bay, (b) the location of the sampling sites (\circ) within Harris Creek, and (c) a bathymetry map of the reef and tripod sampling sites (bathymetry map from: <https://chesapeakebay.noaa.gov/images/stories/habitats/hc3ydcheckinJuly2016.pdf>).

Figure 3.2 A schematic drawing of the gradient approach and sampling manifold on the boat. The ADP is shown in front of the sampling tripod frame to measure hydrodynamics. The dominant flow is in the x direction. Sampling tubes were connected to the tripod at various depths, 5 discrete heights (0.2, 0.4, 0.8, 1.2, and 1.6 m) in June and 6 heights (0.2, 0.4, 0.6, 0.8, 1.1, and 1.5 m) in August. Each sampling tube was connected to a separate diaphragm pump on the boat, which were distributed through tubing on the manifold (b).

Figure 3.3 Total smoothed velocity in June (a) and August (b). Dotted lines represent profile times with $r^2 \geq 0.994$ used to calculate boundary layer parameters.

Figure 3.4 Boundary layer log profile fit for the second August current profile at 09:55. The profile fit was limited to $z < 0.5$ meters above the bottom, where the log layer profile assumption is clearly well satisfied, with an r^2 value of 0.999.

Figure 3.5 Time series of oxygen concentrations during sampling in (a) June and (b) August. Ensemble-averaged dimensionless profiles from time series samples in (c) June and (d) August.

Figure 3.6 Time series of DIC concentrations (a) and ensemble-averaged dimensionless profiles (b) from time series samples in June.

Figure 3.7 Time series of NH_4^+ (a,b) and NO_x (e,f) during sampling, in June and August respectively. Ensemble-averaged dimensionless profiles from time series of NH_4^+ (c,d) and NO_x (g,h) in June and August respectively.

Figure 3.8 Time series of N_2 concentrations during sampling in (a) June and (b) August. Ensemble-averaged dimensionless profiles from time series samples in (c) June and (d) August.

Figure 3.9 Time series of SRP concentrations during sampling in (a) June and (b) August. Ensemble-averaged dimensionless profiles from time series samples in (c) June and (d) August.

Figure 4.1 Map of study area showing (a) the Nanticoke River a tributary to the Chesapeake Bay and (b) the location of the sampling site (○) within the Nanticoke River.

Figure 4.2 Respiration-based sediment fluxes of (a) oxygen (i.e. sediment oxygen demand) and (b) DIC. Mean \pm SE (n=4). Asterisks indicate significant difference between sampling sites for each month (one-way ANOVA, $\alpha=0.05$).

Figure 4.3 Sediment fluxes of (a) NH_4^+ , (b) NO_x , and (c) N_2 . Mean \pm SE (n=3-4). Asterisks indicate significant difference between sampling sites for each month (one-way ANOVA, $\alpha=0.05$).

Figure 4.4 Sediment fluxes of (a) direct denitrification (Dw) and coupled nitrification-denitrification (Dn) and (b) DNRA. Mean \pm SE (n=3).

Figure 4.5 SRP fluxes from sediment collected from harvested, non-harvested, and control sites. Mean \pm SE (n=3-4).

Figure 5.1 Map of Chesapeake Bay showing (a) a comparison site at Harris Creek and (b) the Nanticoke River, a tributary to the Chesapeake Bay and the location of the aquaculture lease (○) where oysters were collected.

Figure 5.2 Drawn to scale diagram of incubation chamber. The base, sides, lid, and impeller were made of PVC, but the ends of the impeller contained magnets to turn the impeller.

Figure 5.3 Regression of average oyster total length against average oyster tissue biomass during the months May, July, and September.

Figure 5.4 Regressions of average oyster tissue biomass against oxygen demand during (a) May, (c) July, and (e) September. Regressions of average oyster length against oxygen demand during (b) May, (d) July, and (f) September. Blue dots represent oysters that were collected from a Harris Creek restoration site in 2017.

Figure 5.5 Regressions of average oyster tissue biomass against DIC fluxes during (a) May, (c) July, and (e) September. Regressions of average oyster length against DIC fluxes during (b) May, (d) July, and (f) September.

Figure 5.6 Regressions of average oyster tissue biomass against denitrification during (a) May, (c) July, and (e) September. Regressions of average oyster length against

denitrification during (b) May, (d) July, and (f) September. Blue dots represent oysters that were collected from a Harris Creek restoration site in 2017.

Figure 5.7 Regressions of average oyster tissue biomass against NO_x fluxes during (a) May, (c) July, and (e) September. Regressions of average oyster length against NO_x fluxes during (b) May, (d) July, and (f) September. Blue dots represent oysters that were collected from a Harris Creek restoration site in 2017.

Figure 5.8 Regressions of average oyster tissue biomass against NH_4^+ fluxes during (a) May, (c) July, and (e) September. Regressions of average oyster length against NH_4^+ fluxes during (b) May, (d) July, and (f) September. Blue dots represent oysters that were collected from a Harris Creek restoration site in 2017.

Figure 5.9 Regressions of average oyster tissue biomass against SRP fluxes during (a) May, (c) July, and (e) September. Regressions of average oyster length against SRP fluxes during (b) May, (d) July, and (f) September. Blue dots represent oysters that were collected from a Harris Creek restoration site in 2017.

Figure 5.10 Respiration-based oyster driven fluxes of oxygen demand normalized by (a) oyster and (b) oyster dry weight. Respiration-based oyster driven fluxes of DIC normalized by (c) oyster and (d) oyster dry weight. Mean \pm SE (n=4). Asterisks indicate significant difference between sampling sites for each month (one-way ANOVA, $\alpha=0.05$).

Figure 5.11 Denitrification rates normalized by (a) oyster and (b) oyster dry weight. NO_x fluxes normalized by (c) oyster and (d) oyster dry weight. NH_4^+ fluxes normalized by (e) oyster and (f) oyster dry weight. Mean \pm SE (n=4). Asterisks indicate significant difference between sampling sites for each month (one-way ANOVA, $\alpha=0.05$).

Figure 5.12 SRP fluxes normalized by (a) oyster and (b) oyster dry weight. Mean \pm SE (n=4). Asterisks indicate significant difference between sampling sites for each month (one-way ANOVA, $\alpha=0.05$).

Figure 5.13 Regressions of (a) polychaete abundance and (b) polychaete biomass against chamber denitrification rates.

Chapter 1: Introduction and overview

Coastal systems and estuaries worldwide are experiencing oxygen declines caused by increased nutrient loading (nitrogen (N) and phosphorus) and organic matter (Breitburg et al. 2018), and the oyster is one ecosystem engineer expected to help mitigate these effects (B. L. Bayne 2017). The eastern oyster *Crassostrea virginica* (Gmelin 1791), provides ecosystem service benefits including habitat stabilization, enhanced seafood production, and biofiltration of the water column (Peterson et al. 2003; Piazza et al. 2005; Dame et al. 1984). Despite the oyster's habitat-forming capabilities, factors such as increased exploitation, changes in water quality, and diseases have contributed to a decline in oyster habitat around the world (Kirby 2004; Beck et al. 2011). Although oyster restoration efforts and shellfish aquaculture have increased globally to counteract the overall decline of intertidal and subtidal oyster reefs, the rate of expansion and associated water quality impacts are relatively unknown (Dumbauld et al. 2009; Beck et al. 2011; Shumway 2011; Coen and Bishop 2015).

Across the freshwater-to-marine continuum, human population growth has contributed to nutrient over-enrichment and excess primary production, resulting in “cultural eutrophication” (Nixon 1995; Paerl et al. 2018). Chronic eutrophication from nutrient sources, such as urban and industrial waste, septic systems, agricultural, lawn and golf course fertilizers, as well as loss of nutrient sinks such as wetlands, contribute to low oxygen “dead zones”, loss of seagrasses, and stimulation of harmful algal species (Cloern 2001; Burkholder and Shumway 2011; Paerl et al. 2018). Due to the significant

cost of removing nitrogen from wastewater effluent via tertiary treatment, wastewater nitrogen removal is not universal, and societal economic priorities in the watershed need to be assessed prior to investment in mitigation (NRC 1993; Glibert et al. 2015; Paerl et al. 2018). In addition to wastewater treatment upgrades, eutrophication mitigation strategies typically focus on land-based discharge nutrient reductions (United States Clean Water Act. 1972; *The European Union Water Framework Directive 2000/60/EC* 2000). Once controls of major point and nonpoint sources are implemented, innovative nutrient management controls such as oysters may address pollution remaining in coastal systems (Cornwell et al. 2016; Bricker et al. 2018).

Oyster-associated nutrient remediation has classically been proposed as a means of “bioextraction”, given that filter feeding can reduced nutrient and phytoplankton concentrations (US Clean Water Act. 1972; EU 2000; Crawford et al. 2003; Shumway et al. 2003). Nitrogen can be stored in oyster tissues after filtration of seston from the water column. For example, Newell and Jordan (1983) observed that *C. virginica* can digest and absorb about 50% of the particulate N in the water column. Another way oysters interact with the nitrogen cycle is by enhancing benthic-pelagic coupling through the transfer of nutrients in biodeposits to sediments. Oysters release biodeposits by either rejecting less nutritious particles (pseudofeces) to the sediment immediately or digesting nutritious particles and defecating (feces) within 24 hours (Newell and Jordan 1983; Ward et al. 1994; Newell et al. 2005). Once biodeposits land on oxic sediments, aerobic bacteria oxidize organic matter and allow for the canonical microbial conversion of oxidized N to N_2 , a process generally termed denitrification; (Seitzinger 1988; Rysgaard et al. 1994). Other processes such as anammox also can produce N_2 (Burgin and

Hamilton 2007). Denitrification does not solely occur in sediments and oysters in reef environments have been associated with enhanced denitrification rates (Kellogg et al. 2013; Smyth et al. 2013; Humphries et al. 2016; Caffrey et al. 2016; Arfken et al. 2017). However, ecosystem services cannot be provided by oysters if there are so few remaining wild shellfish reefs for direct harvesting (Beck et al. 2011).

Consequently, oyster aquaculture and restoration are two means of fisheries enhancement that can increase oyster-associated ecosystem services. Based on the recent “The State of World Fisheries and Aquaculture” report by the Food and Agriculture Organization of the United Nations, aquaculture has become an increasingly important contributor to global food production (Figure 1.1). Aquaculture food production is growing faster than other major food production sectors with an annual growth of 5.8 percent during the period 2001-2016 (FAO UN 2018). Molluscs (i.e. clams, oysters, mussels) make up 21% of the total world aquaculture production, with cupped oysters (*Crassostrea* spp.) increasing by 32 percent from the years 2010 to 2016 (FAO UN 2018). Similarly, interest in oyster restoration has increased substantially with the total number of scientific papers containing the words “oyster restoration” increasing by about 6-fold from the year 2000 to 2017 (Web of Science 2018; Figure 1.2). Oyster restoration is taking place on the Atlantic coast of North America and Gulf of Mexico (*C. virginica*), Pacific coast of North America (*Ostrea lurida*), and Europe and the UK (*Ostrea edulis*; Allison and Murphy 2017). Work assessing ecosystem services provided by oyster restoration and aquaculture has largely focused on the benefits associated with filtration and biodeposits (Dame et al. 1989; Dame et al. 1992; Nelson et al. 2004; Lunstrum et al. 2017); however, recent work suggests that denitrification is enhanced by oysters even in

the absence of associated sediments (Kellogg et al. 2013; Smyth et al. 2013; Caffrey et al. 2016; Arfken et al. 2017), indicating that we may be underestimating the total amount of nitrogen being removed following the increase of filter feeding bivalve biomass to a habitat.

Rates of nitrogen fluxes associated with oyster reefs have been determined as net denitrification rates, potential denitrification rates, and individual coupled processes in various environmental conditions. These methodologies have produced contrasting results regarding whether or not oyster reefs influence denitrification (Kellogg et al. 2013; Piehler and Smyth 2011a; Smyth et al. 2013; Hoellein and Zarnoch 2014). This isn't the first time scientists have struggled with denitrification methodology. In fact, this has been ongoing in the terrestrial and aquatic sciences for decades (Groffman et al. 2006). Measuring denitrification rates associated with oysters can be especially complicated, considering a number of experimental artifacts that may arise without careful consideration of environmental conditions, such as the inclusion of sufficient benthic habitat, minimizing sediment disturbance, maintaining temperatures and oxygen concentrations, and incorporating realistic boundary-layer physical conditions (Kellogg et al. 2013). A comparison of different methods and components of oyster habitat may elucidate uncertainties surrounding what is driving denitrification rates.

In oyster restoration and aquaculture, various environmental factors may alter organic matter availability and therefore denitrification rates. Ongoing studies of oyster-associated denitrification from restored reefs suggest that denitrification rates are positively correlated with total oyster reef biomass (Cornwell et al. unpublished; Figure 1.3); however, it is unclear whether there are allometric relationships between

denitrification rate and oyster size (Cornwell et al. 2016). Other than oyster density, aquaculture cultivation methods are expected to impact nutrient cycling by either increasing or decreasing the exchange rate of nutrients between the sediment and water column (Lunstrum et al. 2017; Stokesbury et al. 2011). For example, a review by Coen (1995) observed that environments experiencing dredge harvesting on leased bottoms recover from major disturbances within a few weeks or months; however, most of this previous work focused on the impact of turbidity and disturbance on species biodiversity rather than water and sediment biogeochemistry. Together, the expansion of oyster aquaculture and restoration provide a unique opportunity to study how oysters impact sediment biogeochemistry.

First, the mechanisms that drive oyster-associated denitrification are unclear. Although denitrification rates scale with oyster dry weight biomass, there is a large amount of variability surrounding this relationship (Figure 1.3). Therefore, in Chapter 2 of this dissertation, I conducted field sampling and replicated laboratory flux chamber incubations with and without sediments to assess how much of the denitrification and nutrient fluxes occurring on restored oyster reefs are associated with oyster clumps and whether overall nutrient dynamics are controlled by the underlying/adjacent sediments or the oysters themselves.

Hypothesis 1: *In coastal environments influenced by oyster sustainability efforts, oysters will dominate rates of denitrification and associated biogeochemical fluxes, with sediments playing a minor role in overall rates.*

Next, acclimated restored reef incubation trays were used to estimate fluxes as close to *in situ* reef conditions as possible; however, flow rates and residence times are

difficult to replicate in the laboratory. In Chapter 3, a boundary layer gradient approach was implemented over a restored reef to compare estimated fluxes with fluxes measured from enclosure experiments with similar oyster densities.

Hypothesis 2: *Incubations of oyster clusters alone and in situ gradient measurements are both alternatives to acclimated segmented reef enclosures and valuable for resolving large-scale variability.*

Finally, environmental conditions associated with aquaculture activities are expected to impact sediment biogeochemistry. Thus oyster size and dredging activities may be affecting total nitrogen removal and overall water quality. In Chapter 4, I conducted field sampling at an on-bottom aquaculture facility to determine how harvest practices alter the benthic environment and biogeochemical cycles. I characterized nutrient fluxes and metabolism for a range of oyster year-classes during different seasons in Chapter 5.

Goal: *Environmental conditions along with oyster restoration and aquaculture activities will control sediment and water column biogeochemistry and therefore influence the magnitude of individual nitrogen cycle processes.*

Hypothesis 3a: *On-bottom aquaculture harvest will lead to more coupled nitrification-denitrification.*

Hypothesis 3b: *The size of oysters in on-bottom aquaculture plays a substantial role in determining rates of denitrification, with older year-classes resulting in higher rates.*

Taken together, this work will provide new information on the methods used to estimate oyster-associated biogeochemical fluxes and will place the role of oysters relative to sediments into perspective. In addition to NO_x concentrations in the water

column, temperature, and organic matter availability, changes in oyster-associated denitrification rates are attributed to oyster grow-out methods. As demonstrated by the high denitrification rates measured from all incubations including oysters, oysters may contribute to nitrogen mitigation strategies if they are grown in environmental conditions that support sediment denitrification.

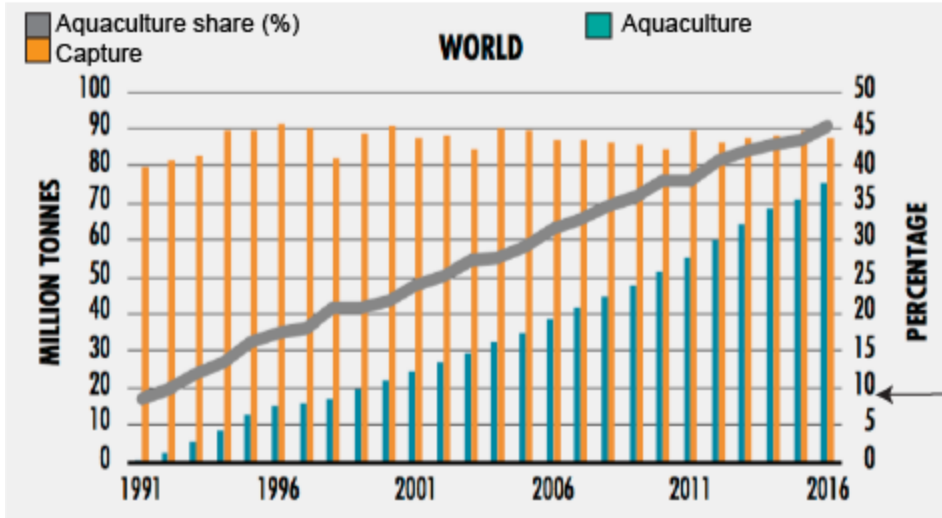


Fig. 1.1 Adapted from FAO 2018. Aquaculture contribution to total fish production (excluding aquatic plants). The arrow on the right-hand side denotes the portion of aquaculture made up of molluscs.

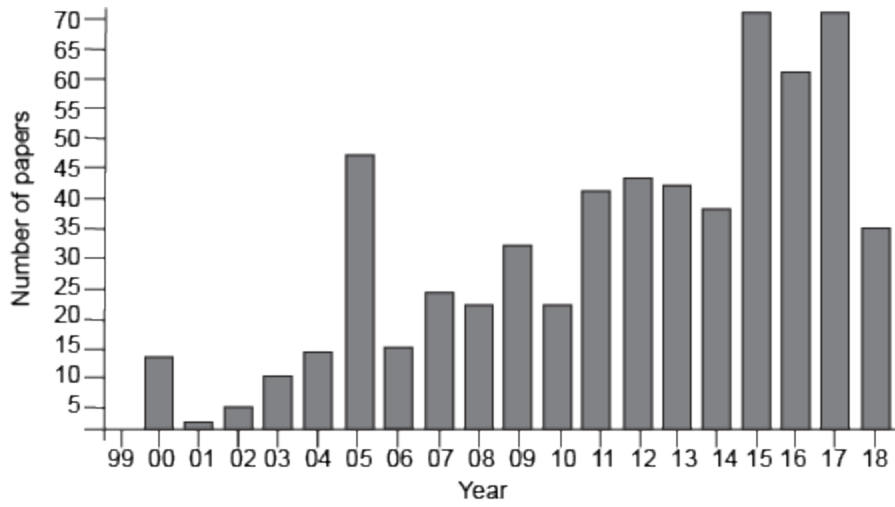


Fig. 1.2 Number of new papers per year on “oyster restoration” from a Web of Science search on August 31, 2018.

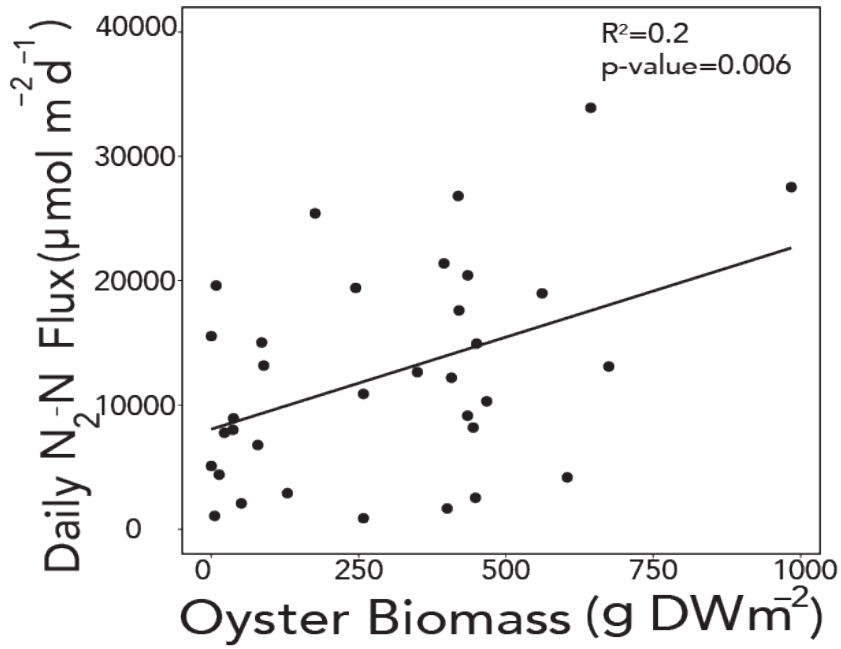


Fig 1.3 Denitrification rates from acclimated restored oyster reef trays versus oyster dry weight biomass (Cornwell et al. unpublished). Data are from restored oyster reef in Harris Creek following methods from Kellogg et al. (2013).

Chapter 2: Confirmation that live oyster clusters perform the majority of denitrification and nutrient fluxes on restored oyster reefs

Abstract

Oyster reef restoration can significantly increase benthic denitrification rates. Methods applied to measure nutrient fluxes and denitrification from oyster reefs in previous studies include incubations of sediment cores collected adjacent to oyster clumps, benthic chambers filled with intact reef segments that have undergone *in situ* equilibration and *ex situ* incubation, and cores with single oysters. However, fluxes of nutrients vary by orders of magnitude among oyster reefs and methods. This study compares two methods of measuring nutrient fluxes and metabolism fluxes on restored oyster reefs: incubations including intact segments of oyster reef and incubations containing oyster clumps without underlying sediments. Fluxes of oxygen (O₂), dissolved inorganic carbon (DIC), ammonium (NH₄⁺), combined nitrate and nitrite (NO₂₊₃), di-nitrogen (N₂), and soluble reactive phosphorus (SRP) were determined in June and August in Harris Creek, a tributary of the Chesapeake Bay, Maryland, USA. Regression of fluxes measured from clumps alone against those measured from intact reef segments showed significant positive relationships for O₂, DIC, NH₄⁺, and SRP (R² = 0.920, 0.61, 0.26, and 0.52, respectively). Regression of clump fluxes against the oyster tissue biomass indicates significant positive relationships for O₂ and NH₄⁺, marginally significant and positive relationships for DIC and N₂, and no significant relationship for NO₂₊₃ or SRP. Although these results demonstrate that the incubation of oyster clumps

without underlying sediments does not necessarily result in accurate rates for most biogeochemical fluxes, this work supports the need to understand the balance between the metabolism of oysters and local sediments to accurately estimate biogeochemical rates.

Introduction

In Chesapeake Bay, populations of the native oyster *Crassostrea virginica* have experienced substantial decline due to overfishing, disease, and habitat loss (Wilberg et al. 2011). Oyster restoration has been applied as a management strategy with the dual goals of rebuilding the commercial fishery and restoring ecosystem services and benthic habitats (Cercio and Noel 2007; Beck et al. 2011). Oyster-associated ecosystem services that enhance nitrogen (N) removal are being considered for approval as best management practices (BMPs) in the Chesapeake Bay (Cornwell et al. 2016) where nitrogen inputs are a primary cause of eutrophication (Hagy et al. 2004; Kemp et al. 2005). Chronic eutrophication from N sources, such as septic systems and fertilizer runoff, can result in low oxygen “dead zones”, loss of seagrasses, and expansion of harmful algal blooms (Cloern 2001; Burkholder and Shumway 2011; Paerl et al. 2018). Oysters can remove N if filtration of particulate N (Grizzle et al. 2008) is followed by assimilation and sequestration of nutrients into tissues and shells, deep burial of nutrients in sediments, or enhancement of denitrification (Newell et al. 2005).

Oysters and other reef organisms appear to create optimal conditions for N removal via denitrification. Oysters remove oxygen through respiration (Boucher and Boucher-Rodoni 1988), re-oxidation of reduced N, S and Fe, and biodeposit

rem mineralization (Dame et al. 1992), which creates anaerobic environments for denitrifiers to reduce oxidized forms of N (NO_2^- and NO_3^-) to N_2 gas. Although the rem mineralization of biodeposits can result in fluxes of NH_4^+ from reefs (Newell et al. 2005; Dame et al. 1984), this form of N may become available to denitrification by coupled nitrification- the conversion of NH_4^+ to NO_3^- . Under aerobic conditions, attenuation of NH_4^+ concentrations via nitrification is associated both with living oysters and oysters shell (Caffrey et al. 2016) and with surfaces of other members of the macrofaunal community (i.e., polychaetes and amphipods) and bivalve soft tissues (Welsh and Castadelli 2004). Given that reefs can provide as much as 50 m^2 of surface area per square meter of reef (Bahr 1974), it is likely that they promote nitrification by providing an abundance of oxic surfaces on which they can grow. Despite this knowledge, the mechanisms that control this coupled process and eventual nitrogen removal by denitrification remain poorly understood.

Although observations show that denitrification associated with oysters effectively removes nitrogen (Piehler and Smyth 2011a; Kellogg et al. 2013; Humphries et al. 2016; Arfken et al. 2017), methodologies and results vary widely. Methods used to estimate denitrification and nutrient cycling associated with oysters include: benthic tunnels (Dame et al. 1984), sediment core incubations with the addition of oyster biodeposits (Newell et al. 2002; Holyoke 2008), incubations of sediment cores collected adjacent to oyster reefs (Piehler and Smyth 2011a; Smyth et al. 2013; Hoellein et al. 2015; Smyth et al. 2015; Westbrook 2016; Smyth et al. 2018), incubations of live oysters without substrate (Caffrey et al. 2016), *in situ* experimental chambers that encompass intact reef segments (Humphries et al. 2016), and *in situ* equilibration of intact reef

segments with *ex situ* incubation and measurement (Kellogg et al. 2013). Many of these studies do not include oysters or the highly abundant reef-associated organisms that alter biogeochemical cycles (Piehler and Smyth 2011a; Nizzoli et al. 2007). Although progress has been made in developing methods for measuring nutrient fluxes from oyster reefs, less progress has been made in directly comparing flux measurements from the entire reef (acclimated oyster clumps plus sediment) to oysters alone. Oysters alone, here called “oyster clumps”, refer to live juvenile and adult oysters attached to shell or each other along with the associated reef community. Clumps typically had barnacles, mussels, tunicates and other sessile filter-feeding organisms attached and included small motile organisms such as polychaete worms, amphipods and mud crabs. The relative importance of oysters clumps in stimulating total reef denitrification remains a critical gap in our knowledge.

Much of the work on oyster-associated denitrification focuses on the filtration of organic matter from the water column and its deposition on sediments as feces and/or pseudofeces (i.e., biodeposits; (Newell et al. 2002). Biodeposits concentrate organic matter on the aerobic sediment surface where the supply of labile carbon is expected to stimulate conversion of oxidized forms of N (NO_3^- and NO_2^-) to N_2 gas by denitrifying bacteria (Henriksen 1988; Seitzinger 1988; Risgaard-Petersen et al. 1994; Newell et al. 2005). In addition to oysters, restored reefs provide habitat for other filter-feeding organisms (e.g. mussels, tunicates, and barnacles) as well as deposit-feeding and bioturbating organisms, all of which can enhance N removal (Rodney and Paynter 2006; Nizzoli et al. 2007; Kellogg et al. 2013).

Contrary to studies that have focused on the impact of biodeposits on sediment denitrification, recent literature suggests live oysters are denitrification hot spots (Kellogg et al. 2013; Smyth et al. 2013; Caffrey et al. 2016; Arfken et al. 2017). Incubations of intact segments of oyster reef have produced some of the highest rates of denitrification, which can be attributed to the filtration of organic matter from the water column by oysters and reef-associated filter-feeders (Kellogg et al. 2013). Incubations comparing live oysters to bare sediment have shown that live oysters have higher rates of denitrification (Smyth et al. 2013), whereas incubations of shell have shown either lower or similar rates to live oysters (Caffrey et al. 2016; Arfken et al. 2017). While experimental separation of oyster reef components helps locate where denitrification occurs, extrapolation from these studies to entire reef systems is problematic without the inclusion of associated reef organisms and underlying sediments. In addition, microbiome structures from live and dead shell, sediment, and oyster digestive glands suggest that the transformation of NO_2^- to N_2 is not controlled by the abundance of complete denitrifiers in the sediment but rather by complex interactions within the microbial community (Arfken et al. 2017). None of these previous studies have directly determined the relative importance of oyster clumps in determining denitrification rates measured from entire restored reefs.

We combined field sampling and replicated laboratory flux chamber incubations with and without sediments to assess whether the denitrification and nutrient fluxes occurring on oyster reefs are associated with oyster clumps. We hypothesized that oysters alone would provide accurate estimates of denitrification compared to those measured from reef segments containing oysters and sediment, whereas oxygen demand and

inorganic nitrogen dynamics (i.e. $\text{NO}_{2/3}^-$ and NH_4^+) measured from oysters alone may differ from whole reef incubations, due to the exposure of new surface area and absence of sediment microbial communities. This prediction was made following knowledge that denitrification was consistently higher from restored reef sites compared to control sediments (Kellogg et al. 2013), with the expectation that samples with higher oyster clump biomass densities would have higher biogeochemical rates.

Materials and methods

Study area and field sampling

A restored reef in Harris Creek ($38^{\circ}45.129'$ N, $76^{\circ}18.571'$ W), a tributary to the Choptank River, Maryland, USA (Fig 2.1) was chosen for the study area. The reef was restored by placement of 28.19 million juvenile oysters set on shell on 6.53 ha of suitable substratum in 2012 (NOAA). In 2015, the density of live oysters across the entire reef averaged 20.39 oysters per m^{-2} (NOAA).

Experiments were conducted in early and late summer (June and August) 2017 using the *in situ* equilibration of intact segments of oyster reef (hereafter “reef segments”) with *ex situ* incubation approach (Kellogg et al. 2013). This work is a part of a larger ongoing project using equilibrated segments of oyster reef to understand spatial and seasonal patterns of nutrient fluxes in Harris Creek; however, the focus of this work is to determine the importance of oysters relative to intact reef segments. At least one month prior to incubations, divers embedded base trays filled with sediment, oyster shell, and live oysters in the substratum flush with surrounding sediments. Sediments consisted of fine-grained muds interspersed with shell fragments, also termed “shell hash”. Oyster

biomass densities in trays ranged from 57 to 574 g DW m⁻² and the volume of sediment in the tray was on the order of 10 L, which reflect the natural deep sediment column and varying oyster densities present on the restored reef. After trays had equilibrated in the field for at least one month, divers capped the base trays with a pvc pipe midsection fitted with a lid and intact reef segments were returned to Horn Point Laboratory, Cambridge, MD where reef segments were placed in filtered Choptank River water with the temperature adjusted to Harris Creek conditions (23.3°C in June to 28°C in August). An empty tray filled with only filtered river water served as a “blank”. Prior to each set of incubations, trays were aerated for ~1 h to bring oxygen concentration to saturation. At the start of each incubation, chambers were capped with a stirring lid containing ports for sample collection, but sealed the sample from the surrounding water bath and stirred the water column with a motor-driven impeller (Kellogg et al. 2013). As part of the larger project, reef segments were incubated first in the dark, then with illumination. After these incubations were complete, a subset of these samples (4 samples in June and 6 samples in August) was selected for additional study based upon whether the sample had at least one oyster over ~75 mm visible on the surface sediment. For each tray selected, the live oysters and oyster clumps were carefully removed from each tray, placed in clean and empty incubation chambers, aerated for ~1 h, and incubated in the dark (Fig 2.2). Our study focused on comparing the results from these “clump only” incubations to results from the dark incubations of the 10 intact reef segments from which they were removed. Fluxes for reef segments not selected for clump only incubations because oysters were too small or absent are not presented as part of the present study.

Oyster abundance and biomass

Once incubations were complete, samples were rinsed over a 12.5-mm mesh sieve and all material was frozen for later analyses. For each sample, all live oysters were counted and measured to the nearest mm. Shell lengths were converted to grams of oyster tissue dry weight from seasonal length to biomass regressions based upon samples collected from Harris Creek, MD 2015 (Kellogg et al. unpubl. data). The area of an individual tray (0.1 m^2) was then used to calculate the oyster biomass density (g DW m^{-2}).

Biogeochemical flux measurement

Solutes (NH_4^+ , NO_2^- , SRP) and dissolved gases (O_2 , N_2 , Ar, $\text{DIC}=[\text{H}_2\text{CO}_3]+[\text{HCO}_3^-]+[\text{CO}_3^{2-}]$) were collected approximately every 45 minutes (4 times total) during each set of incubations from a sampling tube fitted in the lid, while a water replacement tube pulled water from the water bath. Sampling intervals were determined based upon changes in dissolved oxygen (FireSting O_2 -Mini oxygen meter), and incubations of reef segments and oyster clumps alone had the same incubation duration. Final oxygen concentrations for reef segments and oyster clumps ranged from $0.14 \pm 0.06 \text{ mmol l}^{-1}$ (mean \pm SD) in June to $0.15 \pm 0.04 \text{ mmol l}^{-1}$ in August. Dissolved gases were preserved with 10 ml of 50% saturated HgCl_2 , tightly sealed, submerged in water, and held at or slightly below incubation temperature until analysis. Solute samples were filtered through a 0.45 mm pore-size filter and kept frozen for analysis. N_2 , O_2 , and Ar concentrations were measured on a membrane-inlet mass spectrometer (Kana et al. 1994) within 2 weeks of collection. DIC concentrations were measured using an infrared-

based analyzer (Apollo SciTech; Cai and Wang 1998) with a calibration coefficient of variation that ranged from 0.03 to 0.06 % with an average standard deviation of ± 6.09 mmol l⁻¹. Phenol/hypochlorite colorimetry was used to determine NH₄⁺ concentrations (Parsons 2013). NO_{2/3}⁻ was analyzed spectrophotometrically following Doane and Howarth (Doane and Horwath 2003), while a composite reagent of molybdic acid, ascorbic acid, and trivalent antimony were used to determine SRP concentrations (Parsons 2013). Concentrations of gases and nutrients were regressed versus time to obtain a slope. Fluxes were considered significant if they had an $R^2 \geq 0.80$ and the change in concentrations over the incubation were greater than the precision of the analyses (Cornwell et al. 1999). When it was significant, the slope of the “blank” was subtracted from the slope of sample fluxes to remove the effects of water column processes. Areal rates were determined based on the equation:

$$F = \frac{\Delta C}{\Delta t} * \frac{V}{A}$$

where F is the flux (mmol m⁻² hr⁻¹), $\Delta C/\Delta t$ is the slope (mmol L⁻¹ hr⁻¹), V is the volume of overlying water (L), and A is the area of the incubated tray segment (m⁻²). The overlying water volume was determined by subtracting the volume of sediment measured in the tray and the displacement volume of the live oysters from the total incubation chamber volume.

Statistical Analyses

We used a series of criteria to determine whether clump fluxes were representative of reef segment fluxes at this specific site. If the clump fluxes accurately estimate reef segment biogeochemistry, we would expect the two approaches to be highly

correlated ($R^2 \geq 0.80$), have correlation coefficients that did not differ significantly from one, and have intercepts that did not differ significantly from zero. All statistical analyses were performed in R 3.1 using its “base” and “stats” packages (R Core Team 2013). Linear regression was used to determine the slope and whether there were significant linear relationships between fluxes measured from clumps without sediments and fluxes measured from reef segments. For fluxes that had a significant positive relationship, we used a two-tailed t-test of slope to determine whether the regression coefficient was significantly different from the expected slope of one. If the results from the incubation of oysters alone were an accurate estimate of intact reef segments, the correlation coefficient would be one. When slopes did not differ significantly from one, we used a linear model function to determine whether the intercept of the regression line was significantly different from zero. In addition, we used linear regression to test for relationships between biogeochemical fluxes and oyster biomass. Significance level for statistical tests was set at $\alpha = 0.05$. P-values between 0.05 and 0.10 were considered marginally significant.

Results

Biogeochemical fluxes

The majority of fluxes for clumps alone showed positive relationships with fluxes from reef segments (Fig 2.3). Overall, fluxes from clumps alone increased with increasing biomass density (Fig 2.4).

Regression of oxygen fluxes from clumps against those from reef segments (Fig 2.3a) demonstrated a significant ($p < 0.001$), highly correlated ($R^2 = 0.92$) positive

relationship. However, the regression coefficient from the comparison of both methods was significantly greater than the predicted slope of one ($t = -4.71$, $p = 1.5 \times 10^{-3}$) with clumps generally overestimating oxygen demand, especially at high flux rates. The relationship between clump oxygen demand and oyster clump biomass density was significant and positive ($p = 0.02$, $R^2 = 0.49$; Fig 2.4a).

DIC-based respiration rates did not differ significantly between the two incubation methods. Regression analyses (Fig 2.3b) demonstrated a significant positive relationship between clump and reef segment fluxes ($p = 0.008$) but were not as highly correlated ($R^2 = 0.61$) as oxygen-based respiration rates. The relationship between the two methods was not significantly different from the predicted slope of one ($t = 0.24$, $p = 0.81$) and the intercept was not significantly different from the predicted value of zero ($t = 0.23$, $p = 0.82$). DIC fluxes tended to increase with oyster biomass, but were only marginally significant ($p = 0.09$, $R^2 = 0.31$; Fig 2.4b).

Regression of NH_4^+ fluxes from clumps against those from reef segments (Fig 2.3c) demonstrated a significant ($p = 0.012$) positive relationship with correlation similar to that for DIC fluxes ($R^2 = 0.56$). In addition, the regression coefficient from the measured relationship was not significantly different from the expected relationship ($t = 0.41$, $p = 0.69$) and the intercept was only slightly not significantly different from zero ($t = 2.13$, $p = 0.07$). However, NH_4^+ fluxes measured from oyster clumps consistently overestimated rates measured from reef segments. NH_4^+ fluxes from oyster clumps alone had a significant positive relationship with oyster clump biomass ($p = 0.008$, $R^2 = 0.60$; Fig 2.4c).

Combined nitrate and nitrite concentrations were variable within the time course of experiments resulting in few regressions of concentration against time indicative of significant fluxes ($R^2 > 0.080$). For the five clump fluxes that were significant, regression analyses found no relationship ($p = 0.32$, $R^2 = 0.321$) between $\text{NO}_{2/3}^-$ fluxes from clumps versus those measured from reef segments (Fig 3d) and showed a trend towards a negative relationship between fluxes using the two different measurement approaches. Likewise, $\text{NO}_{2/3}^-$ fluxes were not related to oyster clump biomass ($p = 0.67$, $R^2 = 0.05$; Fig 2.4d).

Rates of denitrification measured from clumps alone did not have a significant relationship ($p = 0.24$, $R^2 = 0.16$; Fig 2.3e) to rates measured from reef segments but did show a slight tendency for the relationship to be positive, with denitrification rates from oyster clumps overestimated at the lower end of reef segment measurements and underestimated at the higher end. Regression of clump denitrification rates indicated a marginally significant positive relationship with oyster clump biomass ($p = 0.07$, $R^2 = 0.36$; Fig 2.4e).

Regression analyses found a significant positive relationship between SRP fluxes measured from clumps and those measured from reef segments ($p = 0.019$) with a degree of correlation ($R^2 = 0.5172$) similar to those for DIC and NH_4^+ (Fig 2.3f). The regression coefficient for this relationship was significantly lower than the expected slope of one ($t = 3.85$, $p = 0.004$). Similar to denitrification, incubations of clumps alone overestimated SRP fluxes at the lower end and underestimated fluxes at the higher end of reef segments. SRP fluxes were not significantly correlated with oyster biomass ($p = 0.45$, $R^2 = 0.07$; Fig 2.4f).

Discussion

The majority of flux rates measured from clumps fell within the range of values measured for reef segments, which supports that much of the metabolism occurs within the clumps rather than in underlying sediments. While it is clear that removing clumps from the reef surface resulted in experimental artifacts, it is expected that methods that incubate sediments adjacent to oyster reefs would likely miss a significant proportion of the nutrient and gas fluxes that are occurring. A number of efforts have pointed to the oyster as a potential denitrification hotspot; yet, direct comparisons of whole reef communities and their associated organisms to oyster clumps and associated organisms alone have not been made. The addition of cleaned bivalves to sediment without bivalves may result in less efficient denitrification than an acclimated reef (Smyth et al. 2013) or rates that cannot be extrapolated to entire systems because they are not consistent with natural conditions. Our approach takes the importance of the oysters, associated-macrofauna, and shell microbial communities into consideration by leaving these components as undisturbed as possible. The present study builds on previous findings that oysters are associated with high denitrification rates by providing a direct measure of how oyster clumps compare to an acclimated reef segment, although the clumps alone had very little dynamic range compared to the whole reef segment.

Overall, fluxes of DIC, NH_4^+ , and SRP measured from oysters alone were correlated with reef segment flux rates. During the trial run in June, we were concerned that the removal and placement of oyster clumps in new trays would result in dislodged labile organic matter and sediment from the shells. Nonetheless, the regressions of concentrations versus time to calculate fluxes were linear and significant for all nutrients,

except for $\text{NO}_{2/3}^-$, indicating that for the most part, the incubation of clumps did not dramatically increase variation in biogeochemical processes within the time course of experiments. Our results provide evidence that oysters support much of the metabolism on the reef; however, it is worth noting that none of the clump fluxes met all of the criteria required for an accurate estimate of reef segment fluxes, such as highly correlated ($R^2 \geq 0.80$) variables, correlation coefficients that did not differ significantly from one, and intercepts that did not differ significantly from zero.

Although both measurement approaches were correlated for O_2 and DIC-based respiration rates, oyster clumps overestimated O_2 fluxes at the higher end of reef segments rates. The increase in O_2 demand was likely due to the reoxidation of reduced chemical species occurring on the newly exposed surface area on the bottom of the clumps, considering previous studies have observed the development of anoxic sediments and increases in reduced chemical species below oysters during warmer months (Holyoke 2008; Diaz and Rosenberg 1995). In contrast to O_2 fluxes, DIC-based respiration from oysters alone were the only fluxes that met the criteria of having a slope that was not significantly different from one and an intercept not significantly different from zero, indicating that remineralization rates were minimally affected the by the removal and placement of clumps.

Regression of NH_4^+ fluxes demonstrated that incubation of clumps alone produces a consistent error in measurements across flux rates that results in an overestimate of reef segment fluxes. It was uncertain why we observed higher NH_4^+ fluxes when oysters were incubated alone (Fig 2.3) but these results may suggest that dissimilatory nitrate reduction of nitrate to ammonium (DNRA) increased. DNRA can be promoted when the

availability of organic carbon increases, NO_3^- concentrations are low, and free sulfide (H_2S and S^{2-}) concentrations in adhered sediment are high (Tiedje 1988; Burgin and Hamilton 2007; Hardison et al. 2015). Another possible explanation is that incubation of oyster clumps alone removed much of the shell hash surface area that would support nitrification and the removal of NH_4^+ . We speculate that DNRA was stimulated when oysters clumps were incubated alone by concentrations of reduced sulfides that were exposed on the bottom of the oyster clumps.

Even though N_2 and $\text{NO}_{2/3}^-$ fluxes from clumps were not significantly correlated with fluxes from reef segments, N_2 fluxes tended to increase with increasing reef segment rate while $\text{NO}_{2/3}^-$ showed the opposite trend. As noted above, the increase in NH_4^+ fluxes and decrease in $\text{NO}_{2/3}^-$ fluxes measured from oysters alone may have allowed denitrification rates from oysters alone to have a positive relationship with whole tray estimates. Alternatively, rates of nitrification could have been reduced in our oyster only incubation simply through loss of surface area. The bottom of the *ex situ* incubation trays contain a large amount of shell and shell hash with high surfaces which could support high rates of nitrification. Interestingly, the underlying shell and shell hash does not appear to support high mineralization rates given minimal loss in DIC flux when the oyster clumps are incubated separately.

Regression of SRP fluxes from the two measurement approaches found that clump fluxes underestimated higher rates, suggesting strong binding of P to oyster shell. In addition, high CO_2 :SRP or $\sum\text{N}$:SRP ratios suggest that remineralized P was retained. Positive relationships between several flux rates and oyster tissue biomass within the clump samples provides further evidence that much of the biogeochemical activity occurs

within oyster clumps rather than in underlying sediments. Fluxes of both O_2 and NH_4^+ showed a significant positive correlation with oyster biomass and fluxes of DIC and N_2 showed marginally significant positive correlations. Similarly, work by Green et al. (Green et al. 2012) has shown that *Crassostrea gigas* densities are positively correlated with CO_2 and CH_4 fluxes, while Smyth et al. (Smyth et al. 2015) have reported that rates of denitrification measured adjacent to reefs were positively correlated with oyster (*C. virginica*) densities. Given the spatial limitations of this work, future research should assess whether the observed relationships hold up at other sites with different sediment characteristics and hydrological conditions. Although the results from this subset of work are only from one site and season, this research is in agreement with previous observations that oysters stimulate denitrification and other biogeochemical transformations in reef environments (Kellogg et al. 2013; Smyth et al. 2013; Arfken et al. 2017).

Implications

In situ approaches for measuring oyster denitrification and other biogeochemical fluxes are logistically challenging (Humphries et al. 2016; Smyth et al. 2018), but incubations must include oysters if the goal of the research is to accurately quantify oyster reef biogeochemical flux rates. The observation that the incubations of oysters alone generally fall within the range of measured reef segment rates suggest that oyster clumps are driving reef-associated biogeochemistry. Even though the denitrification measured from oysters without sediment was lower than the entire reef segment, the oysters provide a conservative measure of the reef denitrification (Figure 2.5). Similarly,

we were able to confirm that oysters alone account for the majority of the nitrogen transformations, with stoichiometric plots consistent with the expected Redfield ratio for marine algae (Fig 2.6; Kellogg et al. 2013). Nitrification supported by oyster shell surface area is likely key to maintaining high rates of denitrification in our study. In addition, despite the potential for production or dissolution of carbonates (Waldbusser et al. 2011), this work suggests that the use of DIC, instead of oxygen may be preferred for determining total nitrogen transformations considering DIC fluxes were consistent between treatments. From these experiments, estimates of nitrogen removal as an ecosystem service are best characterized by including the whole community: sediments, oysters, and the oyster-associated metazoan community. We recognize that whole community incubations are considerably more difficult than incubations of oysters or sediments; however, other approaches will necessarily result in low estimates of denitrification. This study highlights the role that oysters play in nutrient transformations and the importance of including intact segments of oyster reefs in incubations for a complete assessment of denitrification and other biogeochemical fluxes.

The data herein point to an important consideration in the determination of whether oyster-associated N removal should be a BMP for overcoming eutrophication. Much of the data available for BMP consideration focuses on the role that oysters play in stimulating denitrification in the surrounding sediments, rather than within the reef and associated organisms. As demonstrated by the high rates of N transformations from clumps of oysters alone, the coupled processes occurring on oyster reefs are complex, and require an improved understanding of the environmental drivers stimulating oyster-associated denitrification to establish oysters as a BMP.

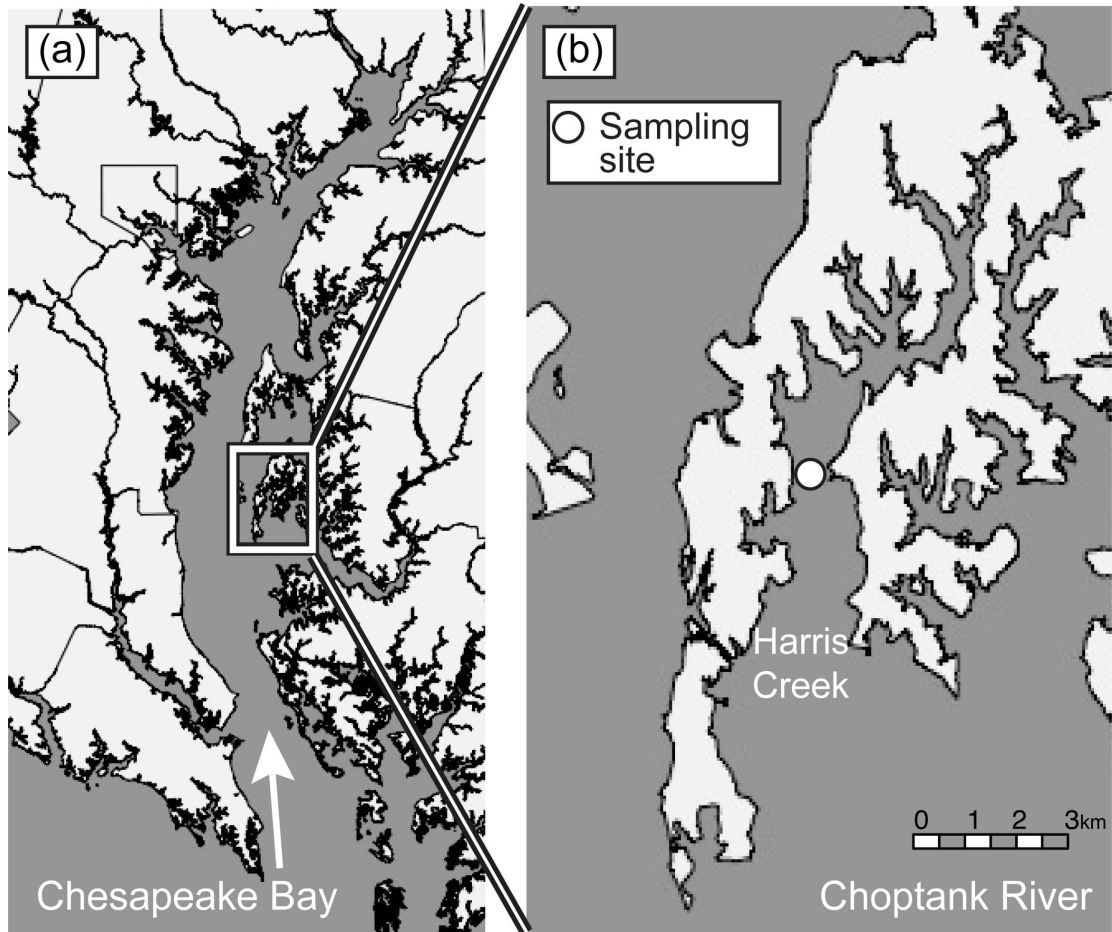


Fig 2.1 Map of study area showing (a) the Choptank River a major tributary to the Chesapeake Bay and (b) the location of the study site (○) within Harris Creek.

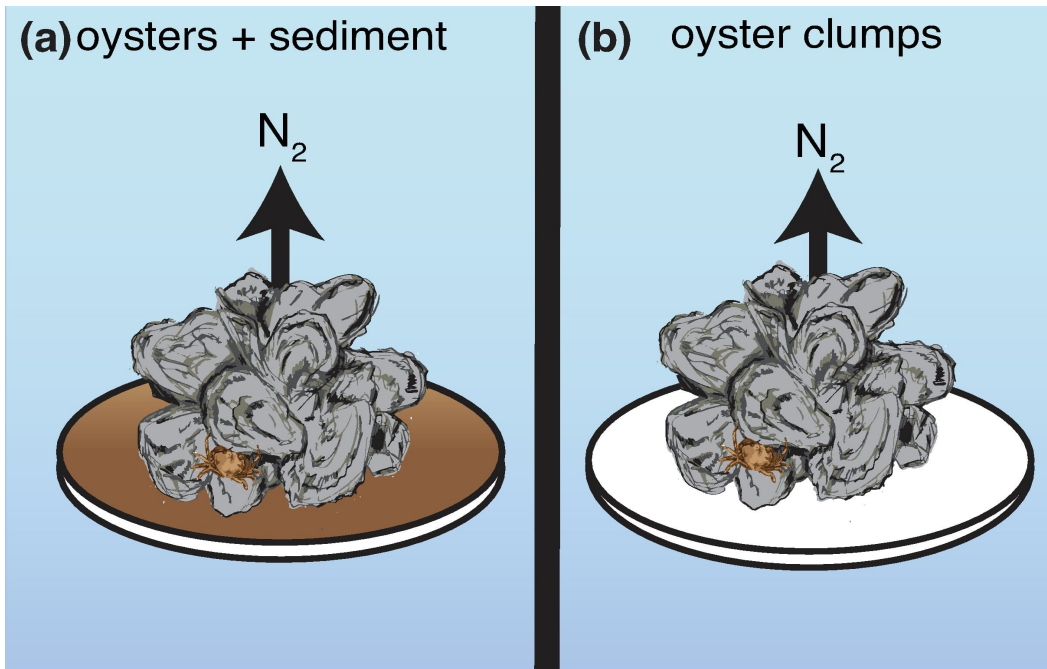


Fig 2.2 Diagram of (a) acclimated oysters and sediment for dark and light incubations and (b) oyster clumps alone for dark incubations.

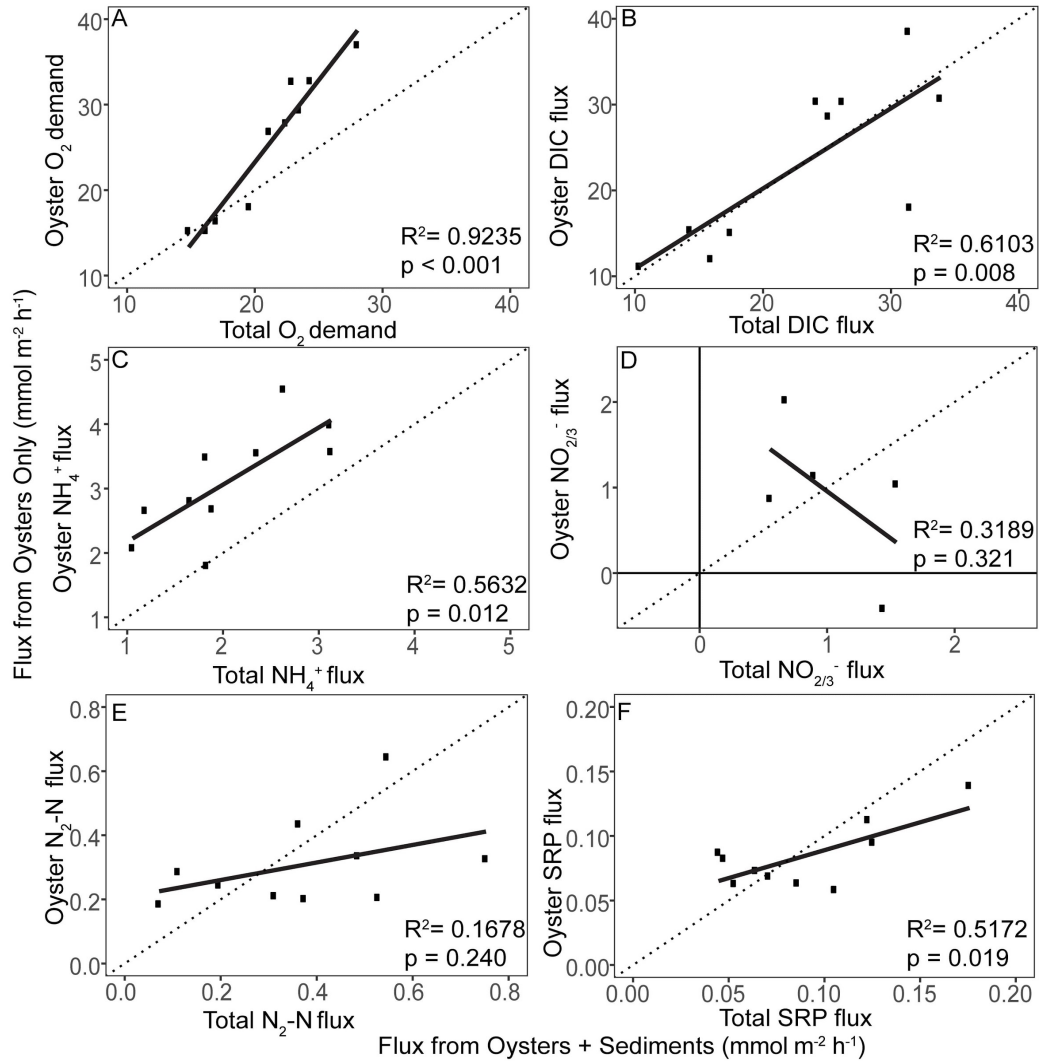


Fig. 2.3 Regressions of fluxes from oyster clumps against those from reef segments. Regressions of (a) oxygen demand (b) DIC (c) NH_4^+ (d) $\text{NO}_{2/3}^-$ (e) N_2 (f) and SRP fluxes.

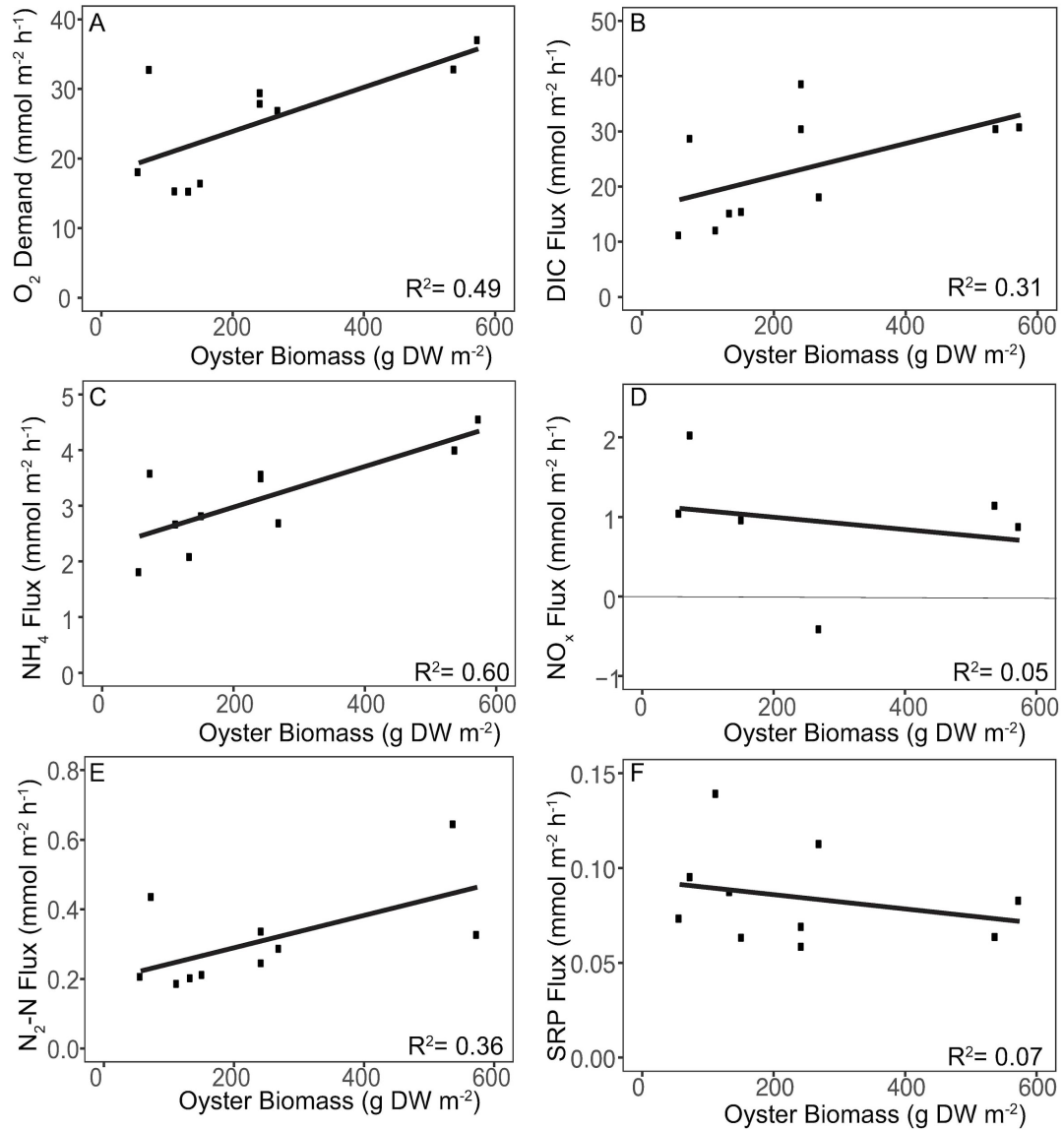


Fig. 2.4 Regressions of fluxes from oyster clumps against oyster biomass. Regressions of (a) oxygen demand (b) DIC (c) NH₄⁺ (d) NO_{2/3}⁻ (e) N₂ (f) and SRP fluxes.

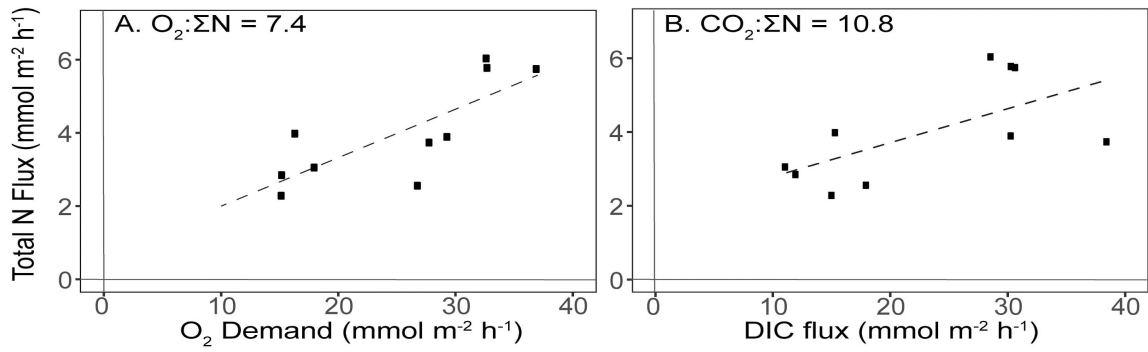


Fig. 2.6 Stoichiometric plots using O₂, DIC, and ΣN (sum of NH₄⁺, NO_{2/3}⁻, and N₂-N) from individual fluxes of oysters alone. We assume that CO₂:O₂ is a 1:1 in the plot of (a) total N flux versus O₂ demand and get a CO₂:ΣN ratio of 7.4. This is compared to an actual plot of (b) total N flux versus DIC flux, which had a CO₂:ΣN ratio of 10.8. Both ratios are similar to the Redfield elemental ratio for marine algae (106:16).

Chapter 3: Application of an *in situ* gradient approach to determining oyster reef concentration gradients and biogeochemical fluxes

Abstract

Studies focused on quantifying the nutrient ecosystem services in oysters reefs and oysters clusters have been shown to effectively remove nitrogen through denitrification. Complex community structure and spatial variability in oyster reef environments make it difficult to measure biogeochemical fluxes over intact reefs while accounting for all relevant environmental variables that potentially influence nitrogen cycling processes. Although enclosures or chamber experiments can include oysters and other reef associated organisms to directly measure their impacts on nutrient cycling, it is difficult to replicate natural circulation and other sources of large-scale variability within an enclosed experimental chamber. This work couples nutrient and gas concentration data from the water column with physical measurements to provide a noninvasive measure of chemical gradients and biogeochemical fluxes over a restored oyster reef. This study compared oyster reef biogeochemical fluxes measured using benthic chambers (*in situ* equilibration followed by *ex situ* incubation) to an *in situ* vertical gradient approach. A pumping system and current meter were deployed to collect a sequence of depth profiles to estimate the fluxes of di-nitrogen (N_2), dissolved inorganic carbon (DIC), oxygen (O_2), and nutrients from the oyster reef. While biogeochemical rates varied considerably, benthic chambers provided better constrained results than the vertical gradient approach. Above the oyster reef, time series and ensemble-averaged normalized profiles reveal that oxygen was removed at the sediment-water interface, whereas DIC, NH_4^+ , N_2 , and SRP

were produced at the bottom. The gradient approach produced O_2 , DIC, and NH_4^+ flux estimates that were in the same direction and order of magnitude as benthic chamber flux estimates. Observations from this work reveal how these contrasting methods fit into our current toolbox for understanding how oysters modify biogeochemical cycles.

Introduction

Restoration efforts to increase oysters in the Chesapeake Bay are of particular interest because oysters provide a number of ecosystem services, specifically enhanced wildstock populations, habitat for associated organisms, shoreline stabilization, and improved water quality (Coen and Humphries 2017). Water quality benefits provided by oysters have been studied largely from the perspective of the influence of bivalves on water column concentrations of nitrogen and phytoplankton biomass (Dame et al. 1992; Dame and Libes 1993; Nelson et al. 2004). Other than measurements of NH_4^+ excretion from oyster reefs (Dame et al. 1984; Volaric et al. 2018; Reidenbach et al. 2013b), there is a lack of understanding of how oysters influence other *in situ* water column concentrations. Oyster-associated biogeochemical fluxes are commonly measured using enclosures or chamber experiments (Kellogg et al. 2013; Smyth et al. 2013; Humphries et al. 2016); however, oyster reefs create a complex environment with a dynamic diffusive boundary layer (Reidenbach et al. 2013b) that is difficult to reproduce within experimental incubations. The preferred methodology for quantifying scalar fluxes from the benthos that incorporates *in situ* flow is the aquatic eddy covariance method, but this method can only be used to measure oxygen fluxes (Volaric et al. 2018) because only oxygen concentrations can be reliably measured *in situ* at a fast enough rate. Therefore, a

challenge remains to effectively determine realistic estimates of the net influence of oyster reefs on benthic biogeochemical fluxes.

Oysters primarily influence water column biogeochemistry through suspension feeding and biodeposit production. Oxygen is removed through oyster respiration (Boucher and Boucher-Rodoni 1988), biodeposit remineralization, and re-oxidation of reduced N, S, and Fe (Dame et al. 1992). Similarly, concentrations of DIC increase with oyster respiration and shell dissolution but can decrease with shell production (Waldbusser et al. 2011; Green et al. 2012; Jackson et al. 2018). Nitrogen and phosphorus are removed from the water column when bivalves filter phytoplankton and store nitrogen and phosphorus in their tissues (Newell et al. 2005; Grizzle et al. 2008). When biodeposits settle on the sediment oxic surface layer organic P is oxidized to PO_4^{3-} ; however, if biodeposits settle to anoxic sediments, PO_4 will no longer efficiently adsorb to iron complexes (Krom and Berner 1981). Oysters can stimulate nitrogen removal by supporting increased rates of denitrification in sediments and within the oyster tissues and shells (Smyth et al. 2013; Kellogg et al. 2013; Arfken et al. 2017). Biodeposits concentrate labile carbon on aerobic sediment surfaces which are expected to support the canonical conversion of oxidized forms of nitrogen (NO_3^- and NO_2^-) to N_2 gas by denitrifying bacteria (Henriksen 1988; Seitzinger 1988; Risgaard-Petersen et al. 1994; Newell et al. 2005). In contrast, if deposition is highly focused over a portion of sediment, the sediments can become depleted in oxygen and will allow sulfide and NH_4^+ to accumulate (Kaspar et al. 1985; Asmus and Asmus 1991; Newell 2004; Giles et al. 2006). Although oysters can increase NH_4^+ concentrations through excretion, NH_4^+ concentrations can be reduced by nitrifiers associated with bivalve soft tissues (Welsh

and Castadelli 2004) and ultimately provide a source of oxidized nitrogen for denitrification. Therefore, both live oysters and benthic habitat must be considered in investigations of oyster influences on benthic biogeochemical fluxes.

Different types and quantities of habitat have been included in oyster-associated incubation experiments, ranging from single oysters (Caffrey et al. 2016; Smyth et al. 2013), sediments adjacent to reefs (Piehler and Smyth 2011b), and encapsulated whole reef habitats (Kellogg et al. 2013; Humphries et al. 2016). A number of considerations need to be made during incubations, such as: the inclusion of benthic biota and habitat (Jackson et al. 2018), minimization of sediment disturbance, maintenance of *in situ* temperatures, avoidance of excessive oxygen depletion, and the representation of natural bottom boundary flow conditions (Kellogg et al. 2013). Despite the fact that enclosures are expensive and do not incorporate *in situ* flows, the encapsulation of reefs *in situ* or acclimated trays are currently the only techniques that can obtain a suite of biogeochemical fluxes from the entire oyster reef habitat.

Previous studies that estimated scalar fluxes by coupling water quality parameters and physics have found that flow speed is one of the major drivers of sediment and oxygen fluxes over oyster reefs (Reidenbach et al. 2013b; Volaric et al. 2018). Flow has been integrated into oxygen and sediment scalar flux measurements over oyster reefs with the eddy correlation technique (Reidenbach et al. 2013b; Volaric et al. 2018) and an *in situ* portable tunnel (Dame et al. 1992). The eddy correlation technique is suitable for the determination of sediment and O₂ fluxes, considering oxygen electrodes and optical backscatter sensors can resolve concentration fluctuations caused by turbulent flows, i.e., sensors with response times in the range of 0.1-1s (Lorrai et al. 2010). Currently, most

nutrient and gas parameters cannot be measured at a high enough frequency to apply the eddy correlation technique. Two other autonomous methods, the gradient flux method and the control volume approach have been used to estimate grazing by benthic suspension feeders (Jones et al. 2009); however, the control volume requires more samples and deals with areas and volumes larger than a tidal cycle. The gradient approach uses the mean gradients in momentum and chemical parameters in the bottom boundary layer to calculate a fluxes. Previously, Takeshita et al. (2016) and McGillis et al. (2011) applied the gradient approach on coral reefs to measure O₂ and pH fluxes. Their work used continuous measurements of pH and O₂ to distinguish gradients in concentrations above the benthos and accurately estimate fluxes. This suggests that the simultaneous measurement of flow speed profiles and water chemistry profiles may offer a cost-effective and unintrusive method for estimating other biogeochemical fluxes.

In this study, we collected discrete water sample profiles and current profiles to understand nutrient dynamics over a restored oyster reef and to estimate fluxes above the reef using the gradient flux approach. These estimates were compared to fluxes measured from enclosure experiments taken within the same week. The gradient approach was applied *in situ* over a restored reef in June and at a site adjacent to the restored reef in August. Enclosure experiments involved laboratory incubations of acclimated oyster trays filled with sediment and oyster densities similar to those observed in the field for comparison. The goals of this study were to use the gradient approach to (1) understand nutrient dynamics over a restored oyster reef, (2) test whether a discrete nutrient profile sampling regime might provide accurate flux estimates, and (3) compare these results inside and outside of the reef.

Methods

Study Site

The study sites were located in the Harris Creek Oyster restoration site, a tributary to the Choptank River, Maryland, USA. The gradient approach was applied within a restored reef during the month of June (38° 45' 7.164" N, 76° 18' 37.188" W) and outside of the same reef in August (38° 45' 5.83" N, 76° 18' 41.04" W; Fig 3.1). The reef was restored in 2012 by placement of 28.19 million juvenile oysters set on shell on 6.53 ha of suitable substratum, and in 2015 the density of live oysters across the entire reef averaged 20.39 oysters per m⁻² (NOAA). Results from the gradient approach were compared to “reef segment” incubations conducted within the same week using the *in situ* equilibration of intact segments of oyster reef with an *ex situ* incubation approach (Kellogg et al. 2013). The average abundance of oysters used in the “reef segment” incubations ranged from 33±5.2 ind. m⁻² in June to 63±9 ind. m⁻² in August.

Materials and Procedures

Gradient approach

The gradient flux method used the near-bed nutrient and gas concentration gradient and the vertical turbulent diffusivity to estimate fluxes. The currents close to the bed were measured with an Aquadopp Profiler (2 MHz ADP, Nortek) with sampling above the blank at 0.13 m and subsequent measurements every minute at 0.03 m intervals. Mean velocities exhibit a logarithmic profile in well-developed turbulent boundary layers, which is associated with the generation of turbulence by shear at the

bed. Once we identified intervals for log profile fitting, limited the vertical extent of the observations appropriately, smoothed the time series, and selected specific vertical profiles to analyze, the general turbulent boundary layer equation (Eqn 3.1) was fit to individual profiles. Eqn 3.1 (Schlichting and Gersten 2000) represents the "law of the wall," where $U(z)$ is the speed at height z , κ (0.41) is the von Karman's constant, u_* is the shear velocity, d is the zero plane displacement, and z_0 is the roughness parameter. This approach was also used for flow over an oyster reef (Reidenbach et al. 2013a).

$$U(z) = \frac{u_*}{\kappa} \ln \left(\frac{z-d}{z_0} \right) \quad 3.1$$

We used the nonlinear curve-fitting toolbox in Matlab to fit the observed profiles at the chosen time.

Gradients in nutrients and gases were directly assessed from water samples. Water sampling occurred during two 3-h experiments conducted once in June and August following tray incubation experiments. A tripod was placed on the reef facing the main direction of the flow with tubing attached at 5 discrete heights (0.2, 0.4, 0.8, 1.2, and 1.6 m) in June and 6 heights (0.2, 0.4, 0.6, 0.8, 1.1, and 1.5 m) in August above the pads on the tripod (Fig 3.2). Tubes closest to the sediment-water interface are expected to represent the summation of local effects (i.e., oysters, microbes, and sediments) over some benthic footprint just upstream of the sampling tripod (Paola 1985), and therefore "sediment-water interface" refers to all of the biogeochemical processes within that footprint. The intake tubes were facing the mean flow to reduce potential mixing caused by the tripod frame. Water samples were collected at 6 time points in June (11:07, 11:59, 12:20, 12:42, 13:06, and 13:33) and August (09:16, 09:55, 10:26, 10:55, 11:22, and

11:48) via 7-m length of tubing and separate diaphragm pumps operating at 6000 mL min⁻¹. Sampling times were chosen to bracket slack tide in both months (slack before ebb in June, slack before flood in August), which is when the largest biogeochemical gradients were expected (equation 3.2). The 1-cm diameter tubing was attached to the tripod and ended with a PVC manifold distributing water to 3 outlets to fill triplicate sample vials or syringes. The sampling intervals were based on the time required to process and appropriately store 6 different types of nutrient and gas samples. Solutes (NH₄⁺, NO_{2/3}⁻, SRP) and dissolved gases (O₂, N₂, Ar, DIC=[H₂CO₃]+[HCO₃⁻]+[CO₃²⁻]) were collected from each depth approximately every 30 minutes. Dissolved gas samples (7 mL) were taken in triplicate and were preserved with 10 µl of 50% saturated HgCl₂, tightly sealed, submerged in water, and held at or slightly below incubation temperature until analysis. Solute samples were filtered through 0.45 mm pore-size filters and kept frozen for analysis. Surface and bottom water temperatures and salinities were measured using a YSI (Quatro) at the time water samples were taken. N₂, O₂, and Ar were measured on a membrane-inlet mass spectrometer (Kana et al. 1994) within 2 weeks of collection. An infrared-based analyzer was used to measure DIC with a calibration coefficient of variation that ranged from 0.14 to 0.2 % with an average standard deviation of ±4.69 µmol l⁻¹ (Apollo SciTech; Cai and Wang 1998). NH₄⁺ concentrations were determined based on phenol/hypochlorite colorimetry, whereas SRP analysis involved a composite reagent of molybdic acid, ascorbic acid, and trivalent antimony (Parsons 2013). Concentrations of NO_{2/3}⁻ were measured spectrophotometrically following Doane and Horwath (2003).

Biogeochemical fluxes were calculated using equation 3.2a with respect to the logarithm of height (Jones et al. 2009) and solving for F_B in equation 3.2b

$$C(z) = \frac{F_B}{\kappa u_*} \ln \frac{z}{z_c} + C_B \quad (3.2a)$$

$$F_B = \frac{\delta C}{\delta \ln z} \kappa u_* \quad (3.2b)$$

where F_B represents the total flux toward or away from the bed. Measured values of $C(z)$ and z at 0.2 and 0.4 meters above bottom were used for these calculations, with u_* estimated at each sampling time as described above.

Individual profiles of nutrients and gases were ensemble-averaged to estimate typical gradients in nutrient or gas concentrations formed above the bottom during each experiment (Jones et al. 2009). Nutrient and gas profiles were normalized by depth-averaged concentrations and averaged over all sampling times for each sampling date, with error bars representing the standard deviation from the normalized concentration. This also allowed for direct comparison to the longer duration laboratory flux experiments.

Reef segment incubation approach

The fluxes estimated using the gradient approach were compared to a subset of reef segments collected the same week and incubated using an *in situ* equilibration and *ex situ* incubation approach described hereafter (Kellogg et al. 2013). Divers embedded pvc trays filled with sediment, oyster shell, and live oysters flush with surrounding sediments approximately one month prior to incubations. Once the trays were acclimated in the field

for a month, the base tray was capped off with a pvc midsection with a sealed lid by divers. The reef segments were returned to Horn Point Laboratory, Cambridge, MD within 2 hours. Trays were submerged in Choptank River water adjusted to ambient temperatures of 23.3° C in June and 28° C in August, and a “blank” tray was filled with filtered river water. Following an aeration period of approximately 1 h, chambers were capped with a motor-driven impeller stirring lid containing ports for sample collection (Kellogg et al. 2013). The trays were incubated first in the dark, then with illumination; because the gradient approach was conducted during the day, we only show the data from the illuminated incubations.

All solutes and dissolved gases collected for the gradient approach were also collected during the incubation approach. Samples were pulled from a sampling tube fitted to the lid, while a water replacement tube pulled water from the water bath every 45 minutes (4 times total) for each set of incubations. Oxygen concentrations were measured using a FireSting O₂-Mini oxygen meter to determine sampling intervals, with final oxygen concentrations ranging from 0.19± 0.001 mmol l⁻¹ in June to 0.16±0.069 mmol l⁻¹ in August. Dissolved gases and solutes were preserved, stored, and analyzed as described in the previous section. Fluxes were estimated by regressing the concentrations of nutrients and gases versus time to obtain a slope. The slope was deemed significant if it had an R²≥0.80 and was subsequently corrected by the slope of the “blank” if it was significant to remove water column processes effects (Owens and Cornwell 2016). We compared the gradient approach flux estimates to rates from trays with oyster densities closest to those on the restored reef. An areal flux (F ; mmol m⁻² hr⁻¹) was determined from the equation:

$$F = \frac{\Delta C}{\Delta t} * \frac{V}{A} \quad 3.3$$

Where $\Delta C/\Delta t$ is the slope ($\text{mmol L}^{-1} \text{hr}^{-1}$), V is the volume of the water in the tray (L), and A is the area of the bottom of the incubation chamber (m^2).

Assessment

Physical conditions

Maximum current speeds in the bottom boundary layer were $<0.14 \text{ m s}^{-1}$ in June and August (Fig 3.3) The results of June boundary layer current profile fitting at the three times indicated in Figure 3.3a are presented in Table 3.1.

Table 3.1 - Boundary layer profile fitting parameters for June observations

Time	$u(.216\text{m})$	u_* (m/s)	d (m)	z_0 (m)	$C_D(.216\text{m})$	r^2
10:51	0.031	0.0042	-0.019	0.010	0.0183	0.997
13:07	0.117	0.011	0.449	0.0096	0.0089	0.996
13:33	0.126	0.012	0.430	0.010	0.0090	0.994

The average drag coefficient of 0.012 was then used to estimate u_* for all times water samples were taken during the June experiment using:

$$u_* = \sqrt{C_D} * u(0.216\text{m}) \quad (3.4)$$

Differences between the first profile at 10:51 and the last two fits were likely due to their occurrences on opposite phases of the tide, with different directions and upstream

roughnesses. The same procedures were used for the August profile fits at the three times indicated in Figure 3.3b to calculate the boundary layer parameters indicated in Table 3.2.

Table 3.2 Boundary layer profile fitting parameters for August observations.

Time	$u(.216\text{m})$	u_* (m/s)	d (m)	z_0 (m)	$C_D(.216\text{m})$	r^2
09:16	0.107	0.0136	-0.0075	0.0096	0.0161	0.998
09:55	0.069	0.0096	-0.0307	0.0140	0.0194	0.999
11:48	0.037	0.0042	0.0435	0.0048	0.0127	0.996

The average drag coefficient of 0.016 was used to estimate u_* for all water sampling times during the August experiment.

The boundary layer profile fit for the second August log profile is illustrated in Figure 3.4. Here, the profile fit was limited to $z < 0.5$ meters above the bottom, where the log layer profile assumption is clearly well-satisfied. Limiting log layer profile fits to r^2 values ≥ 0.994 ensures that the resulting estimates of u_* have uncertainty bounds $\leq \pm 10\%$ (Gross and Nowell 1983), which also ensures that the estimated drag coefficients are acceptably accurate. The present drag coefficient estimates were lower than that recorded over an oyster reef by (Reidenbach et al. 2013b; $C_D = 0.019 \pm 0.004$ at $z = 0.50$ m) and three different reefs by Volaric et al. (2018), likely because the oyster densities in Harris Creek reefs were much lower than in other cases. Interestingly, the drag coefficient measured outside of the reef was significantly higher than drag coefficients typically measured from sands or muds ($C_D = 0.003$; Gross and Nowell 1983). This may be attributed to the fact that our off-reef site was only 97 m away from the on-reef site, but it is also likely

that the off-reef site had a pre-existing rough bottom. Although the off-reef site was not technically planted for restoration, a bottom survey conducted in 2015 classified the site bottom type as consisting of oyster rubble and biogenic shell (M. Munkacsy, personal communication, November 14, 2018).

Environmental conditions and concentration boundary layers

Environmental conditions changed depending on the sampling month. The average water temperature during sampling in June was 22.7°C, whereas the average temperature in August was 26.6°C. Temperatures during sampling on both dates varied by <1°C. The average salinity was higher in June than August (12.58±0.01 and 11.48±0.17, respectively).

Oxygen time-depth distributions from June and August exhibit a depletion of oxygen from the sampling point closest to the bed (Fig 3.5a,b), while ensemble-averaged normalized profiles from June and August reveal that on average oxygen was removed at the sediment-water interface (Fig 3.5c,d). Bottom oxygen concentrations measured in June were on average 0.83% lower than the depth-averaged concentration and 2.4% lower than surface concentrations. In comparison, bottom oxygen concentrations measured in August were on average 4.0% lower than the depth-averaged concentration and 9.1% lower than surface concentrations. Although oxygen concentrations increase with height above the bottom in August, the ensemble-averaged profile is not as smooth as that observed in June (Fig 3.5c,d). There are no other published data on gradients in oxygen concentrations above oyster reefs, but past studies have shown that oyster reefs have a large oxygen demand (Dame et al. 1992; Kellogg et al. 2013).

DIC time-depth distributions from June indicate production of DIC close to the bottom (Fig 3.6a). Similarly, ensemble-averaged normalized profiles from June display that on average DIC was relatively high directly above the bed (Fig 3.6b). In June, bottom DIC concentrations were on average 0.31% higher than the depth-averaged concentration and 0.36% higher than surface concentrations. Other than the production of DIC above the bed, the ensemble-averaged DIC profile was uniform. The increase in bottom DIC concentrations aligns with our understanding that oysters can impact DIC concentrations through CO₂ release during respiration (Lejart et al. 2012; Frankignoulle et al. 1994).

Concentrations of different inorganic nitrogen forms (i.e., NH₄⁺, NO_{2/3}⁻, and N₂) had varying relationships with height above bottom depending on the sampling date and location (Figs 3.7 and 3.8). NH₄⁺ time series from June show that bottom concentrations were consistently higher, whereas bottom concentrations in August were dependent on the sampling time (Fig 3.7 a,b). Ensemble-averaged NH₄⁺ profiles from both sampling dates show a decrease in concentration with increasing height; however, the concentration of the sample nearest the bed taken in August was markedly lower and deviated from this trend (Fig 3.7 c,d). Bottom concentrations of NH₄⁺ were 22.3% higher than depth-averaged concentrations and 65.7% higher than surface concentrations in June, whereas bottom concentrations in August were 27.9% lower than depth-averaged concentrations but 66.7% higher than surface concentrations. Despite differences in measurement techniques, the June results are in line with observations of consistent NH₄⁺ release during ebb and flood tides by (Dame et al. 1989). Time series of vertical profiles of NO_{2/3}⁻ concentrations show variable gradients directly above the bottom in June, yet a

consistent increase in concentrations of the samples nearest the bed in August (Fig 3.7 e,f). For both sampling dates, ensemble-averaged $\text{NO}_{2/3}^-$ profile concentrations decrease from ~0.75 m above the bottom to the surface, followed by an increase in concentrations with increasing height (Fig 3.7 g,h). On average, bottom $\text{NO}_{2/3}^-$ concentrations were 3.3% lower than depth-averaged concentrations and 3.5% higher than surface concentrations in June. In August, bottom $\text{NO}_{2/3}^-$ concentrations were 1.8% higher than depth-averaged concentrations and 15.8% higher than surface concentrations. These findings suggest that surfaces of biogenic shell off-site in August dominate the formation of a $\text{NO}_{2/3}^-$ concentration gradient, concurring with previous observations of nitrification on oyster shell (Caffrey et al. 2016), whereas live oysters complicated concentration gradients on-site in June. Time series of N_2 concentrations exhibited a consistent increase from samples nearest the bed in June during slack tide, whereas profiles from August did not display an obvious trend (Fig 3.8 a,b). Ensemble-averaged bottom concentrations of N_2 revealed opposite trends depending on the sampling date (Fig 3.8 c,d). In June and August, bottom N_2 concentrations were lower than depth-averaged concentrations, by 0.01% and 0.35%, and surface concentrations, by 0.09% and 0.35%, respectively. These findings agree with *in situ* incubations of oyster reef and cultch by (Humphries et al. 2016), in that rates of denitrification were higher above oyster reef than cultch. It is difficult to measure a defined N_2 gradient without a closed system or strong water-density gradients, therefore gradients in N_2 were more pronounced during slack tide. However, slack tide is not the ideal time to estimate a flux because our assumptions to determine u^* are weakened by the low flow regime.

Time series of SRP profiles in June and August display that SRP concentrations were low and often below levels of detection (Fig 3.9 a,b). Ensemble-averaged SRP profiles were similar to $\text{NO}_{2/3}^-$ profiles, with peaks in average concentrations observed at mid- to bottom-depths (from 0.4 to 0.6 m; Figs 3.7 g,h, 3.9 c,d). Compared to depth-averaged concentrations, bottom SRP concentrations were 0.31% higher in June and 1.7% lower in August. In relation to surface concentrations, bottom SRP concentrations ranged from 0.35% to 26.0% higher in June and August, respectively. Previous *in situ* tunnel estimates of SRP fluxes from oyster reefs found similar results of fluxes depending on the tidal regime (Dame et al. 1984).

Comparisons of biogeochemical fluxes from the oyster reef

The nutrient and gas fluxes estimated using the gradient approach, based on equation 3.2, were highly variable depending on physical conditions. Mean oxygen fluxes using the gradient approach ($-4622.00 \pm 4018.51 \mu\text{mol m}^{-2} \text{hr}^{-1}$) compared reasonably well to fluxes from incubation of reef segments ($-7521.94 \pm 907.30 \mu\text{mol m}^{-2} \text{hr}^{-1}$) in June (Table 3.3). The oxygen fluxes measured in August were much more variable at $-54036.78 \pm 77812.08 \mu\text{mol m}^{-2} \text{hr}^{-1}$ using the gradient technique compared to $-8073.64 \pm 1393.42 \mu\text{mol m}^{-2} \text{hr}^{-1}$ from incubations (Table 3.4), but all estimates still indicated net oxygen uptake by the benthos. The percent error observed between incubation derived oxygen fluxes and the gradient approach estimates was lower on-reef in June (-38.55%) and higher off-reef in August (569.29%). These dichotomous fluxes were likely attributed to the lack of a distinct gradient off-reef in August, from the absence of live oyster-associated respiration. In June, average DIC fluxes using the gradient approach

($39466.43 \pm 30767.57 \mu\text{mol m}^{-2} \text{hr}^{-1}$) were higher than reef segment incubations ($17624.10 \pm 1783.65 \mu\text{mol m}^{-2} \text{hr}^{-1}$; Table 3.3) and had a percent error of 123.93%. The relatively small percent errors from DIC flux estimates on-reef suggest that a clear gradient in concentrations was likely formed and dominated by respiration.

Overall, inorganic nitrogen fluxes derived from the gradient approach did not agree as well as respiration-based measurements. In June, mean NH_4^+ fluxes from the gradient approach ($971.94 \pm 1359.2 \mu\text{mol m}^{-2} \text{hr}^{-1}$) were slightly higher than fluxes estimated using the incubation approach ($680.93 \pm 118.47 \mu\text{mol m}^{-2} \text{hr}^{-1}$). Fluxes estimated using the gradient and incubation approaches were dramatically different in August (-8841.37 ± 17673.30 and $763.8 \pm 264.45 \mu\text{mol m}^{-2} \text{hr}^{-1}$, respectively; Tables 3.3 and 3.4); therefore, the percent error was much lower in June than August (42.74% and -1257.55%, respectively). This is in agreement with past work showing that oysters regenerate NH_4^+ through enhanced deposition and recycling (Holyoke 2008; Dame et al. 1984; Pietros and Rice 2003). In June, $\text{NO}_{2/3}^-$ fluxes using the gradient and incubation approach were the same magnitude; however, the directions of the fluxes were different (-497.54 ± 1018.64 and $469.70 \pm 54.67 \mu\text{mol m}^{-2} \text{hr}^{-1}$, respectively). August $\text{NO}_{2/3}^-$ fluxes showed a similar pattern, with negative flux estimates using the gradient approach ($-906.93 \pm 6930.42 \mu\text{mol m}^{-2} \text{hr}^{-1}$) and positive flux estimates using the incubation approach ($525.93 \pm 64.74 \mu\text{mol m}^{-2} \text{hr}^{-1}$). The percent error in average $\text{NO}_{2/3}^-$ estimates increase from -205.92% in June to -3036.43% in August. Average denitrification estimates from the gradient approach in June had the same magnitude but were in the opposite direction of incubation estimates, with average gradient rates of $-884.80 \pm 6590.13 \mu\text{mol m}^{-2} \text{hr}^{-1}$ and incubation estimates of $128.09 \pm 84.43 \mu\text{mol m}^{-2} \text{hr}^{-1}$. August estimates were very

dissimilar, with average gradient estimates of $-23362.25 \pm 18151.57 \mu\text{mol m}^{-2} \text{hr}^{-1}$ and incubation estimates of $140.74 \pm 29.32 \mu\text{mol m}^{-2} \text{hr}^{-1}$. Variability in estimates were expected from *in situ* measurements from an open system.

Finally, mean SRP fluxes measured from the gradient approach in June were negative ($-48.95 \pm 54.58 \mu\text{mol m}^{-2} \text{hr}^{-1}$) and in the opposite direction of estimates from incubations ($8.48 \pm 16.65 \mu\text{mol m}^{-2} \text{hr}^{-1}$). In August, no gradient was measured directly above the bottom, therefore no estimate was produced using the gradient approach. The gradient approach may have missed the SRP gradient given how low SRP concentrations were.

Table 3.3 Comparison of average nutrient and gas fluxes ($\mu\text{mol m}^{-2} \text{hr}^{-1} \pm \text{SD}$) estimated using the gradient and reef segment incubation approach in June on the restored oyster reef.

	June fluxes ($\mu\text{mol m}^{-2} \text{hr}^{-1}$)	
	Gradient (n=6)	Incubation (n=3)
O ₂	-4622.01 ± 4018.51	-7521.94 ± 907.30
DIC	39466.43 ± 30767.57	17624.10 ± 1783.65
NH ₄ ⁺	971.94 ± 1359.20	680.93 ± 118.47
NO _{2/3} ⁻	-497.54 ± 1018.64	469.70 ± 54.67

N ₂	-884.80 ± 6590.13	128.09 ± 84.43
SRP	-48.95 ± 54.58	8.48 ± 16.65

Table 3.4 Comparison of average nutrient and gas fluxes ($\mu\text{mol m}^{-2} \text{hr}^{-1} \pm \text{SD}$) estimated using the gradient and reef segment incubation approach in August. The gradient approach was conducted just outside of the reef, whereas the reef segments were acclimated within the same reef as June sampling. We were unable to estimate an SRP flux due to the lack of a concentration gradient in SRP.

	August fluxes ($\mu\text{mol m}^{-2} \text{hr}^{-1}$)	
	Gradient (n=6)	Incubation (n=3)
O ₂	-54036.78 ± 77812.08	-8073.64 ± 1393.42
NH ₄ ⁺	-8841.37 ± 17673.30	763.8 ± 264.45
NO _{2/3} ⁻	-906.93 ± 6930.42	525.93 ± 64.74
N ₂	-23362.25 ± 18151.57	140.74 ± 29.32
SRP	No gradient	21.95 ± 26.77

Discussion

In this study, we describe methods that can be used to observe nutrient and dissolved gas gradients very near the bottom under favorable circumstances and subsequently use those concentration gradients to estimate biogeochemical fluxes. On-reef sampling captured consistent gradients in respiration-based measurements (i.e. O₂ and DIC). This finding demonstrates the importance of including oysters and associated biota in biogeochemical flux estimates, considering a number of studies have extrapolated rates of oyster reef associated denitrification from sediments adjacent to reefs (Piehler and Smyth 2011a; Smyth et al. 2015). In addition, NH₄⁺ concentration gradients were particularly well-defined on the reef. *C. virginica* have been found to generate NH₄⁺ fluxes through the remineralization of biodeposits (Dame et al. 1984; Newell et al. 2005). Contrastingly, it was unclear whether NO_{2/3}⁻ was being produced or removed on-reef, whereas NO_{2/3}⁻ was evidently produced off-reef from shell hash. These results support the emerging consensus that nitrification is associated with oyster shell (Caffrey et al. 2016). Although the NO_{2/3}⁻ gradient was weaker on-reef, we can attribute this to denitrifiers associated with the live reef reducing oxidized forms of N (NO₂⁻ and NO₃⁻) to N₂ gas (i.e., denitrification; Arfken et al. 2017). The gradient method offers an important advance in the ability to study the substantial heterogeneity within oyster reefs and the potential export of biodeposits and associated fluxes away from a reef, since it is expected that a few sediment-only cores may not represent the natural oyster reef environment.

The dominant filter feeders in Harris Creek include the eastern oyster (*Crassostrea virginica*), hooked mussel (*Ischadium recurvum*), and sea squirt (*Molgula*

mahattensis; Kellogg et al., n.d.). Based on the most recent assessment of the average live oyster biomass across the reef (22.96 ± 3.75 g DW m^{-2} ; NOAA) and the maximum filtration rate (0.17 ± 0.07 m^3 g^{-1} DW day^{-1} ; Cerco and Noel 2005; Cerco and Noel 2007; Fulford et al. 2007; Ehrich and Harris 2015), the maximum pumping rate for *C. virginica* would be 3.90 ± 0.44 m^3 m^{-2} d^{-1} . Other than work by (Dame et al. 1989) showing that the filtration of particulates from the water column by *C. virginica* increases overall fluxes of carbon, nitrogen, and phosphorus, there have been no previous unobstructed *in situ* estimates of overall biogeochemical concentration gradients over oyster reefs.

The evaluation of this technique revealed that local phenomenon were measured over the restored oyster reef, whereas the technique did not work off-reef. Nevertheless, a comparison of average biogeochemical flux estimates from the gradient approach to incubations reveal that, other than $NO_{2/3}^-$, N_2 , and SRP, the majority of fluxes measured on-reef were in agreement in terms of the average rate and direction of the flux. However, when we compared fluxes from the gradient approach off-reef to incubations of low oyster densities, only a small number of estimates were in agreement. Based on previous work showing that oyster reef remineralization is consistent with the expected Redfield ratio for marine algae of 106C:16N:1P (Kellogg et al. 2013), we may extrapolate fluxes from average oxygen or DIC flux estimates determined using the gradient approach. The implications of our findings are that the combination of a few discrete nutrient and gas samples along with estimates of near-bottom turbulent diffusion rates on an active reef can yield average biogeochemical flux estimates within the range of fluxes previously measured from other oyster reefs (Kellogg et al. 2013; Humphries et al. 2016).

Precise flux estimates from the gradient approach may require strong uptake or regenerative conditions, such as measurements over more biologically active oyster reefs. In order to directly resolve nutrient and gas concentration fluctuations caused by turbulent flows, we would need more samples near slack tide and closer to the bottom. Although the gradient approach is not precise compared to incubations or continuous measurement gradient approaches (Takeshita et al. 2016), future work may be able to achieve higher resolution with less error by conducting work on reefs with a higher abundance of oysters at times and heights when stronger gradients in dissolved gas and nutrient concentrations are expected.

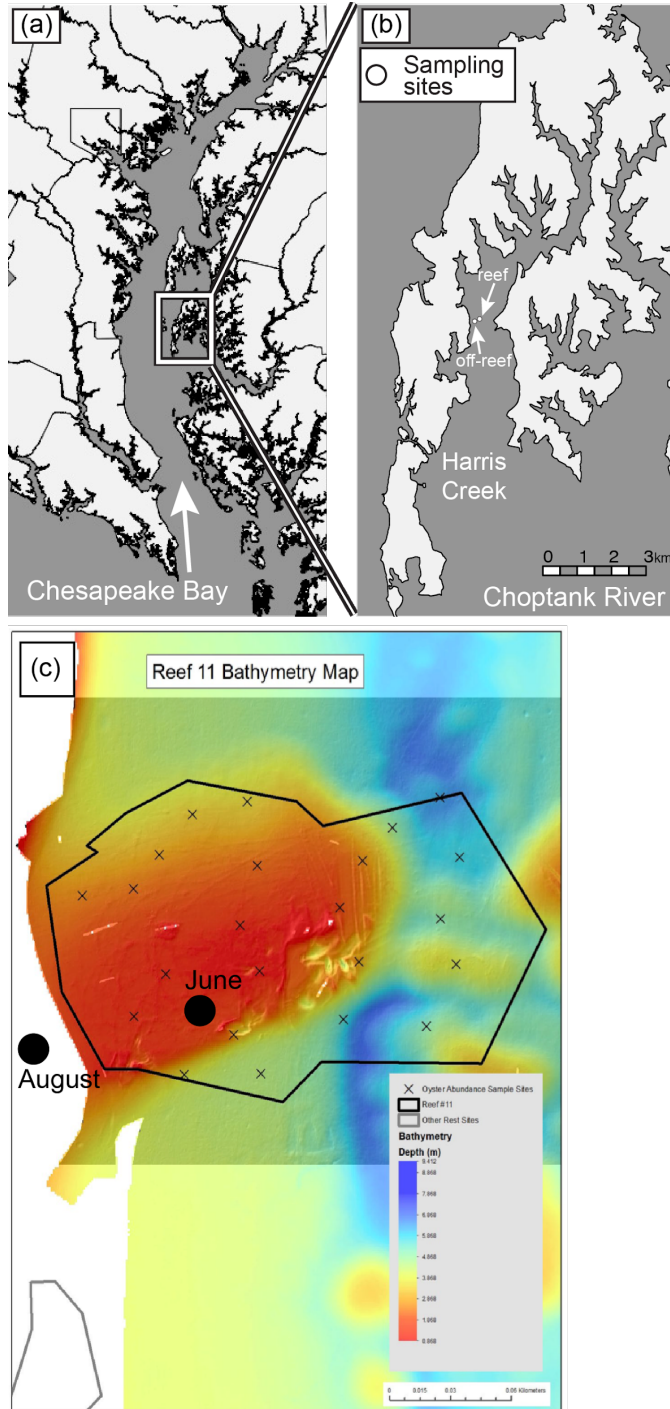


Fig. 3.1 Map of study area showing (a) the Choptank River a major tributary to the Chesapeake Bay, (b) the location of the sampling sites (○) within Harris Creek, and (c) a

bathymetry map of the reef and tripod sampling sites (bathymetry map from:
<https://chesapeakebay.noaa.gov/images/stories/habitats/hc3ydcheckinjuly2016.pdf>).

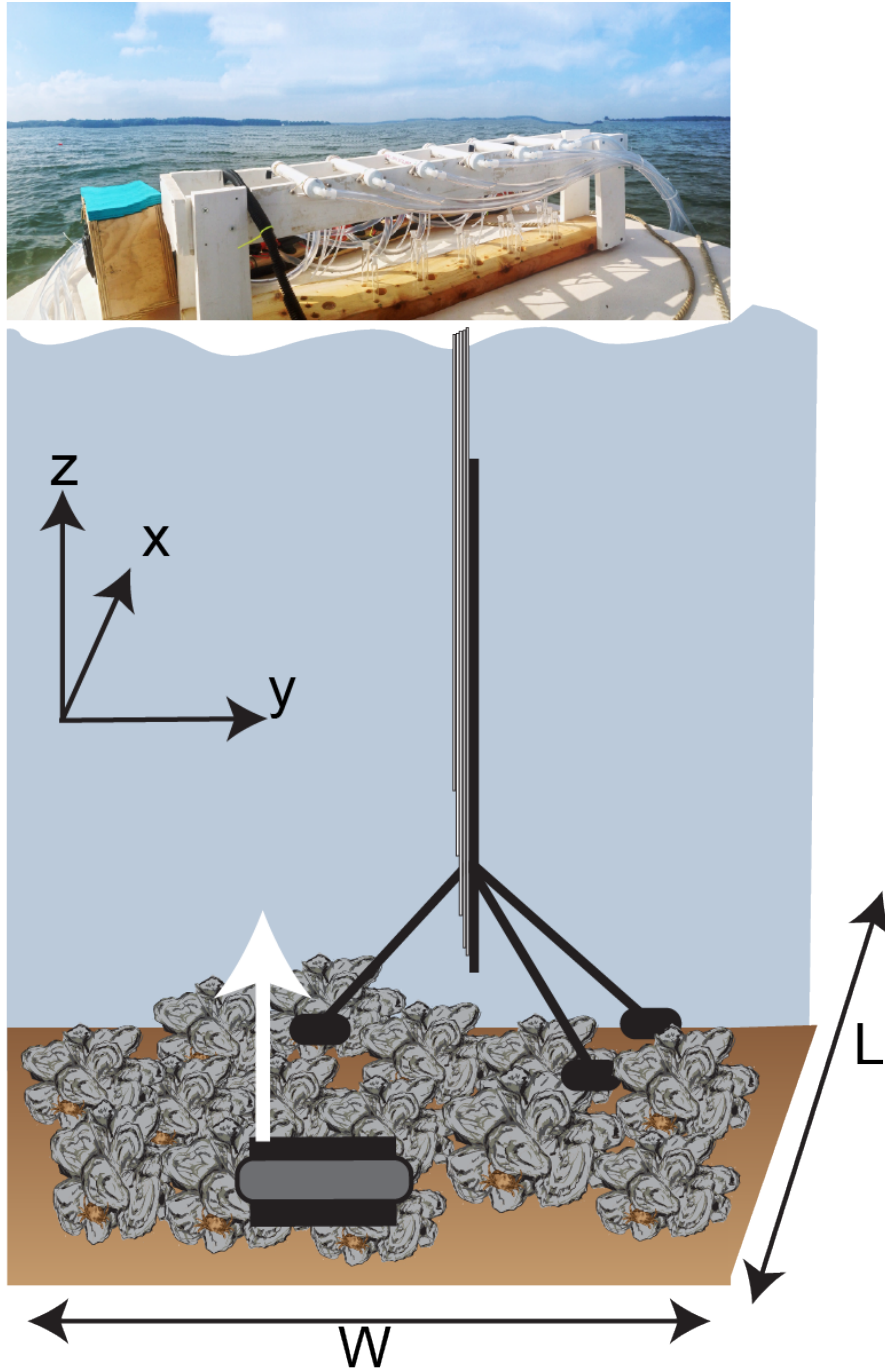


Fig. 3.2 A schematic drawing of the gradient approach and sampling manifold on the boat. The ADP is shown in front of the sampling tripod frame to measure hydrodynamics. The dominant flow is in the x direction. Sampling tubes were connected to the tripod at

various depths, 5 discrete heights (0.2, 0.4, 0.8, 1.2, and 1.6 m) in June and 6 heights (0.2, 0.4, 0.6, 0.8, 1.1, and 1.5 m) in August. Each sampling tube was connected to a separate diaphragm pump on the boat, which were distributed through tubing on the manifold (b).

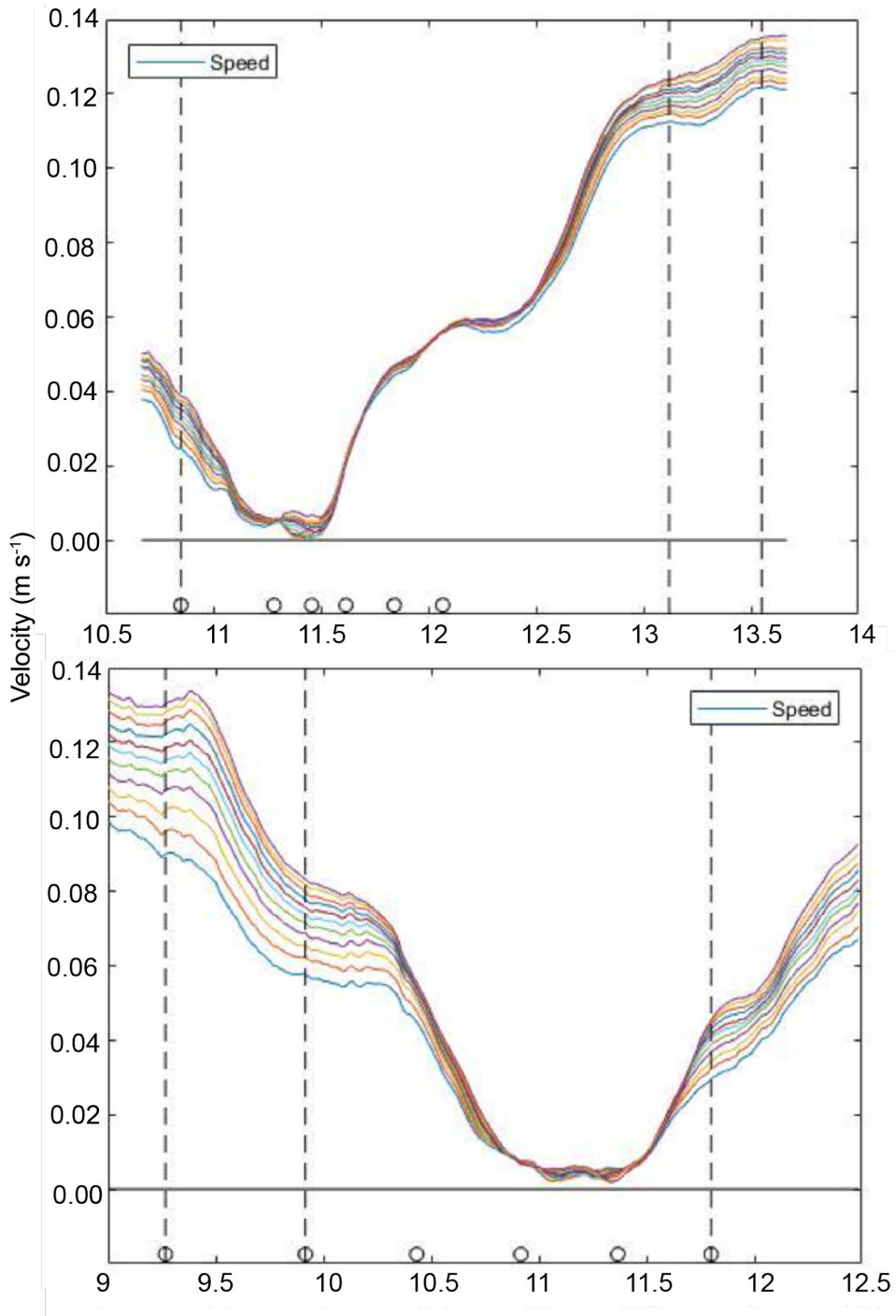


Fig 3.3 Total smoothed velocity in June (a) and August (b). Dotted lines represent profile times with $r^2 \geq 0.994$ used to calculate boundary layer parameters.

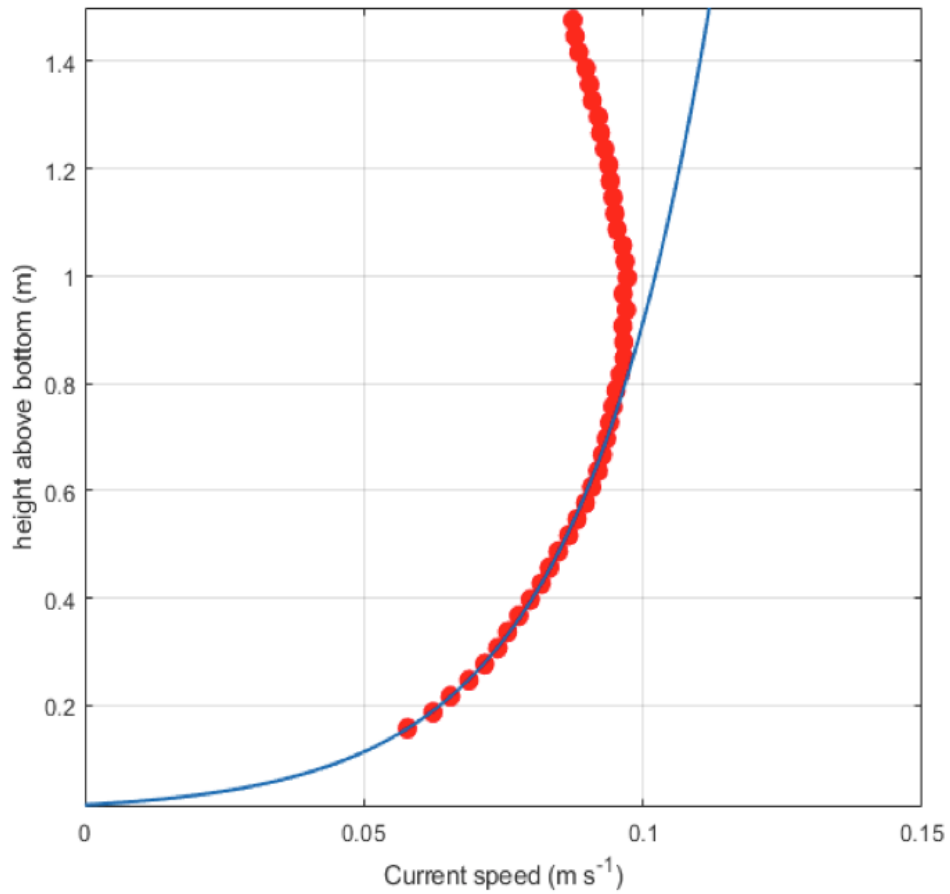


Fig. 3.4 Boundary layer log profile fit for the second August current profile at 09:55. The profile fit was limited to $z < 0.5$ meters above the bottom, where the log layer profile assumption is clearly well satisfied, with an r^2 value of 0.999.

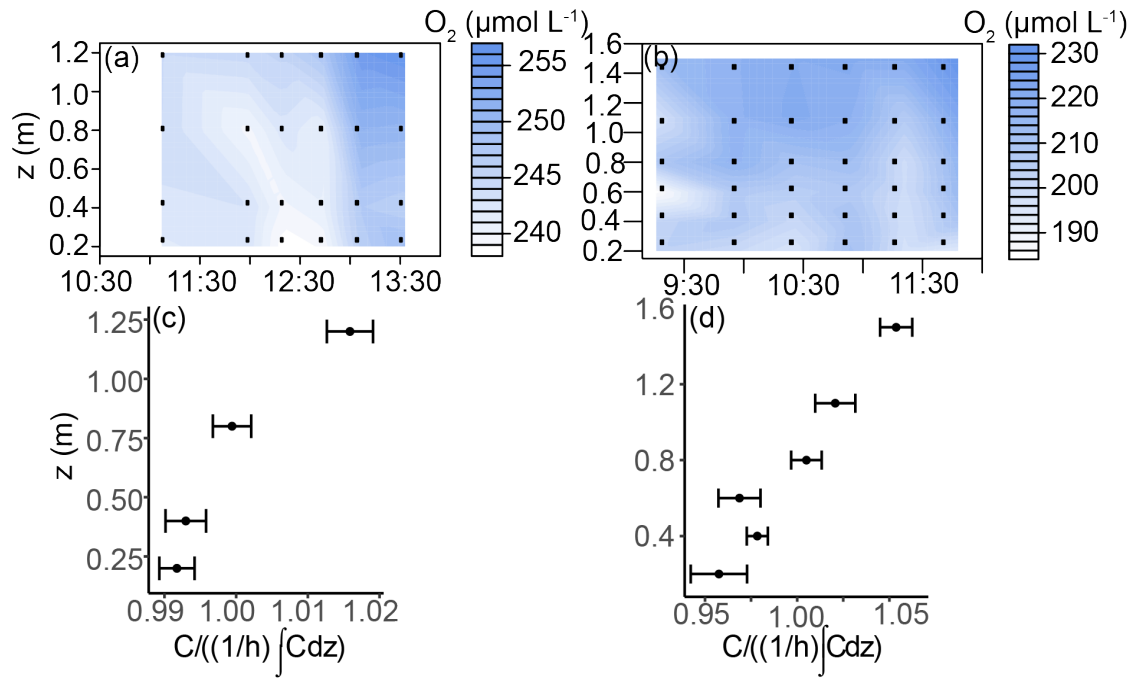


Fig. 3.5 Time series of oxygen concentrations during sampling in (a) June and (b) August. Ensemble-averaged dimensionless profiles from time series samples in (c) June and (d) August.

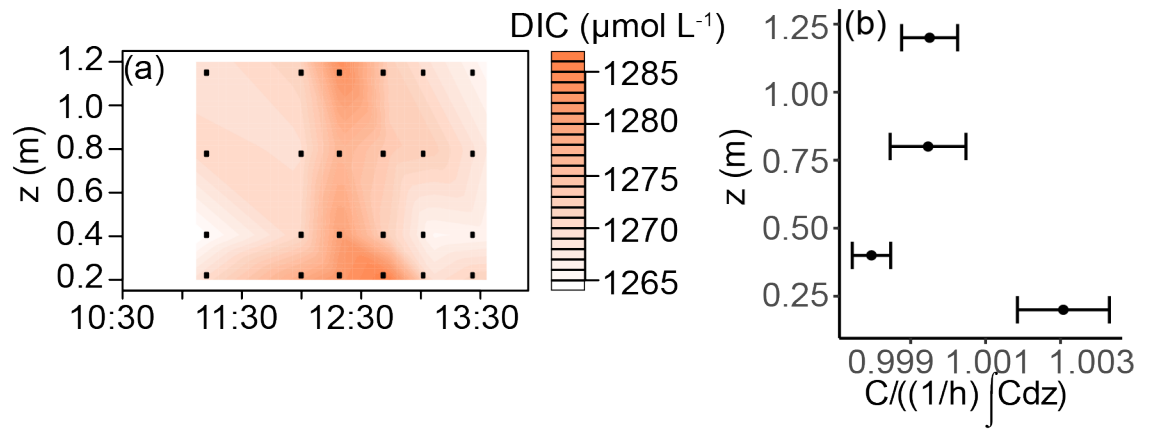


Fig. 3.6 Time series of DIC concentrations (a) and ensemble-averaged dimensionless profiles (b) from time series samples in June.

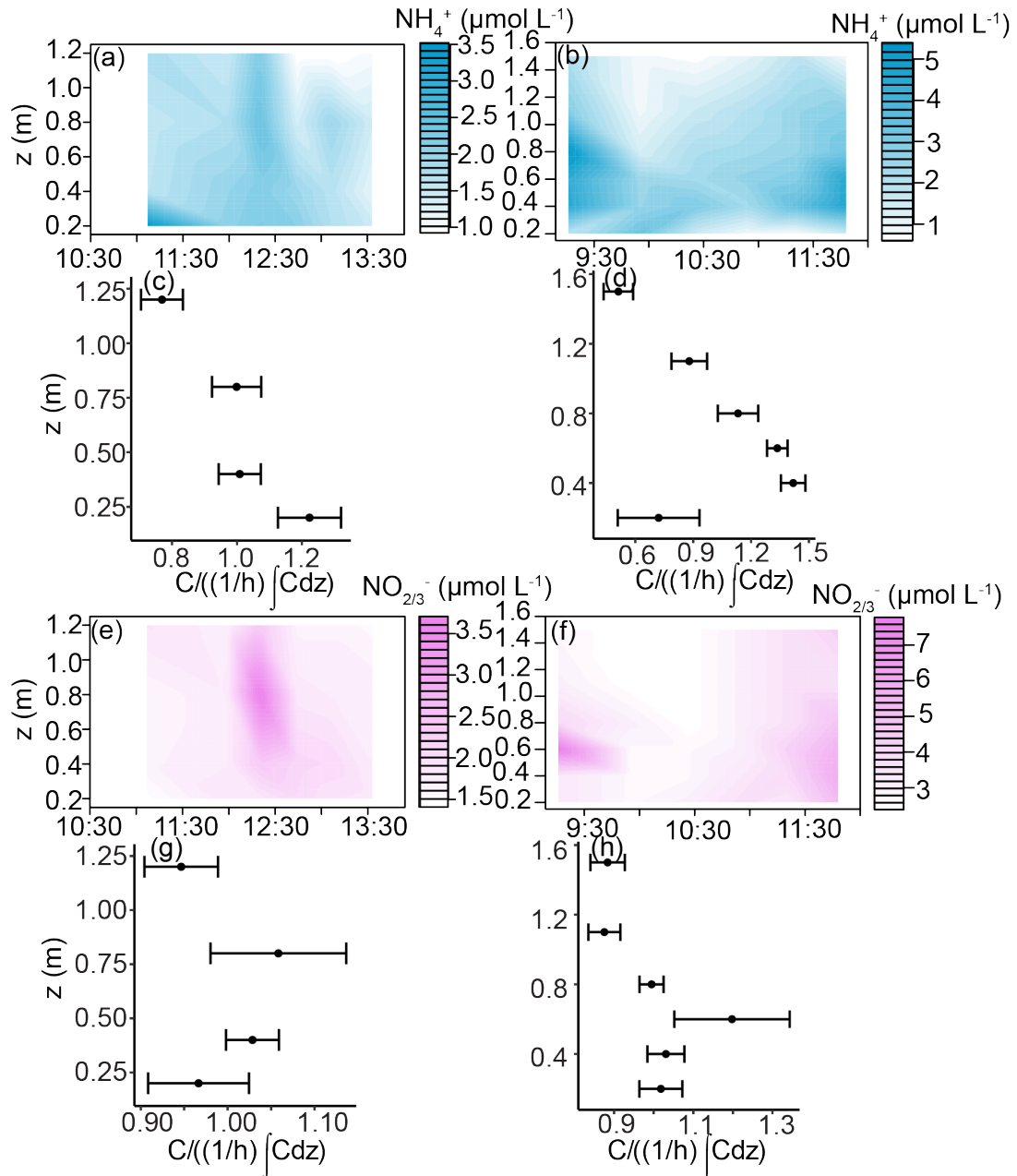


Fig. 3.7 Time series of NH_4^+ (a,b) and NO_x (e,f) during sampling, in June and August respectively. Ensemble-averaged dimensionless profiles from time series of NH_4^+ (c,d) and NO_x (g,h) in June and August respectively.

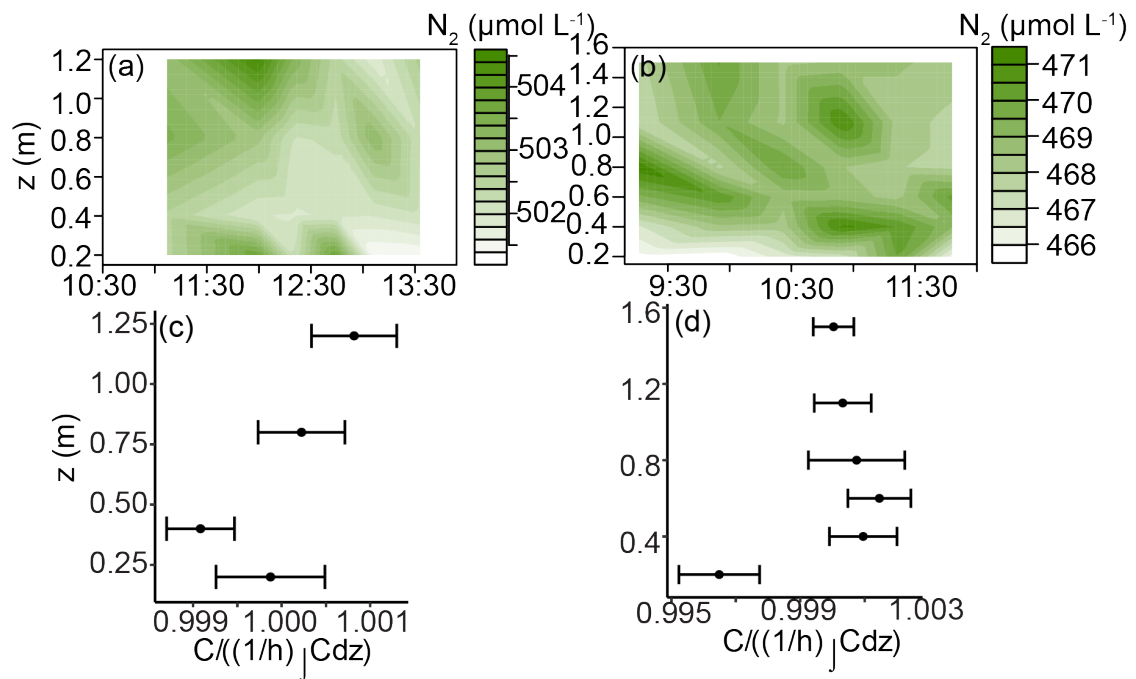


Fig. 3.8 Time series of N_2 concentrations during sampling in (a) June and (b) August. Ensemble-averaged dimensionless profiles from time series samples in (c) June and (d) August.

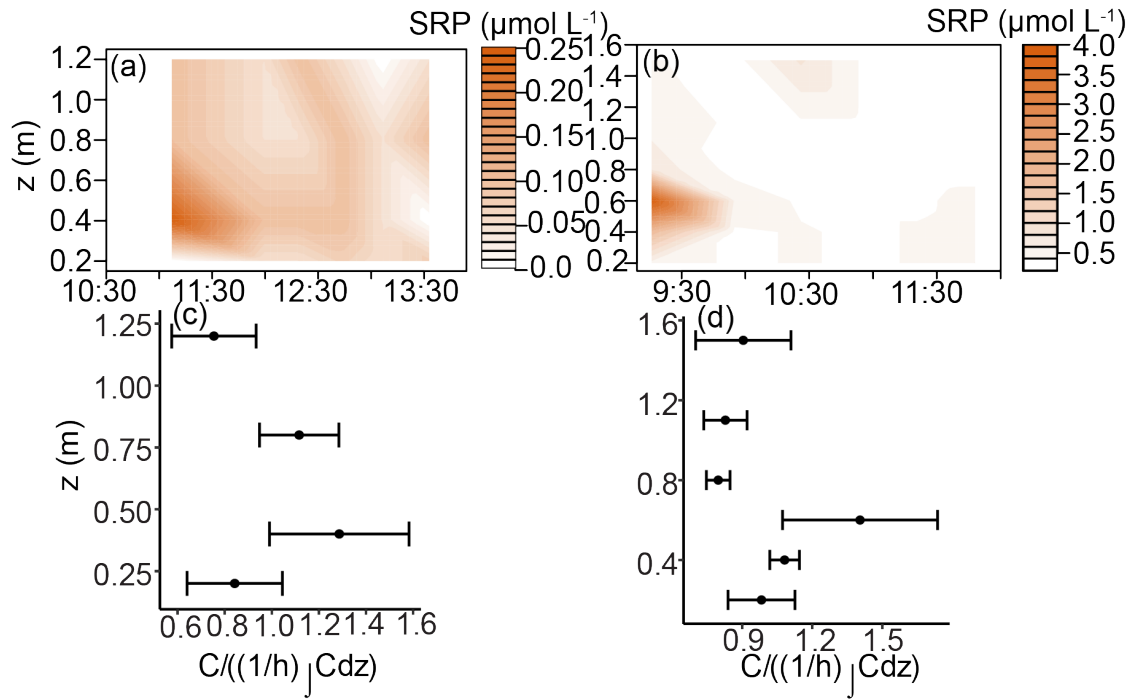


Fig. 3.9 Time series of SRP concentrations during sampling in (a) June and (b) August. Ensemble-averaged dimensionless profiles from time series samples in (c) June and (d) August.

Chapter 4: Impact of oyster aquaculture dredging on sediment biogeochemistry

Abstract

Oyster aquaculture has increased globally to counteract the overall decline of intertidal and subtidal oyster harvest reefs. Sustainability efforts to increase oysters in the Chesapeake Bay are of particular interest because oysters provide ecosystem services that may be applied as best management practices (BMPs) to reduce nitrogen inputs, which are the primary cause of eutrophication. Although observations have shown that aquaculture can stimulate higher rates of denitrification, it is unknown how on-bottom aquaculture and dredging influences sediment biogeochemistry. Our study compares biogeochemical fluxes from sediments that were just harvested in the morning, not harvested, and a reference site with no oysters. Cores were collected from an on-bottom aquaculture lease in the Nanticoke River, Maryland, USA during the months May, July, and September. Results show that denitrification was stimulated at the harvested sites during sampling in May and September, with an average increase relative to reference sites of 404% and 65%, respectively. Sediment oxygen demand increased on average at harvested sites relative to reference sites by 65%, 161%, and 18% in May, July, and September, respectively. Although harvested sites exhibited higher rates of denitrification, seasonal differences in rates were likely dependent on ambient nitrate concentrations and availability of labile organic matter.

Introduction

An estimated 32 percent increase in oyster aquaculture of the genus *Crassostrea* from the years 2010 to 2016 has helped continue to make aquaculture the fastest growing food production sector in the world (FAO UN 2018). Beyond market value, bivalve shellfish have been identified as providing ecosystem benefits of water clarity, habitat for associated organisms, nutrient sequestration, and denitrification (Newell et al. 2005; Coen et al. 2007; Cerco and Noel 2007; Grizzle et al. 2008; Kellogg et al. 2013). Despite growing interest in ecosystem services provided by aquaculture (van der Schatte Olivier et al. 2018), the impacts of aquaculture harvest on sediment biogeochemistry and water quality are poorly understood. For instance, oysters have been shown to stimulate denitrification (Jackson et al. 2018), whereas the concentration of biodeposits in environments with long residence times may hinder denitrification rates underlying aquaculture. At the same time, it is unknown how harvest practices may influence biogeochemistry other than that the harvest of oysters commonly involves bottom-disturbing gear that can cause damage to seafloor habitats (Lenihan and Peterson 2004). Therefore it is important to determine the role bottom harvest may have on determining denitrification rates.

Along with the expansion of molluscan aquaculture (e.g., oysters, scallops, and mussels) to approximately a quarter of the total global aquaculture harvest in 2016 (FAO UN 2018), there is an expectation that shellfish will support nitrogen remediation efforts by mitigating the effects of eutrophication (Bricker et al. 2018; Kellogg et al. 2013; Rose et al. 2014). Oyster aquaculture has direct and indirect interactions with water quality through removal of particulate N from the water-column and the subsequent

bioassimilation of some fraction of these nutrients in tissues (Higgins et al. 2011; Cornwell et al. 2016) and the deposition of biodeposits on sediments (Feinman et al. 2017; Lunstrum et al. 2017; Smyth et al. 2018). Depending on the physical and chemical conditions present surrounding oyster aquaculture operations, the deposition of biodeposits can have a range of ecosystem effects on underlying sediments (Testa et al. 2015). Under aerobic conditions, NH_4^+ generated by remineralization of biodeposits can be oxidized to support subsequent denitrification to N_2 (i.e., coupled nitrification-denitrification; (Henriksen 1988; Seitzinger 1988; Rysgaard et al. 1994; Newell et al. 2005). On the other hand, if deposition is highly focused over a portion of sediment, the sediments will become depleted with oxygen and will allow sulfide and NH_4^+ to accumulate, and will result in a decrease in N_2 fluxes (Kaspar et al. 1985; Asmus and Asmus 1991; Newell et al. 2002; Giles et al. 2006). Other than focusing organic matter to the benthos, suspension feeding bivalves can regulate biogeochemistry by providing a habitat for nitrifying and denitrifying bacteria on their shells and in their tissues (Welsh and Castadelli 2004; Stief 2013; Lunstrum et al. 2017). Bivalve aquaculture induced benthic-pelagic coupling on leases with floating and off-bottom cages has been well characterized (Testa et al. 2015; Humphries et al. 2016; Lunstrum et al. 2017; Smyth et al. 2018), however it is not well known how leased on-bottom aquaculture influences sediment biogeochemistry.

Another process that regulates the efficiency of denitrification is dissimilatory nitrate reduction to ammonium (DNRA). DNRA can be promoted when the availability of organic carbon increases, nitrate concentrations are low, and free sulfide (H_2S and S_2^-) concentrations in adhered sediments are high (Tiedje 1988; Burgin and Hamilton 2007;

Hardison et al. 2015). Studies addressing the competition for NO_3^- by DNRA relative to denitrification in aquaculture suggest that DNRA plays a small role in the overall nitrogen cycling (Smyth et al. 2018), but can make up at least 75% of NO_3^- reduction in sediment below aquaculture (Lunstrum et al. 2017). Although DNRA has been characterized in near-bottom bivalve aquaculture previously (Nizzoli et al. 2006; Lunstrum et al. 2017; Smyth et al. 2018), it is unknown whether DNRA or denitrification will dominate when aquaculture harvest practices disturb the sediments.

Dredging may cause a short-term acceleration of nutrient fluxes (Barnes 1991). Studies have compared chemical parameters between hydraulic dredged and non-dredged clam shellfish bottom (i.e., Kyte and Chew 1975; Meseck et al. 2014) to find few differences in water column chemistry. These studies were conducted using hydraulic dredges, which involve water jets. Contrastingly, dredges with toothed blades are commonly used in the Chesapeake Bay to harvest oysters from aquaculture. Aquaculture dredging will likely mobilize sediments and act as an anthropogenic bioturbation mechanism in the sediments. Based on knowledge that bioturbating organisms can enhance N removal by increasing the surface area of sediments across which oxidized and reduced solutes can be exchanged (Hargrave 1972), we expect that the toothed blades will also increase surface area and subsequent rates of denitrification. It is unknown how aquaculture dredging will influence sediment biogeochemistry and concurrent biogeochemical flux measurements from dredged and non-dredged oyster lease bottom have not been conducted.

Efforts to increase oyster aquaculture in the Chesapeake Bay are of particular interest because oysters may be applied as best management practices (BMPs) to reduce

nitrogen inputs (Cornwell et al. 2016). Anthropogenic nutrient loading is the primary cause of eutrophication in the Chesapeake Bay (Hagy et al. 2004; Kemp et al. 2005), and has been implicated in declines in submerged aquatic vegetation (Orth et al. 2017) and bottom water oxygen (Hagy et al. 2004). As an alternative process for mitigating nitrogen loading, oysters are approved as a BMP for nitrogen assimilated through feeding activities (Cornwell et al. 2016) and are being evaluated for denitrification enhancement (Cornwell, pers. comm.) High positive correlations between nitrogen content in oyster tissue and total shell length (Higgins et al. 2011) are appealing from a regulatory standpoint because they can be estimated from basic assessments of shell length. Quantifying the enhancement of denitrification on oyster aquaculture is considerably more challenging, given the spatial and temporal variability surrounding denitrification estimates (Rose et al. 2014), absence of *in situ* methods, and the incorporation of a representative benthic habitat in incubations. Similarly, the impact of aquaculture harvest practices must be fully understood to accurately characterize oyster aquaculture enhanced denitrification.

Based on the expansion of oyster aquaculture around the world, it is essential to understand the effects of on-bottom aquaculture and dredging on sediment biogeochemistry. The goal of this study was to determine how biogeochemical fluxes shift under bottom oyster aquaculture and dredging, and how fluxes may respond on a seasonal basis. Overall, we investigated the seasonal nitrogen cycling at an on-bottom oyster aquaculture lease from sites that: were harvested prior to sampling, that had not been harvested yet that season, and a reference adjacent to the planted lease. We hypothesized that sediments from within the aquaculture lease that were dredge would

have the highest rates of denitrification, whereas the unplanted site would have the lowest rates of denitrification. We expect that the presence of oysters on the bottom will increase organic matter accumulation and ultimately increase denitrification. In addition, dredging will mechanically bioturbate sediments and increase denitrification. Finally, we assessed the seasonal variability of the biogeochemical fluxes on the lease by taking samples during three different sampling months.

Methods

Study Site

Samples were collected from an oyster aquaculture lease in the Nanticoke River, the largest Chesapeake Bay tributary on the lower Delmarva Peninsula (Fig 4.1a). The water depth at the lease is about 1.5 m, with an average current speed of 0.5 m s^{-1} (NOAA Site 8571476, Roaring Point, MD). The Nanticoke River drains three counties in Maryland and two counties in Delaware. Land use in the watershed is made up of agriculture (40%), urban and suburban development (less than 2%), and forests (The Nature Conservancy 1994).

Sediment cores were collected from three different sites within and adjacent to an oyster aquaculture lease in the Nanticoke River. Triplicate sediment cores were collected from a site on-lease that was harvested the morning of sampling, on-lease that had not been harvested yet during the harvest season, and off-lease as a reference (Fig 4.1b). The harvested and non-harvested sites changed between sampling months because the farmer would rotate harvest each month, but the samples were close enough in distance that they were expected to represent the same habitat (i.e., harvested vs. non-harvested). Samples

were collected once during the months of May, July, and September. Mean density of oysters in the lease was 40 ind m⁻², but this varied depending on the time of the year. Background nutrient data from the Nanticoke River was obtained from Station ET6.2 (<http://data.chesapeakebay.net/WaterQuality>).

Core collection and incubation

Cores (6.35 cm I.D.) were collected using a pole corer, sealed with machined plastic lids fitted with O-rings and stoppers, and submerged in insulated coolers for transportation to the Horn Point Laboratory (<1 h). At the same time, a YSI (Quatro) measured ambient temperature, salinity, and oxygen conditions. Photosynthetically active radiation (PAR) was measured with LiCor (2□) sensors at the surface and 1 m depth. Water samples were collected from below the surface to measure water column respiration from the harvested, non-harvested, and reference sites. Triplicate dissolved inorganic carbon (DIC=[H₂CO₃]+[HCO₃⁻]+[CO₃²⁻]) samples were siphoned from BOD bottles 4 times every 4 hours and preserved with 10 µl of 50% saturated HgCl₂, tightly sealed, submerged in water, and held at or slightly below incubation temperature until analysis. Respiration rates were measured as differences in DIC between initial and final samples divided by incubation times.

At the laboratory, cores were placed in a temperature-controlled walk-in chamber at ambient temperature conditions and submerged in incubation tanks filled with ambient water from the Nanticoke River. Two empty core tubes were filled with ambient water and a stopper at the approximate sediment depth height as blanks. Cores were aerated with individual “T” bubblers made of PVC (Owens and Cornwell 2016) overnight (>12

hrs). Flux incubations began once cores were sealed with machined plastic lids with an O-ring and Teflon-coated magnetic stirrer turned by an external magnetic turntable. Solutes (NH_4^+ , $\text{NO}_2^- + \text{NO}_3^-$, SRP) and gas (O_2 , N_2 , Ar, DIC) samples were collected immediately after chambers were sealed and every ~60 minutes over a period of ~4 h. As shown by PAR measurements, the Nanticoke River is very turbid, therefore cores were not incubated in the light (Table 4.1). Solute samples were filtered through a 0.45 mm pore-size filter and kept frozen for analysis. N_2 , O_2 , and Ar were stored in glass tubes, preserved with 10 μl of 50% saturated HgCl_2 , and were measured on a membrane-inlet mass spectrometer (Kana et al. 1994) within 2 weeks of collection. DIC samples were preserved as described previously and measured on an infrared-based analyzer with a calibration coefficient of variation that ranged from 0.07 to .15 % with an average standard deviation of $\pm 7.45 \mu\text{mol l}^{-1}$ (Apollo SciTech; Cai and Wang 1998).

Fluxes were calculated by obtaining a slope from the regression of gases and nutrients versus time. Slopes with an $R^2 \geq 0.80$ were considered significant fluxes (Cornwell et al. 1999). Effects of water column processes were removed by subtracting a significant water blank slope from sample flux slopes. Areal fluxes (F ; $\mu\text{mol m}^{-2} \text{hr}^{-1}$) were determined using Eqn. 1:

$$F = \frac{\Delta C}{\Delta t} * \frac{V}{A} \quad (1)$$

where $\Delta C/\Delta t$ is the slope ($\mu\text{mol L}^{-1} \text{hr}^{-1}$), V is the volume of the water overlying sediment (L), and A is the area of the core (m^2).

Cores were incubated a second time similar to (Nizzoli et al. 2006). The isotope pairing technique (IPT) was applied with $^{15}\text{NO}_3^-$ added to assess denitrification (Nielsen 1992) and DNRA with a version of the OX/MIMS technique (Yin et al. 2014; Lunstrum

et al. 2017). Denitrification was determined based on ratios of $N_2:Ar$ in the first incubation (Kana et al. 1994) and the production of $^{29}N_2$ and $^{30}N_2$ in the second incubation (Nielsen 1992), whereas DNRA rates were derived from the production of $^{15}NH_4^+$.

Prior to the second incubations, all cores were bubbled again for 1 h, excluding one core from each sampling site which were used for pore water and solid-phase analyses. A sample was pulled from the water bath incubation tanks to measure initial NO_3^- concentrations and a solution of $^{15}N-NaNO_3$ (98 atm%) was added to reach a final concentration of $\sim 20 \mu mol L^{-1}$. The water overlying the cores was stirred for 20 min to allow the addition of ^{15}N to reach the sediment surface (Steingruber et al. 2001). Once the cores were capped, T_0 water column samples were collected for $^{29}N_2$ and $^{30}N_2$ IPT measurements and preserved with 10 μl of 50% saturated $HgCl_2$ and stored under water prior to analysis. After ~ 4 hr, cores were uncapped and subsamples of sediment and water column were taken with a 2.6 cm ID cutoff syringe (Nizzoli et al. 2006; Lunstrum et al. 2017). The sample was mixed with powdered KCl to reach a 2N solution to extract NH_4^+ and kept frozen for analysis. Cores were stirred gently with a rod to allow for the collection of all $^{29}N_2$ and $^{30}N_2$ produced in the core (Steingruber et al. 2001), and after 60s T_f samples were collected and preserved with 10 μl of 50% saturated $HgCl_2$.

Gas ratios were measured a second time using the MIMS with an in-line furnace and copper reduction column heated to $600^\circ C$ to remove O_2 to determine $^{29}N_2$ and $^{30}N_2$ from T_0 and T_f samples (Lunstrum and Aoki 2016). Eqn. 1 was used to determine areal production of $^{29}N_2$ and $^{30}N_2$, and the standard IPT equations were used to calculate denitrification of added $^{15}NO_3^-$ (D15) and ambient NO_3^- (D14; Nielsen 1992). Given that

IPT equations require anammox is not a significant source of N₂, we assumed that anammox was minimal in the Nanticoke River based on knowledge that it occurs in ecosystems with little labile carbon (Burgin and Hamilton 2007).

DNRA rates were determined based on a version of the OX/MIMS technique (Yin et al. 2014; Lunstrum et al. 2017). The OX/MIMS technique measures the production of N₂ following the oxidation of NH₄⁺. The KCl slurry samples were mixed on a shaker table for 30 min, filtered with a 0.45-μm pore size filter to remove particulates, and stored in gas-tight glass vials. Alkaline hypobromite iodine solution (0.2 ml) was added to one of each sample pair to oxidize ¹⁵NH₄⁺ to ³⁰N₂ or ²⁹N₂. Following measurement on the MIMS with in-line furnace, the un-oxidized sample was subtracted from the oxidized sample to determine the production of ³⁰N₂ or ²⁹N₂ from the oxidation of ¹⁵NH₄⁺. Eqn. 1 was used to determine production rates of ²⁹N₂ ($p(^{29}N_2)$) and ³⁰N₂ ($p(^{30}N_2)$). In addition, DNRA from the addition of ¹⁵NO₃⁻ (DNRA₁₅) was calculated based on Eqn. 2.:

$$DNRA_{15} = p(^{29}N_2) + 2p(^{30}N_2) \quad (2)$$

In situ DNRA (DNRA₁₄) was found using Eqn. 3, with the assumption that the ratio of ¹⁵NO₃⁻ and ¹⁴NO₃⁻ used by denitrification would be the same for DNRA (Risgaard-Petersen and Rysgaard 1995):

$$DNRA_{14} = DNRA_{15} \times \frac{D_{14}}{D_{15}} \quad (3)$$

Pore water was collected from three cores, one from the three different sampling sites, on each sampling date. Overlying water was siphoned off the sediment cores and a mini-corer (1.4 cm I.D.) was used to collect the upper 1 cm of sediment for chlorophyll *a* and frozen for later analysis. Cores were extruded under N₂ and the upper 0.5 cm was placed in 50 ml centrifuge tubes, centrifuged for 10 minutes at 3500 rpm, and the supernatant

was filtered with 0.45 μm filters for dissolved sulfide ($\Sigma\text{H}_2\text{S}$: H_2S , HS^- , S^{2-}). Mixed diamine reagent (10 μl) was added to 1 ml of dissolved sulfide samples to fix samples prior to analysis (Cline 1969). The upper 2 cm of sediment was removed from one core from each sampling site for the determination of sediment organic matter (SOM). Sediments were dried for at least 24 h at 60°C then combusted at 525°C for 4 h. The weight of the combusted sample was subtracted from the dried sample and subsequently divided by the total sediment mass to produce SOM (%). Sediment grain size distribution was determined from the upper 2 cm of three cores from each site during the months of May and July (Sweet 1993).

Statistical Analysis

All statistical analyses were performed in R 3.1 (R Development Core Team 2013). Two-way analysis of variance (ANOVA) tested for statistical differences between sampling sites for all benthic fluxes measured, with sampling site type and date as fixed factors, to account for seasonal variability. Tukey HSD tests were applied to assess main effects of differences between sites when site by date interactions were insignificant. One-way ANOVA and Tukey HSD post hoc tests were used when interaction was significant to test the main effect of sites for individual sampling dates. Significance level for all tests was set at $\alpha=0.05$ and homogeneity of variance was established by Levene's test.

Results

Environmental Conditions

Temperatures in the Nanticoke River ranged from 18.5 to 26.2°C, with highest temperatures in July and September (Table 4.1). Salinity varied by 4 units over the course of study, with the lowest salinity measured in July. Light attenuation coefficients (k_d) remained relatively consistent, and the highest coefficient was observed in July.

Table 4.1 Physical and chemical properties of the location of sediment core collection on the aquaculture lease.

	Sampling date		
	May	July	September
Salinity	12.9	8.4	11.3
Temperature (°C)	18.5	26.1	25.6
Irradiance ($\mu\text{mol photons m}^{-2} \text{s}^{-1}$)			
Subsurface	807	1067	400
Depth of 1 m	159	86.3	38
Light attenuation coefficient (k_d)	1.62	2.51	2.35
Irradiance at bottom	98.2	40.8	18.8
Ambient NO_x (μM)	21.2	2.51	0.60

Based on chemical properties recorded at Station ET6.2, concentrations of nitrogen and algal biomass (chlorophyll *a*) varied substantially over time (Table 4.2). NO_x concentrations ranged from a maximum of 24.32 μM in June to a minimum of 0.11 μM in August. Similarly, NH₄⁺ concentrations decreased from 4.22 μM in June to 0.22 μM in September. Concentrations of chl *a* ranged from 9.61 to 32.04 μg L⁻¹. The minimum dissolved oxygen concentration in 2018 was recorded in June (5.20 mg L⁻¹) and steadily increased into October.

Table 4.2 Chemical properties from the surface (0.5 m) and bottom water (3 m) from Station ET6.2 (<http://data.chesapeakebay.net/WaterQuality>) measured from May to October.

Month	Chl (μg/L)		DO (mg/L)		NH ₄ ⁺ (μmol/L)		NO _x (μmol/L)	
	surface	bottom	surface	bottom	surface	bottom	surface	bottom
May	9.61	9.61	6.70	6.00	1.28	2.28	17.92	12.69
June	6.41	5.87	5.20	5.10	4.22	4.22	24.32	25.92
July	19.94	16.55	7.20	6.40	0.61	0.72	0.25	0.64
August	32.04	23.50	6.60	5.80	0.61	1.72	0.11	0.12
September	20.29	17.44	7.80	7.20	0.22	0.50	1.24	1.17
October	13.88	16.38	9.10	8.90	1.06	0.50	4.66	4.67

Sediments at the harvested sites consisted of mostly sand with percentages ranging from 53.4±0.1 in May to 41.9±9.2 in July (Table 4.3). Similarly, the non-harvested sediments were mostly composed of sand (55.4±7.0 and 50.3±5.8% in May and July, respectively). Sediments at the control sites consisted of mostly sand and silt with percentages of sand ranging from 36.9±2.5 to 51.3±4.% and silt ranging from 34.3±4.4 to 46.5±4.5%. In the top 2 cm, SOM was highest at the harvested site (7.49%) and lowest at

the non-harvested site (0.67%). Benthic Chl varied across the three sites, but was lowest during the month of July (Table 4.3). Across the three sites, water column respiration rates did not show an obvious pattern (Table 4.4).

Table 4.3 Sediment characteristics from the control, non-harvested, and harvest sites during May, July, and September. Data are recorded as means \pm SE. n.d. indicates that samples were compromised.

	Control			Non-harvested			Harvested		
	May	July	Sept.	May	July	Sept.	May	July	Sept.
Sand (%)	36.9 \pm 2.5	51.3 \pm 4.1	n.d.	55.4 \pm 7.0	50.3 \pm 5.8	n.d.	53.4 \pm 0.1	41.9 \pm 9.2	n.d.
Silt (%)	34.3 \pm 4.4	46.5 \pm 4.5	n.d.	33.7 \pm 1.5	44.0 \pm 8.8	n.d.	25.9 \pm 7.1	37.3 \pm 1.0	n.d.
Clay (%)	28.8 \pm 3.9	2.2 \pm 1.1	n.d.	10.8 \pm 6.5	5.7 \pm 10.3	n.d.	20.7 \pm 1.7	20.8 \pm 8.3	n.d.
SOM (%)	n.d.	2.89	1.38	0.95	0.67	3.08	1.31	7.49	1.71
Benthic Chl (mg m ⁻²)	14.7	3.04	6.43	14.79	8.09	13.91	5.57	4.35	14.7
H ₂ S (μ M)	98.47	222.5	95.0	94.8	335.0	135.0	113.3	112.5	210.0

Table 4.4 Water column respiration measured during May, July, and September. Rates were determined based on regression.

Month	Site	Respiration ($\mu\text{mol l}^{-1} \text{hr}^{-1}$)	R-squared
May	harvest	0.34	0.87
	nonharvest	0.21	0.83
	control	0.66	1.00
July	harvest	0.36	0.99
	nonharvest	-0.05	0.33
	control	0.02	0.01
September	harvest	0.94	0.85
	nonharvest	1.27	0.83
	control	0.44	0.74

Biogeochemical fluxes

Oxygen fluxes were significantly different between sites ($p < 0.001$) and sampling month ($p < 0.001$), but did not show a significant site by month interaction ($p = 0.108$; Table 4.5, Fig. 4.2a). Other than during sampling in September, oxygen demand was the highest at the harvested sites, with an average rate of $3095 \pm 609 \mu\text{mol m}^{-2} \text{h}^{-1}$ observed in

May. The harvested site was statistically different from the control and nonharvested sites (Tukey HSD, Harvest*Control $p=0.012$; Harvest*Nonharvested $p=0.042$), but the nonharvested and control sites were not statistically different from each other (Tukey HSD, Nonharvested*Control $p=0.86$). DIC-based respiration fluxes did not have a significant site by month interaction ($p=0.117$; Table 4.5, Fig. 4.2b). In addition, there were no significant differences between sites or months ($p=0.317$ and $p=0.240$, respectively). DIC fluxes were highest at the control site in May ($3713\pm580 \mu\text{mol m}^{-2} \text{h}^{-1}$), otherwise fluxes remained fairly constant across the sites and sampling dates.

NH_4^+ fluxes were significantly different between sampling months ($p=0.001$), but were not significantly different between sites ($p=0.131$; Table 4.5, Fig. 4.3a). There was no significant site by month interaction for NH_4^+ fluxes ($p=0.95$). During sampling in May and September, NH_4^+ fluxes were directed into the sediment, whereas fluxes from all sites in July were directed to the water column. NH_4^+ fluxes were elevated at the harvested site in July and were less negative in May and September, with average rate of $94.9\pm29.1 \mu\text{mol m}^{-2} \text{h}^{-1}$ measured in July. Although NO_x fluxes were not significantly different between sampling sites or months ($p=0.350$ and $p=0.280$, respectively), there was a significant site by month interaction ($p<0.001$; Fig. 4.3b). NO_x fluxes from harvested and nonharvested sites were significantly different from control sites in May and September (Tukey HSD ranging from $p=0.017$ to $p=0.033$). NO_x fluxes from nonharvested and harvested sites were not significantly different from each other on all dates (Tukey HSD ranging from $p=0.538$ to $p=0.980$). The control site had the highest NO_x fluxes in May and July, with average rates of 158.2 ± 37.0 and $56.2\pm30.1 \mu\text{mol m}^{-2} \text{h}^{-1}$

¹, respectively. However, the nonharvested and harvested sites had the highest NO_x fluxes in September (102.4±30.5 and 107.8±32.9 μmol m⁻² h⁻¹, respectively).

Denitrification rates had a significant sampling site by month interaction, with higher rates at the harvested site in May and September ($p < 0.001$; Table 4.5, Fig. 4.3c). Denitrification rates from the harvested site were significantly higher than the control and nonharvested sites in May and September (Tukey HSD ranging from $p < 0.001$ to $p = 0.016$). The harvested site had the highest denitrification rates in May, with the average rate more than double the nonharvested site. In May, the majority of denitrification was supported by NO₃⁻ in the water column (Fig. 4.4a). Other than the control site in September, coupled nitrification-denitrification consistently supplied NO₃⁻ during all sampling times with rates ranging from 7.5±2.5 to 33.8±10.2 μmol m⁻² h⁻¹. NO₃⁻ was also reduced via DNRA with average rates ranging from 0 to 29.4±7.7 μmol m⁻² h⁻¹ (Fig. 4.4b). Rates of DNRA were highest at the nonharvested sites in May and July, however rates were highest at the control sites in September.

SRP fluxes were significantly different between sampling months ($p = 0.001$), but were not significantly different between sites ($p = 0.713$; Fig. 4.5). Overall SRP fluxes were low, with the highest rates observed in September. In September, the harvested and control sites had the highest SRP fluxes ranging from 12.7±4.0 to 19.9±10.2 μmol m⁻² h⁻¹, respectively.

Discussion

Biogeochemical fluxes of N₂, O₂, and NO_x from sediments within an aquaculture lease varied depending on whether the site had been planted with shell and spat on shell,

as well as the occurrence of aquaculture dredging. Denitrification rates were stimulated by aquaculture dredging activities and mediated by nitrate concentrations in the water column and the availability of algal biomass (Table 4.5, 4.2, Fig. 4.3c). Increases in denitrification at the harvested sites in July coincided with higher rates of sediment oxygen demand (Figure 4.2a). Meanwhile, fluxes of NO_x were variable depending on whether NO_x consuming processes, such as denitrification, DNRA, and/or benthic assimilation, exceeded sediment NO_x availability.

A growing body of literature has reinforced the idea that bivalves enhance the transportation of organic carbon and nitrogen to sediments, which increases sediment oxygen demand and ultimately stimulates direct or coupled denitrification (Newell et al. 2002; Newell et al. 2005; Hoellein et al. 2015; Smyth et al. 2015; Lunstrum et al. 2017; Smyth et al. 2018). Oxygen demand did not significantly differ between the control and nonharvested sites, likely due to the potential dispersion of biodeposits with high local flows. Previous studies below rack and bag oyster aquaculture have found oxygen demands approximately double those observed at control sites (Lunstrum et al. 2017). In addition, high oxygen demands from clam aquaculture have been linked not only to deposition of organic matter but respiration from including clams in incubations (Murphy et al. 2016). Moreover, the significant differences between oxygen demand at harvested and nonharvested sites indicate that dredging increased oxygen demand by exposing sediment anoxia and stimulating organic matter oxidation (Table 4.5). DIC-based respiration rates did not differ significantly across the sites, suggesting that mineralization rates were not impacted by planting of spat on shell or aquaculture dredging; however,

we do expect a different result upon the inclusion of oysters in incubations based on their respiration.

Prior analysis of oyster reefs (Hoellein et al. 2015; Smyth et al. 2015; Smyth et al. 2018) and bivalve aquaculture (Lunstrum et al. 2017; Smyth et al. 2018) support the emerging consensus that bivalve-associated denitrification is modulated by NO_x concentrations. Enhanced diffusion of water column NO_x in oyster reef-adjacent sediments has been observed (e.g., (Hoellein et al. 2015; Smyth et al. 2015). Previous work focusing on denitrification of added $^{15}\text{NO}_3^-$ to sediments from a rack and bag aquaculture setting suggests that sediments under oyster bags may be effective at removing pulses of NO_3^- (Lunstrum et al. 2017; Smyth et al. 2018). Similarly, observations of increased denitrification rates at clam aquaculture sites compared to bare sediments following additions of NO_3^- have revealed that denitrification associated with bivalve aquaculture was NO_3^- limited (Smyth et al. 2018). Water column concentrations of NO_x are known to regulate N_2 -N exchange (Kemp et al. 1990) in bare, subtidal sediment, and these results indicate that water column NO_x concentrations also play a role in determining how aquaculture dredging impacts sediment biogeochemistry.

Not only did aquaculture plantings and dredging affect N transformations, but fluxes tended to vary seasonally. For example, harvested sites had the highest NH_4^+ efflux in July and reduced NH_4^+ uptake in May and September (Fig. 4.3a), corresponding to higher surface sediment chlorophyll *a* during those sampling months (Table 4.3). As ambient NO_x concentrations decreased from May to July, the percentage of denitrification supported by NO_x from nitrification increased (Fig. 4.5a). These results are consistent with comparisons of seasonal net NO_x and N_2 fluxes (Fig. 4.4b,c). In May,

consumption of NO_x agreed with increased rates of denitrification, whereas discrepancies in sediment uptake of NO_x and net denitrification observed in July and September were likely associated with more coupled nitrification-denitrification. Aquaculture activities appeared to only impact denitrification rates in May and September, whereas rates in July remained the same across sites likely due to low NO_x and algal biomass. In addition, the accumulation of surface porewater H_2S in July may have promoted DNRA over denitrification, but this was not obvious from the DNRA data (Table 4.3, Fig. 4.4b; (Burgin and Hamilton 2007; Hardison et al. 2015).

Across the east coast of the United States, aquaculture activities have been recognized for their enhancement of nitrogen cycling, yet site and methodological differences result in varying ranges. The highest NH_4^+ flux observed at the harvested site ($145 \mu\text{mol m}^{-2} \text{h}^{-1}$) was less than half the average flux observed from rack and back sites by Lunstrum et al. (2017) during similar times of the year. Incubations of cores from below a floating oyster aquaculture lease on the Choptank River, MD yielded NH_4^+ fluxes that were approximately 2-fold larger than those observed from the Nanticoke (Testa et al. 2015). Even though flux ranges were different between these studies, NH_4^+ fluxes consistently increased following aquaculture activities in all cases. Assessments by Smyth et al. (2017) and Lunstrum et al. (2017) in the lower Chesapeake also found NO_3^- fluxes that were on average more than ten-fold lower than those observed in the Nanticoke. An average NO_x flux of $-19.6 \mu\text{mol m}^{-2} \text{h}^{-1}$ was collected from work by (Testa et al. 2015) with samples collected from below floating aquaculture. Despite the low NO_x fluxes observed by Lunstrum et al. (2017) and Smyth et al. (2018), average denitrification rates were more than 6-fold higher in the Nanticoke than the lower Chesapeake Bay.

Stimulation of denitrification rates by bivalve aquaculture activities are consistent with field measurements by Testa et al. (2015), Humphries et al. (2016), Lunstrum et al. (2017), Vieillard (2017), and Smyth et al. (2018). The enhanced denitrification rates observed at nonharvested and harvested sites in May were slightly lower than those reported from sediments below oyster aquaculture suspended mesh bags in Ninigret Pond, RI ($346.1 \pm 168.6 \mu\text{mol m}^{-2} \text{h}^{-1}$; (Humphries et al. 2016). Likewise, Testa et al. (2015) describe similar ranges from a farm site and near-farm site (55.8 ± 20.8 and $72.8 \pm 21.4 \mu\text{mol m}^{-2} \text{h}^{-1}$, respectively). These responses are comparable to those shown by Vieillard below oyster aquaculture lantern nets in Fishers Island, NY during summer months (Vieillard 2017). However, based on discrepancies in denitrification rates in our study using the $\text{N}_2:\text{Ar}$ and IPT methods (Fig. 4.3c and 4.4a) and low rates from previous studies using the IPT method (e.g., Lunstrum et al. 2017; Vieillard 2017; Smyth et al. 2018), we can expect the IPT method to provide slightly lower more conservative rate estimates (Eyre et al. 2002). In the Chesapeake Bay, there is one example of an aquaculture facility that did not experience an increase in denitrification rates following enhanced biodeposition (Higgins et al. 2013), which may be attributed to previously anoxic sediments and low flows. Differences in nitrogen fluxes across studies were most likely due to environmental conditions, such as dispersion of organic matter, temperature, and ambient nutrients.

Implications

An extensive review of bivalve aquaculture by van der Schatte Olivier (2018) has estimated that the value of global ecosystem services provided by bivalve aquaculture

total \$30.39 billion. This value only includes the nitrogen and phosphorus remediation from the biomass removed at harvest (van der Schatte Olivier et al. 2018). Bivalve nutrient offset schemes are in use in Denmark and Sweden (Petersen et al. 2014) and oyster-associated enhanced nitrogen removal is being considered for approval as BMPs in the Chesapeake Bay (Cornwell et al. 2016). Before recommendations can be made, an improved understanding of the environmental variability that modulates aquaculture stimulated denitrification is required. With the addition of denitrification to nutrient offset schemes or BMPs, bivalve aquaculture has the potential to increase the value of the aquaculture industry globally (van der Schatte Olivier et al. 2018).

Given the global trends in bivalve aquaculture production, these findings have implications for aquaculture methodology and eutrophication management. Understanding that oysters and aquaculture gear types influence sediment biogeochemistry has consequences for denitrification efficiency. Harvest during certain times of the year, when NO_x concentrations are high, may more effectively remove nitrogen. This work demonstrates that harvesting techniques matter to biogeochemistry, because on-bottom aquaculture harvest may support more denitrification than floating caged aquaculture due to the direct supply of biodeposits from oysters on the bottom. Compared to floating cages, aquaculture dredging bioturbates sediments and ultimately increase nitrogen removal during certain environmental conditions.. Although dredging stimulated denitrification during some sampling periods, managers must keep in mind that dredging has other ecological impacts, such as mortality of non-target species, destruction of suitable habitat, and suspended sediments (Kaiser et al. 1998; Wilber and Clarke 2001). The fact that oysters stimulate denitrification through increased

biodeposition and sediment oxygen demand must be combined with knowledge of how aquaculture gear types may interact with the environment.

Table 4.5 Benthic fluxes statistical results based on two-way and one-way ANOVAs.

	Oxygen demand			DIC			NH4+			Nox			Denitrification			SRP		
	df	F	p	df	F	p	df	F	p	df	F	p	df	F	p	df	F	p
Two-way																		
Anova																		
Site	2	10.9	<0.001	2	1.2	0.317	2	2.22	0.131	2	1.064	0.35	2	19.65	<0.001	2	0.342	0.713
Month	2	16.34	<0.001	2	1.51	0.24	2	8.838	0.001	2	1.322	0.28	2	18.39	<0.001	2	8.25	0.001
Interaction																		
(Month																		
*Site)	4	2.1	0.108	4	2.06	0.117	4	0.167	0.95	4	6.905	<0.001	4	10.62	<0.001	4	1.78	0.16
One-way																		
Anova site																		
May										2	6.57	0.021	2	15.29	0.001			
July										2	0.692	0.525	2	0.018	0.983			
September										2	6.54	0.017	2	16.27	0.001			

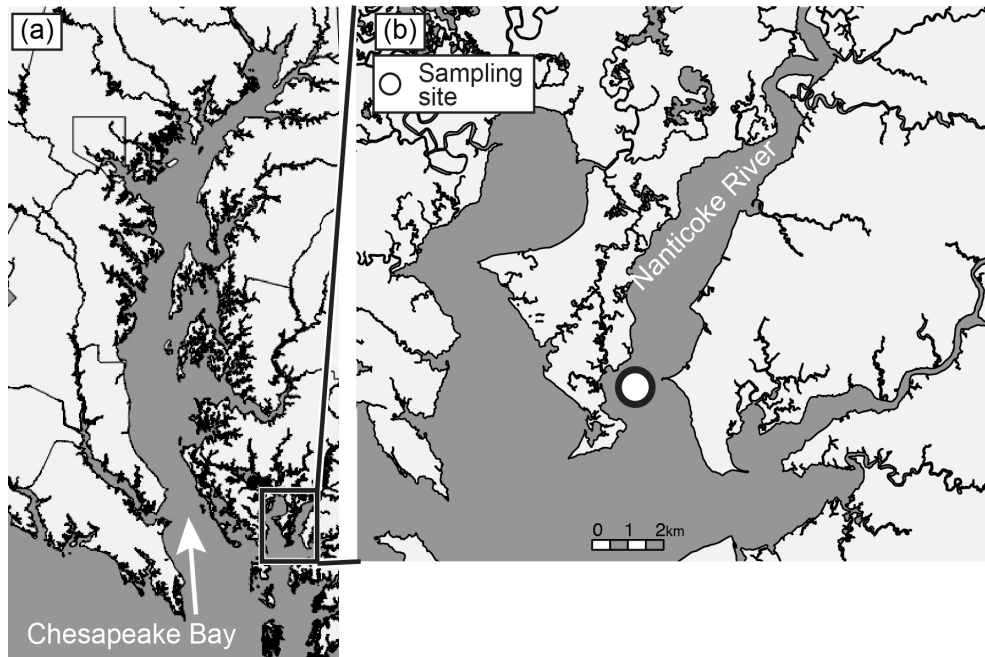


Fig. 4.1 Map of study area showing (a) the Nanticoke River a tributary to the Chesapeake Bay and (b) the location of the sampling site (○) within the Nanticoke River.

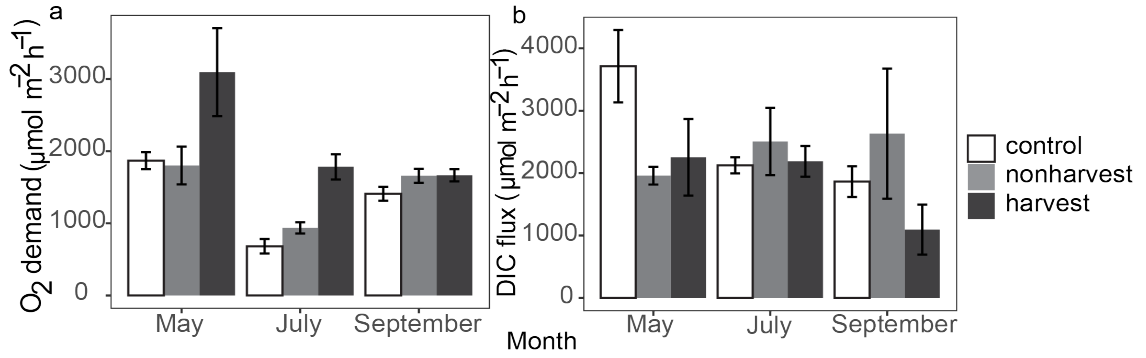


Fig. 4.2 Respiration-based sediment fluxes of (a) oxygen (i.e. sediment oxygen demand) and (b) DIC. Mean \pm SE (n=4). Asterisks indicate significant differences between sampling sites for each month (one-way ANOVA, $\alpha=0.05$).

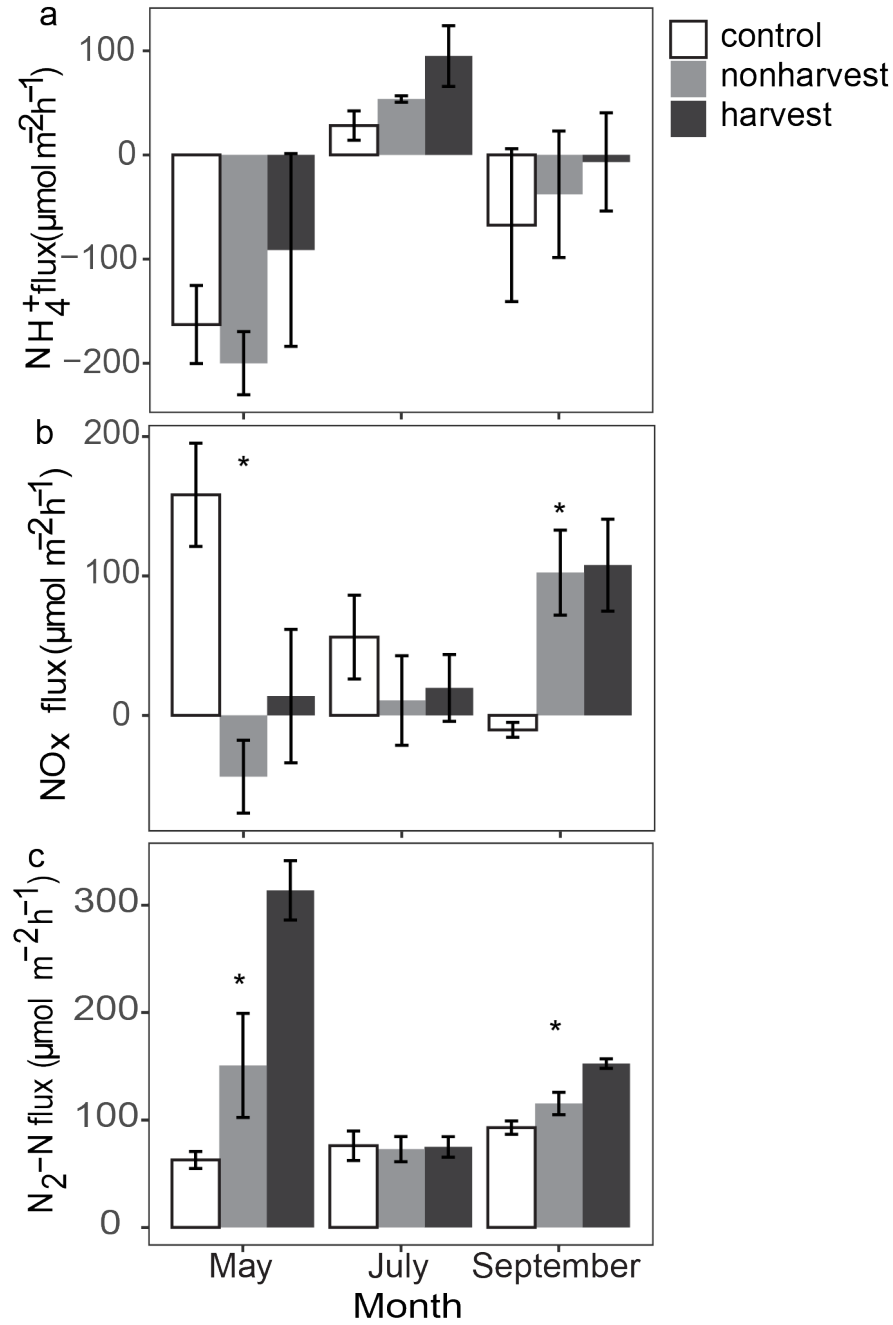


Fig. 4.3 Sediment fluxes of (a) NH_4^+ , (b) NO_x , and (c) N_2 . Mean \pm SE (n=3-4). Asterisks indicate significant differences between sampling sites for each month (one-way ANOVA, $\alpha=0.05$).

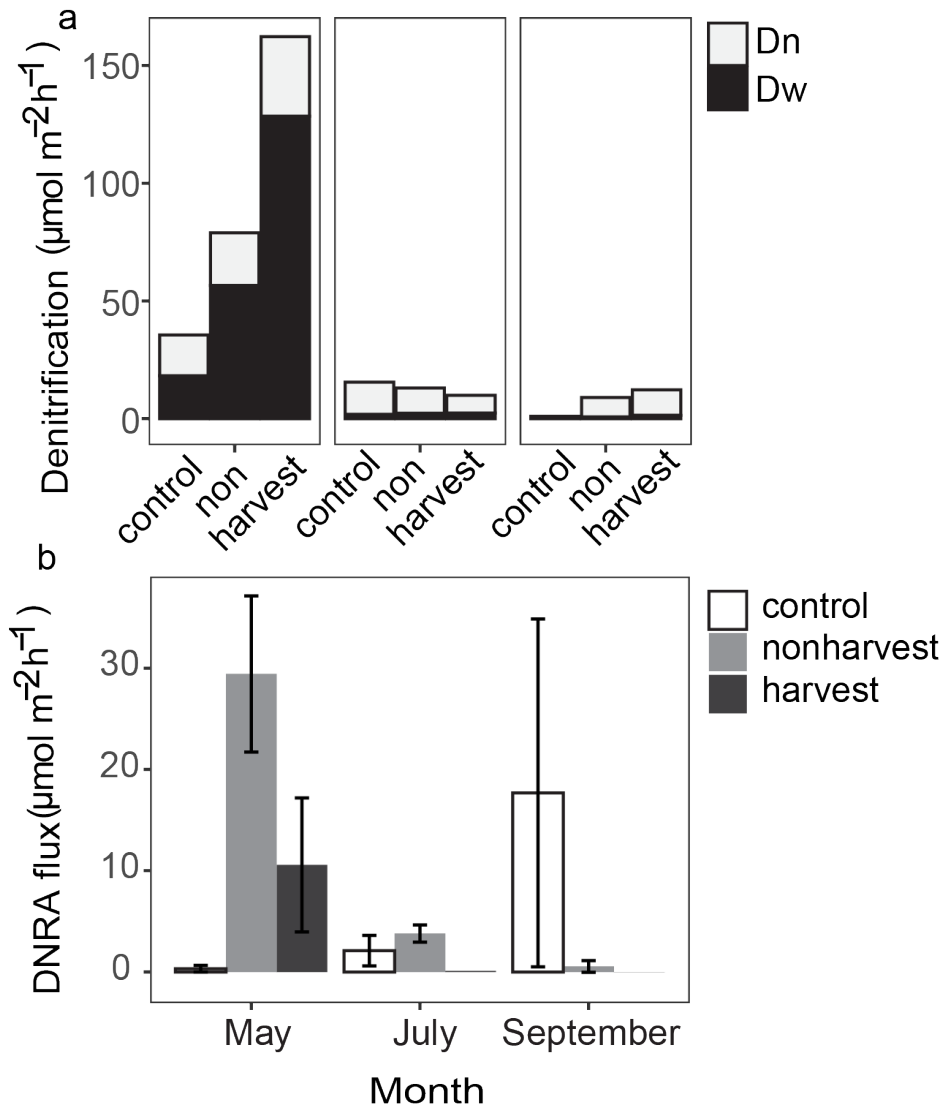


Fig. 4.4 Sediment fluxes of (a) direct denitrification (Dw) and coupled nitrification-denitrification (Dn) and (b) DNRA. Mean \pm SE (n=3).

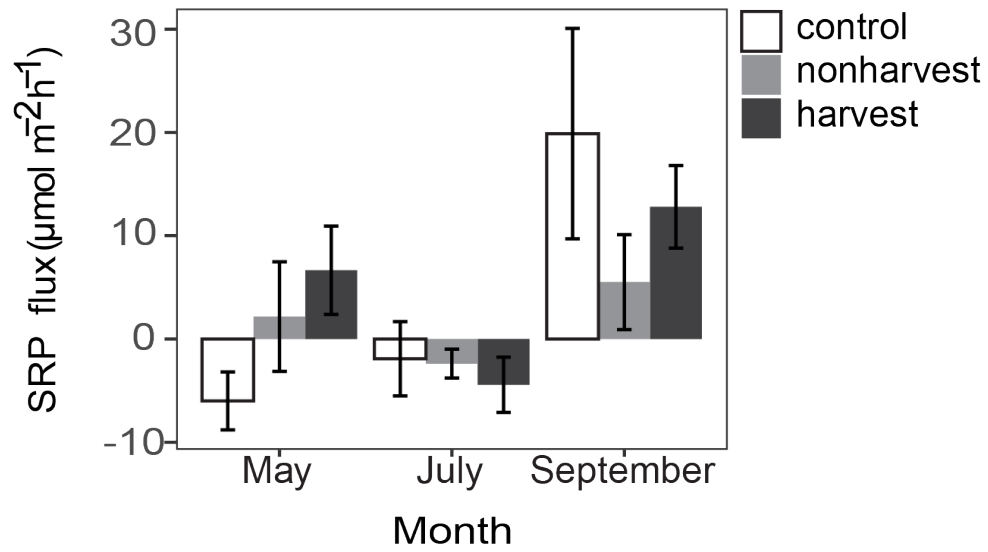


Fig. 4.5 SRP fluxes from sediment collected from harvested, non-harvested, and control sites. Mean \pm SE (n=3-4).

Chapter 5: The effect of oyster year-class on biogeochemistry

Abstract

Around the world, there is growing interest in using bivalves for ecosystem services, such as nitrogen removal via harvest and microbial denitrification of the nitrogen in biodeposits. In this study, we assessed whether there are differences in denitrification rates across a range of oyster year-classes by measuring biogeochemical fluxes from different oyster year-classes reared and harvested from an on-bottom aquaculture lease during the months of May, July, and September. We found that over the course of May-September, oyster biomass declined for a given length, oxygen demand increase, and DIC fluxes increased for larger oysters, confirming that adult oysters were undergoing physiological changes over the course of the season. Oyster biomass and length were positively correlated with denitrification rates during May and September, but the relationship was the opposite in July. Shifts in ambient NO_x concentrations in May, July, and September (13.6 ± 1.3 , 6.2 ± 1.8 , and 22.2 ± 4.9 μM , respectively) were followed by shifts in denitrification rates, with the higher rates observed in May and September. Overall, larger oysters supported higher rates of denitrification, but rates were constrained by ambient NO_x concentrations. Similar to nitrogen assimilation relationships to oyster size, these data may be used by Bay managers to evaluate whether oyster-associated nitrogen removal via denitrification can be quantified based on the total shell length.

Introduction

Over the last half-century, an estimated 85% decline in oyster reefs around the world has coincided with a recent 32% increase in total aquaculture production of *Crassostrea* spp. compared to 2010 production numbers (Beck et al. 2011; FAO UN 2018). The status of the oyster stocks has been of interest not only for their economic importance, but for the oysters' role in mitigating adverse environmental effects of eutrophication through bioassimilation of nutrients and enhancement of benthic-pelagic coupling (Newell 1988; Newell et al. 2005). Strong empirical relationships between total assimilated nutrient content and oyster shell length provide a promising tool for the quantification of nitrogen removal from shellfish harvest numbers (Higgins et al. 2011; Rose et al. 2014; Cornwell et al. 2016). Although it is understood that oysters also remove nitrogen by enhancing the biogeochemical process known as denitrification (Kellogg et al. 2013; Smyth et al. 2013; Caffrey et al. 2016; Arfken et al. 2017; Jackson et al. 2018), it is unknown whether an empirical relation for denitrification rates and oyster size (a proxy for year-class) exists.

In the Maryland waters of Chesapeake Bay, the most recent stock assessment of the Eastern Oyster, *Crassostrea virginica* (Gmelin 1791), has concluded that the current population of adult oysters is half of what it was 18 years ago (MD DNR and UMCES 2018). Meanwhile, the number of oysters harvested from commercial shellfish leases has increased from approximately 1.0 million to 22.2 million in the last 5 years (MD DNR and UMCES 2018). The transition to aquaculture should support a more sustainable fishery and may provide nitrogen removal services that could help mitigate the Chesapeake Bay's long history of eutrophication. As a result, a number of studies have

suggested the use of oyster sustainability efforts (i.e., restoration and aquaculture) as a supplement for reductions in anthropogenic nitrogen loads (Newell 1988; Cerco and Noel 2007; Rose et al. 2014).

Oysters are suspension-feeders and filter out nitrogen from the water column by sorting through phytoplankton and particles greater than $\sim 3\text{-}\mu\text{m}$ diameter (Bayne and Newell 1983; Bayne and Hawkins 1992; Newell 2004). Once particles are captured, nitrogen may undergo a series of different fates. Nitrogen in digested particles may return to the water column as ammonium or other nitrogenous waste products (excretion), become assimilated into shell or tissue biomass, or get deposited on the sediment as biodeposits (Newell et al. 2005). Nitrogen in tissue biomass is removed from the local environment when oysters are harvested and the amount removed can be readily estimated from highly significant relationships between nitrogen content and total shell length (Rose et al. 2014). The fate of nitrogen in biodeposits is the more complex nitrogen removal pathway because in order for it to be removed, biodeposit N must be mineralized to ammonium and ultimately undergo coupled nitrification-denitrification to remove nitrogen from the water in the form of di-nitrogen gas (N_2 ; Newell et al. 2002; Giles et al. 2006; Kellogg et al. 2014; Dame 2016). Coupled nitrification-denitrification requires aerobic environments to exist in close proximity to anaerobic environments by compressing the distance for NO_x diffusion to encounter anaerobic conditions (Rysgaard et al. 1994).

Mineralization of biodeposits also may involve natural decomposition of dissolved organic nitrogen or processing following ingestion by deposit-feeders (Newell et al. 2002; Giles et al. 2006; Kellogg et al. 2014; Dame 2016). Increased biogeochemical

cycling on oyster reefs has been associated with deposit-feeders (Kellogg et al. 2013). For example, extremely large abundances of polychaetes and amphipods have been observed on a restored oyster reef site compared to bare sediments (Kellogg et al. 2013). Polychaetes and amphipods are known to assimilate nitrogen, as well as support microbial nitrification activity internally and externally on the animals themselves (Welsh and Castadelli 2004). Shellfish aquaculture in floating cages has been shown to increase the number of invertebrates in a given environment (DeAlteris et al. 2004), but the abundance of polychaetes and amphipods on on-bottom aquaculture and their role in removing nitrogen is unknown.

Prior studies of the effects of bivalve aquaculture on nitrogen cycling have included incubations of sediment cores below different forms of floating aquaculture (Holyoke 2008; Testa et al. 2015; Humphries et al. 2016; Lunstrum et al. 2017; Vieillard 2017) and incubations of sediment cores including clams (Murphy et al. 2016; Smyth et al. 2018). Much of the work documenting biogeochemical fluxes associated with oysters alone has either used cleaned oysters, or focused on rate comparisons to sediments and shell (Smyth et al. 2013; Caffrey et al. 2016; Arfken et al. 2017). In contrast to sediment flux measurements from aquaculture, denitrification rates from oysters alone, particularly focusing on differences in year-classes (i.e., size) has never been examined. This raises questions as to whether oyster size matters to denitrification rates, and if so, to what extent do these rates contribute to the overall nitrogen cycle.

Based on the growth of aquaculture in the Chesapeake Bay and the potential for oyster-associated denitrification to be applied as a best management practice (BMP), the goal of this study was to evaluate whether there are differences in denitrification rates

across different oyster sizes. Therefore, we measured biogeochemical fluxes from different oyster year-classes reared and harvested from an on-bottom aquaculture lease during the months of May, July, and September. We also measured polychaete biomass attached to oysters for a gradient of year classes to test the hypothesis that denitrification rates would be stimulated by more nitrogen processing in incubation chambers with higher abundances of polychaetes.

Methods

Study area and field sampling

An aquaculture lease in the Nanticoke River (38° 15.691' N, 75° 56.262' W), a tributary to Chesapeake Bay on the lower Delmarva Peninsula, was chosen for oyster collection (Fig. 5.1). The Nanticoke River has a tidal extent of 48 km and a tidal amplitude of <1m (Secor, Houde, and Kellogg 2017). An analysis of the time period from 1957 to 2015 has revealed that peak monthly flow rates typically occur from February to April, and maximum flows in March can make up to 16% of the annual mean flow (Secor, Houde, and Kellogg 2017). The water depth at the lease is about 1.5 m, with an average current speed of 0.5 m s⁻¹ (NOAA Site 8571476, Roaring Point, MD). The average oyster density on the lease is approximately 40 ind. m⁻²; however, the density changes throughout the harvest season. Agriculture is the dominant form of land use in the watershed (40%; The Nature Conservancy 1994).

Oysters were collected with a dredge during the harvest season from spring to late summer (May, July, and September) of 2018. Environmental conditions such as dissolved oxygen, salinity, and temperature were characterized with a YSI (Quatro). Once oysters

were collected, they were aerated in buckets during transport to Horn Point Laboratory (~1 hr) in Cambridge, MD, where oysters were placed in nonfiltered Choptank River water and aerated overnight. In the morning, oysters were placed in custom-designed incubation chambers in filtered Choptank River water adjusted to morning temperature conditions (19.0, 27.0, and 23.1 °C in May, July, and September, respectively). Chambers consisted of a machined bottom with an area of 0.05 m² made from 0.95 cm outer diameter PVC pipe (Fig. 5.2). Prior to each experiment, 12 chambers were each filled with ~6 oysters. The 12 chambers were filled with either small, medium, or large oyster size-classes (63.41±8.72, 90.21±4.99, and 114.77±12.24, respectively; i.e., 4 chambers for each size-class designation; Fig. 5.3). Three chambers were each filled with 6 shells collected from the site. The total number of chambers sampled was 16; one additional chamber was empty and filled with only filtered river water to serve as a “blank” for water column processes. All chambers were aerated prior to the start of incubations for approximately an hour to bring oxygen concentrations to saturation. Following aeration, stirring lids with ports for sample collection were used to seal the chambers from the surrounding water bath and keep the water column stirred with motor-driven magnets (Fig. 5.2). The chambers were incubated in the dark only, based on low light levels observed from photosynthetically active radiation (PAR) measurements made with LiCor (2π) sensors at the surface and 1 m depth.

In order to gauge whether these processes are a local phenomenon or a response that can be measured universally, three incubations using the same trays were conducted in 2017 using oysters from Harris Creek. We overlaid data points generated from incubations of oysters planted for restoration from Harris Creek, a tributary to the

Choptank River, Maryland, USA on Nanticoke River regression panels for the month of September (Figs. 5.4e,f and 5.6-9e,f). The Harris Creek incubations were conducted in August but the water temperature (24.5°C) was closest to that measured in the Nanticoke River in September (25.0°C).

Oyster and polychaete characteristics

After incubations, each oyster was placed in an individual container of 5% ethanol and 95% artificial seawater adjusted to ambient salinities (13.7, 9.1, and 11.6 in May, July, and September, respectively) for 24 hours (method from Shannon Hood et al. unpubl. data). The ethanol treatment forced the polychaetes to emerge from their shell burrows so they could be removed from oysters with forceps. All polychaetes from each oyster or shell were dried together to a constant weight for at least 48 h at 60°C. All oysters were measured to the nearest mm, shucked, and dried to a constant weight at 60°C.

Biogeochemical flux measurement

Based upon changes in dissolved oxygen (FireSting O₂-mini oxygen meter), solutes (NH₄⁺, NO_x=[NO₂⁻]+[NO₃⁻], SRP) and dissolved gases (O₂, N₂, Ar, DIC=[H₂CO₃]+[HCO₃⁻]+[CO₃²⁻]) were collected approximately every 45 minutes. As samples were collected from a sampling tube fitted in the lid, a water replacement tube pulled water from the water bath. By the final time point, dissolved oxygen concentrations reached 260.1±9.2, 146.6±41.9, and 198.3±22.8 μmol l⁻¹ (mean± SD) in May, July, and September, respectively. Dissolved gases were tightly sealed, submerged

in water at temperatures at or below incubation temperatures, following preservation with 10 ml of 50% saturated HgCl₂. Within 2 weeks of collection, a membrane-inlet mass spectrometer (Kana et al. 1994) was used to measure N₂, O₂, and Ar concentrations. An infrared-based analyzer (Apollo SciTech; Cai and Wang 1998) measured DIC concentrations. The DIC calibration coefficient of variation ranged from 0.06 to 0.30% and had an average standard deviation of ±8.5 μmol l⁻¹. Solutes were filtered (0.45 μm pore-size filter) and frozen for analysis. Concentrations of NH₄⁺ were determined with the phenol/hypochlorite colorimetry method (Parsons 2013). Concentrations of NO_x were analyzed spectrophotometrically according to Doane and Horwáth (2003), and SRP following Parsons (2013) using a composite reagent of molybdic acid, ascorbic acid, and trivalent antimony.

Fluxes were determined by first observing the relationship between concentrations of gases and nutrients with time. Regressions with an R² ≥ 0.80 and a change in concentration greater than the precision of analysis were considered significant (Cornwell et al. 1999). The slope of the “blank” was subtracted from the slope of the sample fluxes to remove the effects of water column processes if the blank was significant. Fluxes (F; μmol m⁻² hr⁻¹) were calculated based on the equation:

$$F = \frac{\Delta C}{\Delta t} * \frac{V}{A}$$

where ΔC/Δt is the slope (μmol L⁻¹ hr⁻¹), V is the volume of overlying water (L), and A is the area of the chamber (m⁻²).

Statistical analyses

All statistical analyses were performed with base stats packages in R 3.1 (R Development Core Team 2013). A multiple linear regression was used to investigate whether biogeochemical fluxes depended on oyster size and sampling month, where biogeochemical fluxes were the dependent variable and average oyster size characteristics (i.e., biomass or total length) and sampling month were the independent variables. Assumptions of normality and homoscedasticity were confirmed with normal Q-Q plots and residual vs. fitted plots. Statistical differences between size-classes for biogeochemical fluxes were further analyzed following the separation of incubated oysters into two different size groups: juveniles (50-80 mm) and adults (100-130 mm). A two-way analysis of variance (ANOVA) with size class and sampling month as fixed factors, was followed by post hoc Tukey HSD tests if the interaction between size and date was insignificant. However, the two-way ANOVA was followed by a one-way ANOVA and Tukey HSD to test the main effect of size for each sampling month if the interaction was significant. Although some statistical strength was lost by removing middle ranged size classes, this test provided more insight into whether biogeochemical fluxes depend on oyster length or biomass.

Results

Oyster shell from the aquaculture lease was collected and incubated (68 oyster shells total). From May to September, oxygen demand from shell decreased from 676.2 ± 188.5 to 331.5 ± 188.5 $\mu\text{mol m}^{-1} \text{hr}^{-1} \text{shell}^{-1}$ (Table 5.1). Similarly, DIC fluxes decreased from 1090.9 ± 310.7 to 193.2 ± 23.5 $\mu\text{mol m}^{-1} \text{hr}^{-1} \text{shell}^{-1}$. Denitrification

increased from -83.2 ± 67.7 to $35.8 \pm 18.4 \mu\text{mol m}^{-1} \text{hr}^{-1} \text{shell}^{-1}$ from May to July. A decline in NO_x and NH_4^+ fluxes was observed from May to September.

A total of 210 live oysters were used for flux incubations. A strong positive relationship was observed between total shell length (mm) and oyster tissue dry weight (g) during different sampling times, with a significant multiple linear regression equation found ($F(5, 30) = 26.07, p < 0.001$), with an R^2 of 0.81 (Fig. 5.3). Oyster dry weight increased by 0.027, 0.015, and 0.012 g for each mm of length during May, July, and September, respectively.

Multiple linear regressions were calculated to predict biogeochemical rates based on the oyster biomass and sampling month. Based on differences in size-class biomass observed across sampling months (Fig. 5.3), a second multiple linear regression was used to estimate biogeochemical rates based on oyster length and sampling month. A significant regression equation was found for oxygen-based respiration from oyster biomass and month ($F(5, 31) = 18.04, p < 0.001$), with an R^2 of 0.744 (Fig. 5.4a,c,e). Average oyster length also produced a significant regression equation for oxygen-based respiration rates ($F(5, 31) = 31.8, p < 0.001$), with an R^2 of 0.837 (Fig. 5.4b,d,f). Oxygen-demand increased by 211.4, 489.9, and 1,271.6 $\mu\text{mol m}^{-1} \text{hr}^{-1}$ for each g of biomass and 7.9, 8.3, and 22.5 $\mu\text{mol m}^{-1} \text{hr}^{-1}$ for each mm of length during May, July, and September, respectively. Oysters collected from Harris Creek had oxygen demands that ranged from 747.90 to 1131.54 $\mu\text{mol m}^{-2} \text{h}^{-1} \text{oyster}^{-1}$ (Fig. 5.4e,f). In addition, sampling month and oyster biomass accounted for 74.61% of the variance in DIC-based respiration ($F(5, 28) = 16.45, p < 0.001$), whereas sampling month and length accounted for 75.00% of the variance ($F(5, 28) = 16.80, p < 0.001$; Fig. 5.5). DIC-based respiration increased with each

g of biomass by 404.84, 820.8, and 1,360.62 $\mu\text{mol m}^{-1} \text{hr}^{-1}$ and with each mm of length by 13.7, 14.1, and 23.0 $\mu\text{mol m}^{-1} \text{hr}^{-1}$ in May, July, and September, respectively.

Similarly, biomass and sampling month produced a significant regression equation for denitrification ($F(5, 31)=10.67, p<0.001$), with an R^2 of 0.623 (Fig. 5.6a,c,e). However, average length and sampling month only accounted for 34.07% of the variance in denitrification ($F(5, 31)=3.203, p=0.020$; Fig. 5.6b,d,f). Oyster-associated denitrification decreased by 70.69 $\mu\text{mol m}^{-1} \text{hr}^{-1}$ for each g of biomass during July, but increased by 134.43 and 31.04 $\mu\text{mol m}^{-1} \text{hr}^{-1}$ during May and September, respectively. A similar pattern was observed for each mm of length, with an increase of 4.0 and 0.5 $\mu\text{mol m}^{-1} \text{hr}^{-1}$ in May and September and a decrease by 1.5 $\mu\text{mol m}^{-1} \text{hr}^{-1}$ in July. Oysters collected from Harris Creek had denitrification rates that ranged from 25.35 to 29.90 $\mu\text{mol m}^{-2} \text{h}^{-1} \text{oyster}^{-1}$ (Fig. 5.6e,f). Contrastingly, sampling month and oyster biomass did not explain the observed NO_x fluxes ($F(5, 31)=0.53, p=0.75$), with an R^2 of 0.082 (Fig. 5.7a,c,e). Likewise, sampling month and oyster length only explained 1.68% of the variance ($F(5, 31)=0.11, p=0.990$; Fig. 5.7b,d,f). Oysters collected from Harris Creek had NO_x fluxes that ranged from 92.94 to 111.54 $\mu\text{mol m}^{-2} \text{h}^{-1} \text{oyster}^{-1}$ (Fig. 5.7e,f). A multiple linear regression that used sampling month and oyster biomass as independent variables accounted for 59.41% of the variance in NH_4^+ fluxes ($F(5,31)=8.786, p<0.001$), whereas sampling month and average length accounted for 64.94% of the variance ($F(5,31)=11.48, p<0.001$; Fig. 5.8). During July, NH_4^+ fluxes decreased by 102.63 $\mu\text{mol m}^{-1} \text{hr}^{-1}$ for each g of biomass, whereas fluxes increased with biomass by 43.32 and 125.3 $\mu\text{mol m}^{-1} \text{hr}^{-1}$ in May and September, respectively. A similar pattern was observed for every mm of length, with a decrease of 1.0 $\mu\text{mol m}^{-1} \text{hr}^{-1}$ observed in July and an increase

of 1.5 and 2.3 $\mu\text{mol m}^{-1} \text{hr}^{-1}$ in May and September. NH_4^+ fluxes measured from oysters collected from Harris Creek had a small range (54.91-70.81 $\mu\text{mol m}^{-2} \text{h}^{-1} \text{oyster}^{-1}$; Fig. 5.8e,f). Sampling month and oyster biomass explained 43.75% of the variance in SRP fluxes ($F(5, 31)=4.67, p=0.003$), whereas sampling month and oyster length explained 56.72% of the variance (Fig. 5.9). SRP fluxes decreased by 19.14 $\mu\text{mol m}^{-1} \text{hr}^{-1}$ for each g of biomass July, but increased by 0.27 and 12.68 $\mu\text{mol m}^{-1} \text{hr}^{-1}$ in May and September, respectively. Finally, SRP fluxes measured from oysters collected from Harris Creek ranged from 13.33 to 16.62 $\mu\text{mol m}^{-2} \text{h}^{-1} \text{oyster}^{-1}$ (Fig. 5.9e,f)

The oysters were split into two size classes, juveniles (50-80 mm) and adults (100-130 mm), to assess both oyster abundance-normalized and tissue biomass-normalized fluxes based on size class and sampling month; therefore, a number of samples within the middle size range were removed for analysis. The analysis of oyster abundance-normalized fluxes is expected to characterize the effect of changing biomass during the sampling months, whereas the analysis of tissue biomass normalized fluxes may distinguish whether there is an effect of total length alone. Oyster oxygen demand per oyster had a significant size by month interaction ($p=0.004$), as well as significant variation between size-classes and sampling months ($p<0.001$ and $p<0.001$, respectively; Table 5.2). Average oxygen demand per oyster was consistently higher for adult oysters compared to juveniles, but only significantly different during the month of September (Tukey HSD, $p=0.003$; Fig. 5.10a). Oyster oxygen demand normalized by tissue biomass did not have a significant size by month interaction ($p=0.143$), but there was significant variation between size-classes and sampling month ($p=0.007$ and $p<0.001$, respectively; Table 5.3). Juveniles had the highest average oxygen demand per gram during all

sampling dates, with rates almost double adult rates during May and July (Fig 5.10b). Oyster-associated DIC fluxes did not have a significant size class by sampling month interaction ($p=0.131$), but rates were significantly different across size classes ($p<0.001$) and sampling months ($p<0.001$; Table 5.2). Average DIC fluxes from individual adults were consistently higher than juvenile fluxes (Fig. 5.10c). DIC-based respiration normalized by tissue biomass had a significant size class by sampling month interaction ($p<0.001$) and a significant difference between rates measured during different sampling months ($p<0.001$; Table 5.3). Juvenile and adult DIC-based respiration normalized by tissue biomass were only significantly different during sampling in September ($p=0.002$). On average, adults had higher DIC-based respiration per gram than juveniles during May and September, but this relationship was the opposite in July with an average flux of $1891.35 \pm 224.64 \mu\text{mol m}^{-1} \text{hr}^{-1} \text{g DW}^{-1}$ in juveniles compared to $1446.44 \pm 138.51 \mu\text{mol m}^{-1} \text{hr}^{-1} \text{g DW}^{-1}$ (Fig. 5.10d).

Denitrification did not have a significant size class by sampling month interaction when rates were normalized by the number of oysters in the tray ($p=0.093$; Table 5.2), but there was an interaction when rates were normalized by tissue biomass ($p=0.005$; Table 5.3). Denitrification per oyster and per gram DW were higher for adult size classes during May and September, but fluxes normalized by DW from juveniles were more than double adults during July (Tukey HSD, $p=0.007$; Fig. 5.11b). NO_x fluxes normalized by the number of oysters and tissue biomass did not have a significant size class by sampling month interaction ($p=0.904$ and $p=0.918$, respectfully; Table 5.2 and 5.3); however, on average juveniles had higher NO_x fluxes per gram than adults during all sampling months (Fig. 5.11d). NH_4^+ fluxes for individual oysters had a significant size class by sampling

month interaction ($p=0.005$), in addition to significant variation by size ($p=0.043$) and sampling month ($p=0.039$; Table 5.2). NH_4^+ fluxes from adult oysters were more than double juvenile rates, but were only significantly different in September (Tukey HSD, $p=0.005$; Fig. 5.11e). Similarly, NH_4^+ fluxes per gram had a significant size class by sampling month interaction ($p<0.001$), as well as significant variation by size ($p=0.005$) and sampling month ($p<0.001$; Table 5.3). Average NH_4^+ fluxes per gram were higher from juvenile incubations than adults during May and July, but a significant difference was only observed during July (Tukey HSD, $p=0.005$; Fig. 5.11f). An opposite pattern was observed in September, with average NH_4^+ fluxes from adult incubations higher than juvenile rates (145.97 ± 19.76 and $120.49\pm 19.62 \mu\text{mol m}^{-1} \text{hr}^{-1} \text{g DW}^{-1}$, respectively).

SRP fluxes per oyster and per gram DW had a significant size class by sampling month interaction ($p<0.001$ and $p=0.002$, respectively) and a significant difference between months ($p<0.001$ for both; Tables 5.2 and 5.3). Fluxes normalized by the number of oysters for adults were nearly three-fold higher than juveniles in May and September, but the reverse was true in July (Fig. 5.12a). SRP fluxes normalized by tissue biomass from juvenile incubations were more than 3-fold higher than adult fluxes in July (Tukey HSD, $p=0.009$), but average SRP fluxes were higher from adults than juveniles in May and September (Fig. 5.12b).

Polychaete abundances were higher in July and September than May (Fig. 5.13). Regression analyses demonstrated a positive relationship between denitrification rates and polychaete abundance ($R^2=0.29$), but the relationship was not significant ($p=0.135$; Fig. 5.13a). Regression of denitrification rates against polychaete biomass in September demonstrated a significant ($p=0.037$) and slightly correlated ($R^2=0.29$) positive

relationship (Fig. 5.13b). Otherwise, regression analyses found no other relationships between denitrification and polychaetes.

Discussion

This work has shown that oyster size, whether it is measured as biomass or length, plays an important role in determining biogeochemical fluxes occurring on oyster aquaculture leases. Seasonal shifts in ambient NO_x concentrations, as well as oyster biomass for a given oyster length, mirrored changes in average denitrification rates observed from May to September. Oyster biomass was associated with changes in denitrification rates, but the relationships changed depending on the sampling month. As expected, oyster respiration (e.g. O_2 and DIC fluxes) was significantly and positively associated with oyster size during every sampling month. However, shifts in respiration slopes and weaker correlations, suggest that oysters were possibly stressed in July. The dichotomous denitrification relationships observed with sampling date indicate that fluxes depend on size, season, and NO_x concentrations.

The decline in adult oyster biomass along with the increase in oxygen demand and DIC fluxes from May to September suggest that adult oysters were undergoing physiological changes over the course of the season. These observations fit within our understanding of the empirically observed condition called routine metabolic rate (RMR; Peters 1983; Bayne 2017). The concept of RMR considers that an oyster's metabolic rate depends on the amount of food that has been consumed, the temperature, and physiological condition (reproductive state and environmental stresses; Bayne 2017). It was assumed that the oysters in our experiment were consuming the same food and that

the temperature conditions were the same on a given incubation day; therefore, any variability observed in RMR was likely due to the oyster's physiological condition.

As for the physiological state, the diploid oysters were likely at different reproductive stages, depending on their size. In Chesapeake Bay, spawning periodicity ranges from early June to early October, with peaks in July (UMD 1953; Kennedy 1986). Moreover, the decrease in oyster biomass from May to July is consistent with relationships of the weight of eggs spawned and prespawning soft-tissue dry weight for *Crassostrea virginica* produced by (Cox and Mann 1992; Mann et al. 1994). The assessment of oyster tissue dry weight in two Louisiana estuaries, also found that oyster biomass decreased post-spawning (Westbrook 2016). The increase in oxygen demand for larger oysters from May to September is comparable to those shown by (Tran et al. 2008) where oysters after spawning had higher oxygen consumption rates, which were interpreted as due to higher rates of biosynthesis of proteins and glycogen. Based on work by (Shumway and Koehn 1982), oxygen demand in acclimated oysters increased with temperature and salinity. Similarly, DIC fluxes from adult oysters were approximately 2-fold higher in July, compared to May. These responses are consistent with those shown by (Lejart et al. 2012) from *Crassostrea gigas* in France, with seasonal variation in DIC fluxes observed only in adults.

Not only did respiration rates shift, but shifts in maximum denitrification rates from adult oysters were supported by changing ambient NO_x concentrations. NO_x concentrations were the highest in May ($13.6 \pm 1.3 \mu\text{M}$) and September ($22.2 \pm 4.9 \mu\text{M}$) and the lowest in July ($6.2 \pm 1.8 \mu\text{M}$). The increase in oyster-associated denitrification rates with ambient NO_x concentrations confirms our understanding that denitrification

rates from sediments are commonly regulated by water column concentrations of NO_x (Kemp et al. 1990). Previous studies at clam aquaculture sites that supplied NO_3^- additions to sediments have associated the elevated NO_3^- with higher rates of denitrification (Smyth et al. 2018).

Considering NO_x concentrations were the highest in September and maximum denitrification was observed in May, discrepancies in denitrification rates from adults and periodicity of spawning in Chesapeake Bay raises the question of whether denitrification was also related to glycogen stores. Glycogen plays an important role in the oyster gametogenic cycle, and concentrations within oysters in Maryland are often at a maximum in May and at a minimum immediately after spawning (Sidwell et al. 1979; Kennedy et al. 1996). As oxygen demand for larger oysters increased from May to September, the respiratory quotient (RQ; moles of carbon dioxide liberated per mole of oxygen consumed) decreased from 1.01 to 0.75, suggesting that carbohydrate (glycogen) utilization may have fueled lipid synthesis to supply developing oocytes with yolk in May (Bayne 2017). Similarly, the atomic ratio of moles of oxygen consumed per mole of nitrogen excreted (NH_4^+) is used as a metabolic index (O/N) to suggest the balance between proteins, lipids, and carbohydrates metabolized in energy production as well as the quality of food (Bayne 2017). O/N values from large oysters were 7.96, 15.21, and 10.75 in May, July, and September, respectively, indicating that the utilization of carbohydrates (i.e. glycogen) may have been at a peak in July. Moreover, the pattern in O/N values mirrors seasonal shifts in adult denitrification rates. Given the fact that O/N and RQ are difficult to interpret and the goal of this work was not to understand oyster biochemical energy storage cycles, I suggest that a more comprehensive study of oyster

biochemical composition and associated denitrification rates be conducted. Unlike sediments, where denitrification rates are mostly constrained by environmental conditions, oyster-associated denitrification rates also depend on changes in oyster biology.

Similar to denitrification, NH_4^+ fluxes increased with increasing biomass and length during May and September, whereas fluxes were negatively correlated with biomass and on average two-fold higher in July. NH_4^+ fluxes measured in our incubations were equal to the sum of excretion and microbial processes associated with the oyster (i.e., ammonification or DNRA). Excretion consists of the combination of losses from protein recycling (endogenous) and waste incurred during assimilation of dietary nitrogen (exogenous; Bayne 2017). Increases in excretion rates with temperature have been observed for *Ostrea edulis* (Hutchinson and Hawkins 1992; Beiras et al. 1995). Across the globe, *Crassostrea gigas* in China showed a similar pattern with higher NH_4^+ excretion in the summer during spawning and lower rates in the winter (Mao et al. 2006). In addition, the quality of food is important, considering variability in NH_4^+ fluxes has been attributed to how oysters regulate imbalances between the nitrogen in their diet and nutritional demand (Bayne 2017). Small oysters have high demands for protein-nitrogen to support somatic growth and consequently their tissue C:N may be as low as 3.5 (Bayne 2009). Shifts in NH_4^+ fluxes from juvenile oysters may have been associated with the C:N ratio of available food (Bayne 2017). Contrastingly, NO_x fluxes in May had a slightly negative relationship with size (Fig. 5.7a,b). Therefore, the removal of NO_x by larger oysters was most likely responsible for the maximum rates of denitrification

observed in May. Overall, oyster size played an important role in nitrogen transformations.

Taking into account the few reports of oyster-associated fluxes, this work presents a more detailed case of how oysters alone influence biogeochemistry. Similar biogeochemical fluxes were measured from incubations of oysters collected from Harris Creek restoration sites (Figs. 5.4e,f and 5.6-9e,f), which proves that this is not a phenomenon that only occurs in the Nanticoke River. The majority of the overlaid points fell within the standard error or on the regression lines for all of the biogeochemical fluxes measured. The biogeochemical fluxes we observed with oysters from the Nanticoke River are within the ranges reported from another study of oysters incubated alone from Harris Creek (Jackson et al. 2018). Compared to rates measured with oysters from the Nanticoke, (Caffrey et al. 2016) reported denitrification rates that on a per oyster basis are approximately 10-fold less ($0.31 \mu\text{mol h}^{-1} \text{oyster}^{-1}$), which may be attributed to the incubation of single oysters in smaller core tubes. Similar to our results, data from incubations of single scrubbed oysters from Calico Creek, North Carolina suggest denitrification rates on the order of $400 \mu\text{mol m}^{-2} \text{h}^{-1} \text{oyster}^{-1}$ (Smyth et al. 2013). Estimates of oyster-associated denitrification from the Nanticoke River and other comparative studies validate that oysters support enhanced denitrification.

Implications

Although measuring oysters alone may provide conservative estimates of total ecosystem biogeochemical fluxes (Jackson et al. 2018), these findings have important implications for nitrogen removal mitigation efforts in the Chesapeake Bay. Nitrogen

inputs reaching the lower Nanticoke River are on the order of $58.0 \times 10^{-3} \text{ kg N yr}^{-1}$ (US EPA 2010), therefore using an annual adult oyster denitrification-based removal rate of $6.75 \mu\text{mol h}^{-1} \text{ oyster}^{-1}$, an acre planted with 100 bushels of adult oysters (~ 230 oysters bushel $^{-1}$; MD DNR and UMCES 2018) would remove $38.1 \text{ kg N yr}^{-1}$ (0.06%). There are a number of caveats in extrapolating oyster-associated denitrification from three sampling months to an entire year; however, the amount of nitrogen removed may become more significant as aquaculture continues to increase in the future. For example, in the Maryland portion of the Chesapeake Bay alone, the number of oysters planted on leases increased from 231.7 million in 2012 to 301.3 million in 2016.

In addition, incubations with triploid oysters, which do not reproduce, may produce results with less seasonal variation than diploids. Understanding relationships between seasonal fluxes and the oyster life cycle have consequences for nutrient substrate availability for the total sediment and oyster ecosystem. More importantly, nutrient reduction studies associated with bivalves have largely focused on processes occurring in adjacent sediments (Holyoke 2008; Piehler and Smyth 2011; Smyth et al. 2015; Hoellein et al. 2015; Lunstrum et al. 2017). The classic view of enhanced denitrification response following oyster biodeposition neglects the importance of oyster biology and physiology to biogeochemical processing.

Table 5.1 Biogeochemical fluxes measured from shell collected from an aquaculture lease. N.s. means that none of the three shell incubations were significant (i.e., $R^2 > 0.80$).

Shell biogeochemical fluxes ($\mu\text{mol m}^{-2} \text{hr}^{-1} \text{shell}^{-1}$)	May	July	September
Oxygen demand	676.2±188.5	164.9±86.5	331.5±61.0
DIC	1090.9±310.7	362.0±35.4	193.2±23.5
N ₂	-83.2±67.7	35.8±18.4	n.s.
NO _x	129.1±108.6	48.4±20.3	-111.2±67.6
NH ₄ ⁺	153.6±36.7	9.3±28.8	n.s.
SRP	12.2±6.3	7.1±1.7	n.s.
Average shell length (mm)	95.1±9.0	96.1±2.0	106.0±5.0

Table 5.2 Biogeochemical fluxes normalized per oyster with statistical results based on two-way and one-way ANOVAs.

	Oxygen demand			DIC			NH4+			NOx			Denitrification			SRP		
	df	F	p	df	F	p	df	F	p	df	F	p	df	F	p	df	F	p
Two-way																		
Anova																		
Size	1	9.10	0.007	1	2.35	0.142	1	9.66	0.005	1	0.663	0.426	1	3.38	0.081	1	3.55	0.075
Month	2	43.86	<0.001	2	49.68	<0.001	2	25.03	<0.001	2	0.276	0.762	2	12.92	<0.001	2	13.46	<0.001
Interaction (Size*Month)	2	2.17	0.143	2	13.20	<0.001	2	12.56	<0.001	2	0.086	0.918	2	7.14	0.005	2	8.32	0.002
One-way																		
Anova size																		
May				1	0.09	0.771	1	0.10	0.759				1	0.44	0.529	1	0.03	0.861
July				1	2.34	0.177	1	17.68	0.005				1	15.29	0.007	1	14.09	0.009
September				1	25.70	0.002	1	0.84	0.396				1	0.04	0.840	1	1.02	0.351

Table 5.3 Biogeochemical fluxes normalized by grams of oyster tissue dry weight with statistical results based on two-way and one-way ANOVAs.

	Oxygen demand			DIC			NH4+			NOx			Denitrification			SRP		
	df	F	p	df	F	p	df	F	p	df	F	p	df	F	p	df	F	p
Two-way																		
Anova																		
Size	1	17.70	<0.001	1	17.12	<0.001	1	4.67	0.043	1	0.37	0.549	1	1.33	0.2627	1	0.75	0.398
Month	2	20.73	<0.001	2	10.49	<0.001	2	3.85	0.039	2	0.32	0.73	2	2.40	0.1175	2	10.40	<0.001
Interaction (Size*Month)	2	7.38	0.004	2	2.26	0.131	2	7.05	0.005	2	0.10	0.904	2	2.69	0.0934	2	11.68	<0.001
One-way																		
Anova size																		
May	1	4.00	0.085				1	3.39	0.108							1	0.73	0.422
July	1	0.49	0.515				1	2.97	0.136							1	7.21	0.036
September	1	24.76	0.003				1	17.60	0.005							1	12.37	0.013

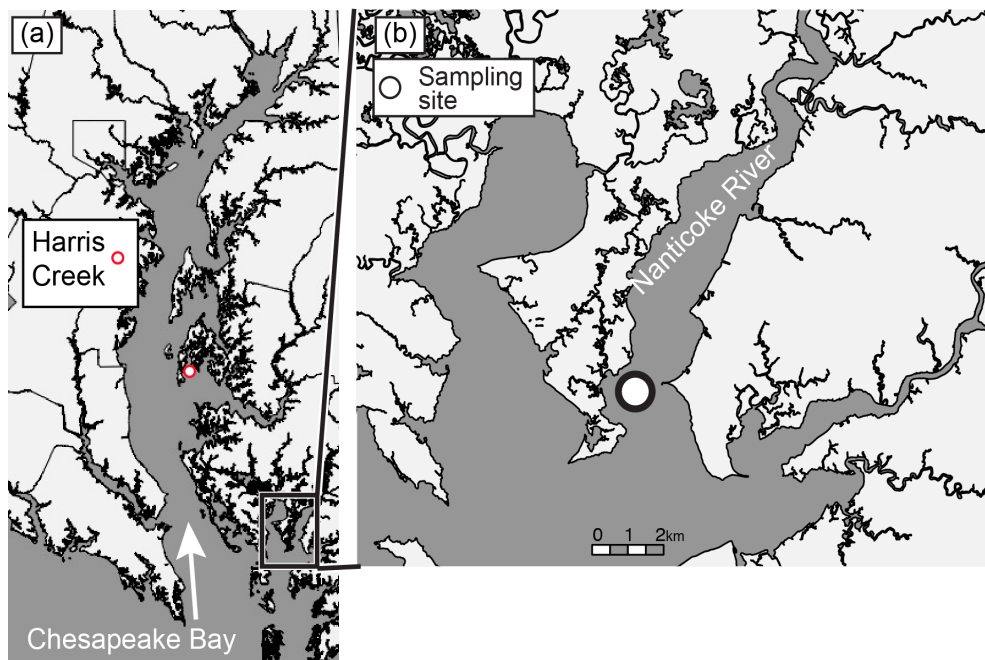


Fig. 5.1 Map of Chesapeake Bay showing (a) a comparison site at Harris Creek and (b) the Nanticoke River, a tributary to the Chesapeake Bay and the location of the aquaculture lease (○) where oysters were collected.

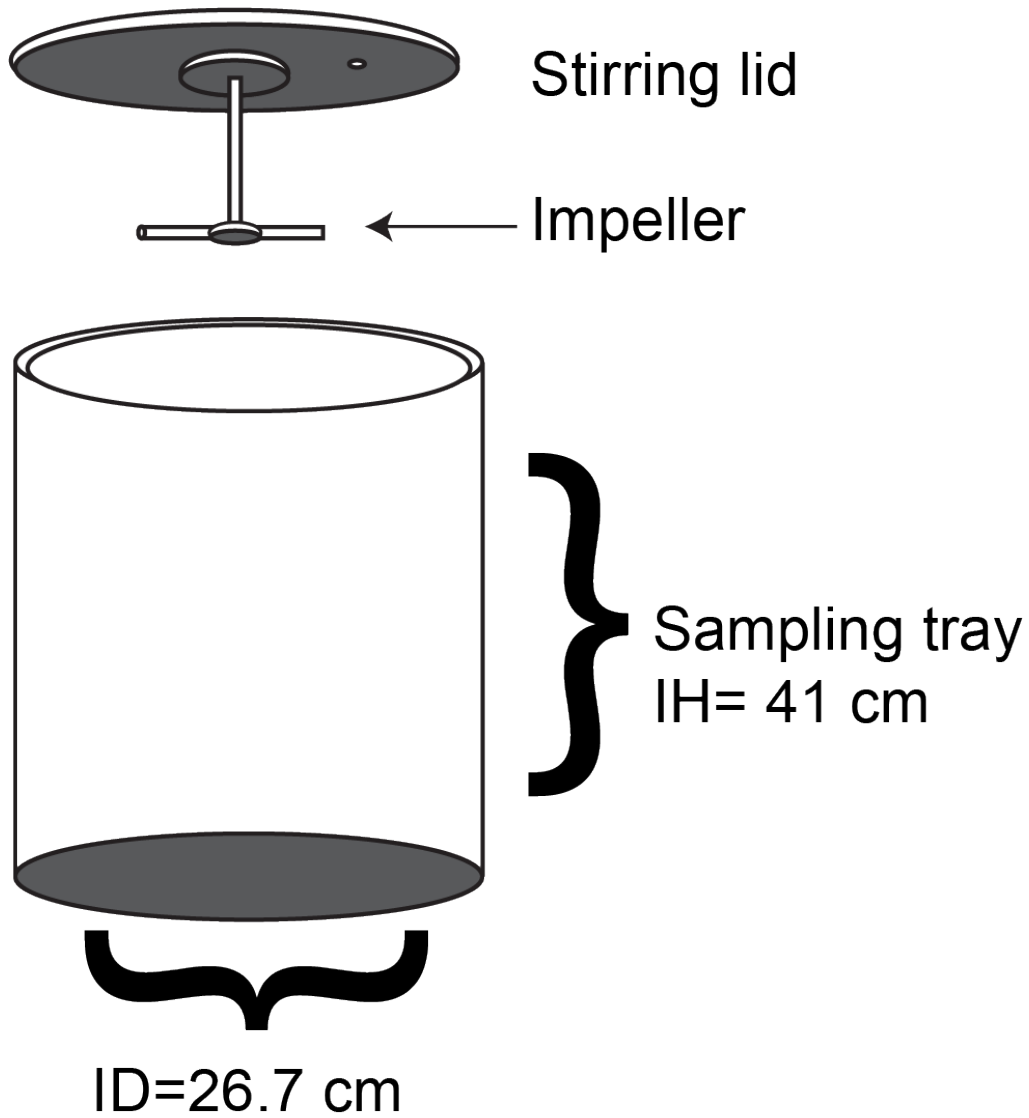


Fig. 5.2 Drawn to scale diagram of incubation chamber. The base, sides, lid, and impeller were made of PVC, but the ends of the impeller contained magnets to turn the impeller.

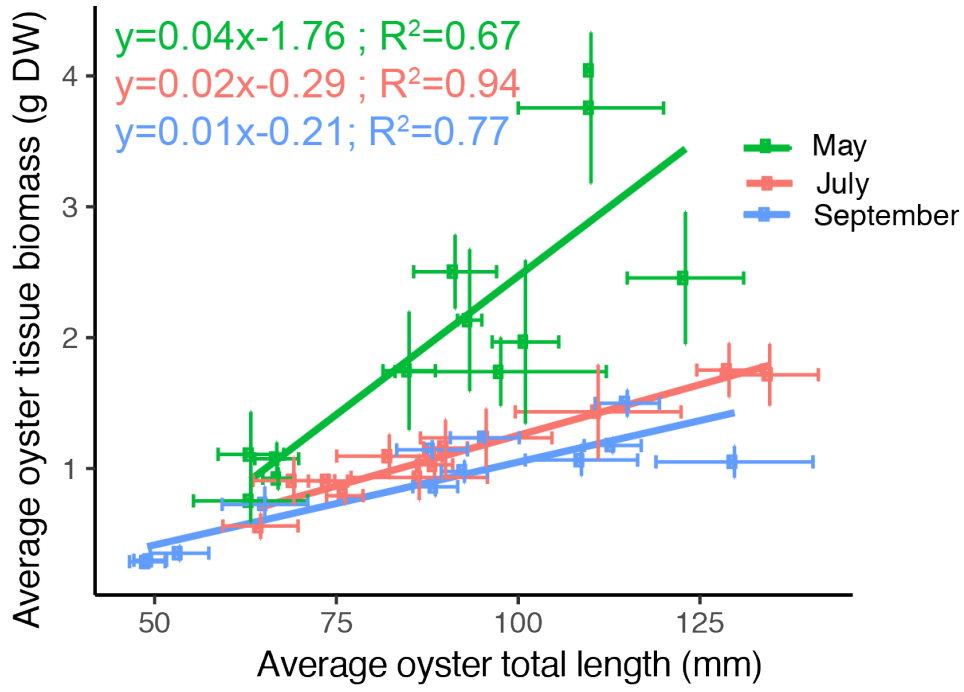


Fig. 5.3 Regression of average oyster total length against average oyster tissue biomass during the months May, July, and September.

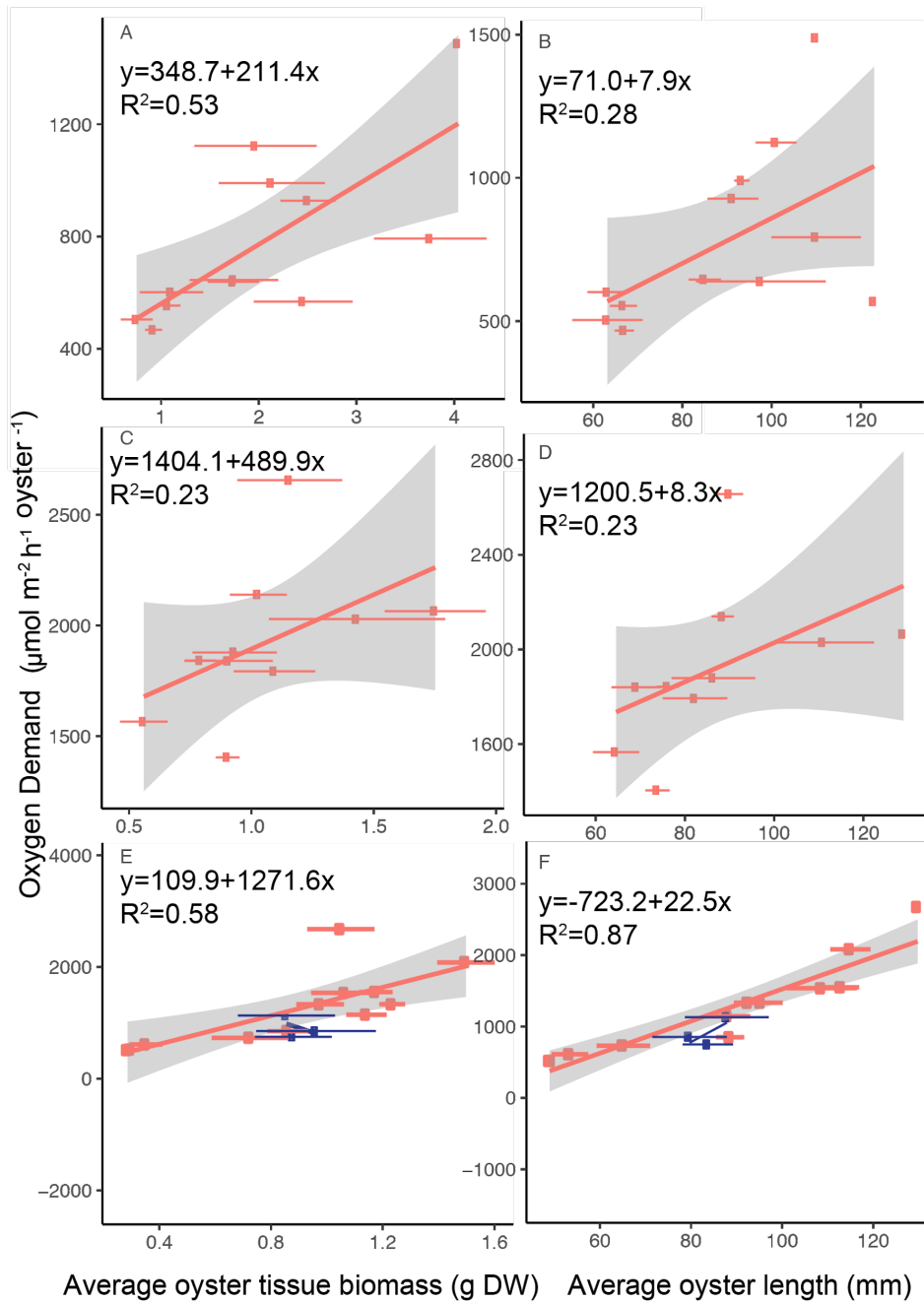


Fig. 5.4 Regressions of average oyster tissue biomass against oxygen demand during (a) May, (c) July, and (e) September. Regressions of average oyster length against oxygen demand during (b) May, (d) July, and (f) September. Blue dots represent oysters that were collected from a Harris Creek restoration site in 2017.

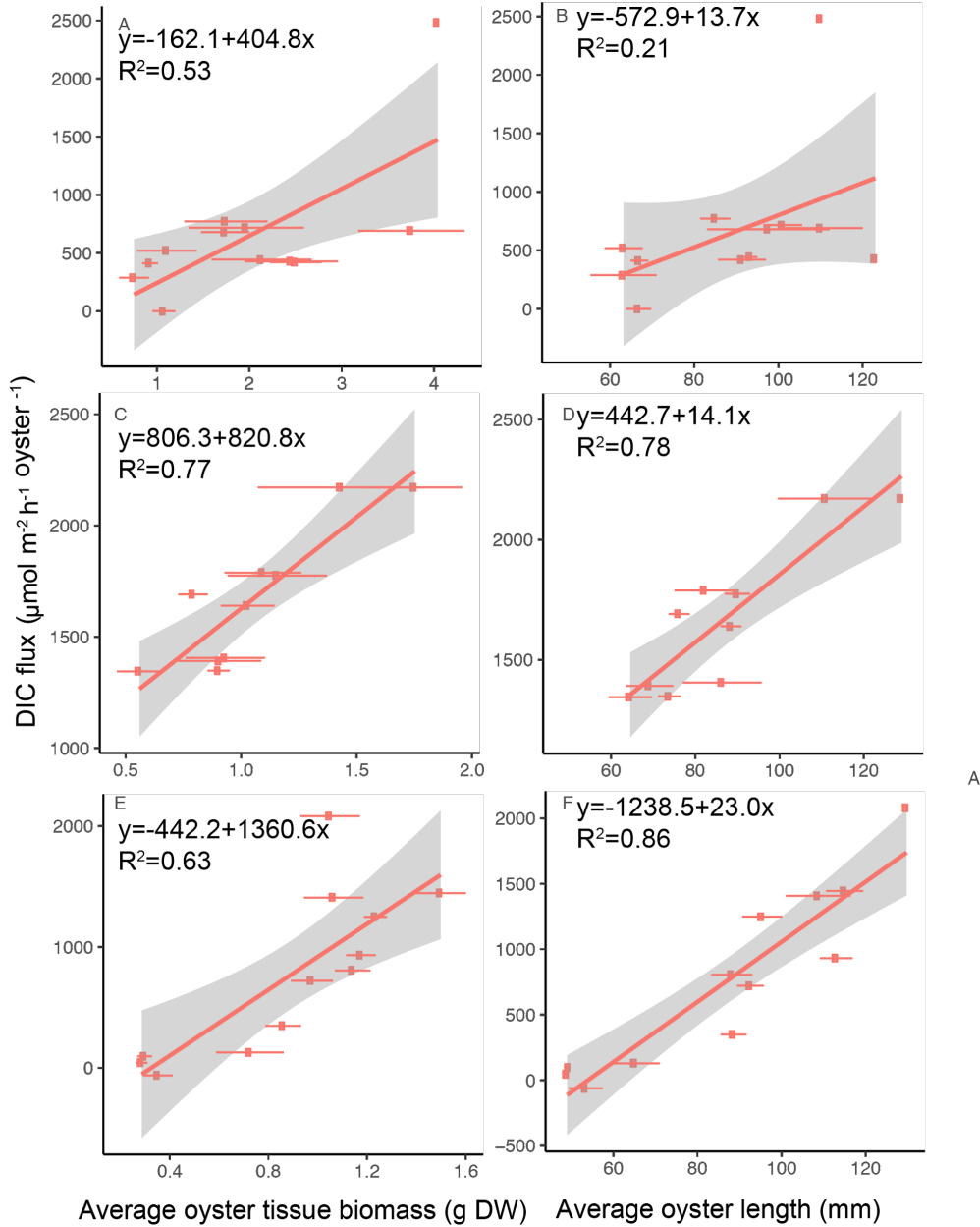


Fig. 5.5 Regressions of average oyster tissue biomass against DIC fluxes during (a) May, (c) July, and (e) September. Regressions of average oyster length against DIC fluxes during (b) May, (d) July, and (f) September.

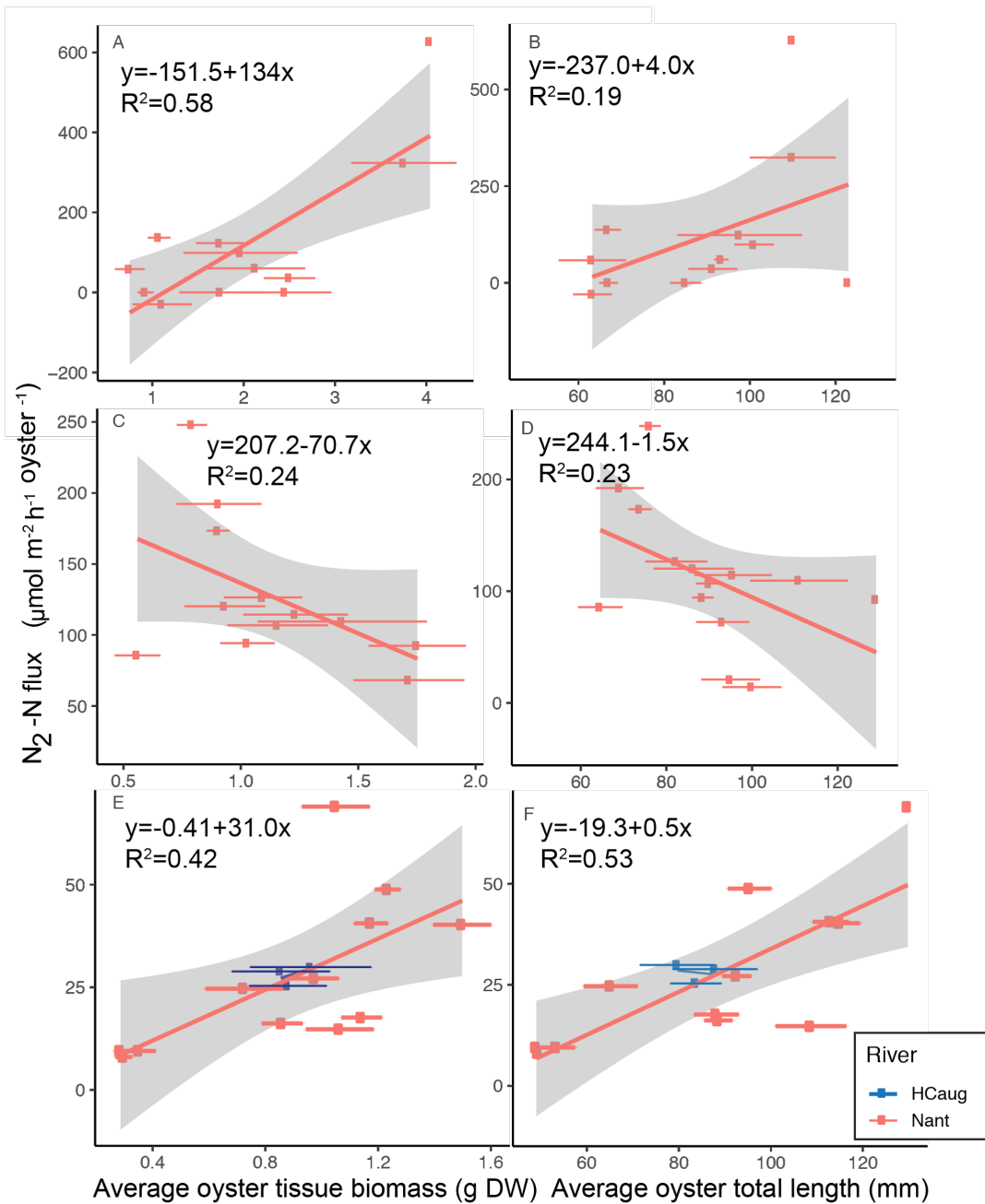


Fig. 5.6 Regressions of average oyster tissue biomass against denitrification during (a) May, (c) July, and (e) September. Regressions of average oyster length against denitrification during (b) May, (d) July, and (f) September. Blue dots represent oysters that were collected from a Harris Creek restoration site in 2017.

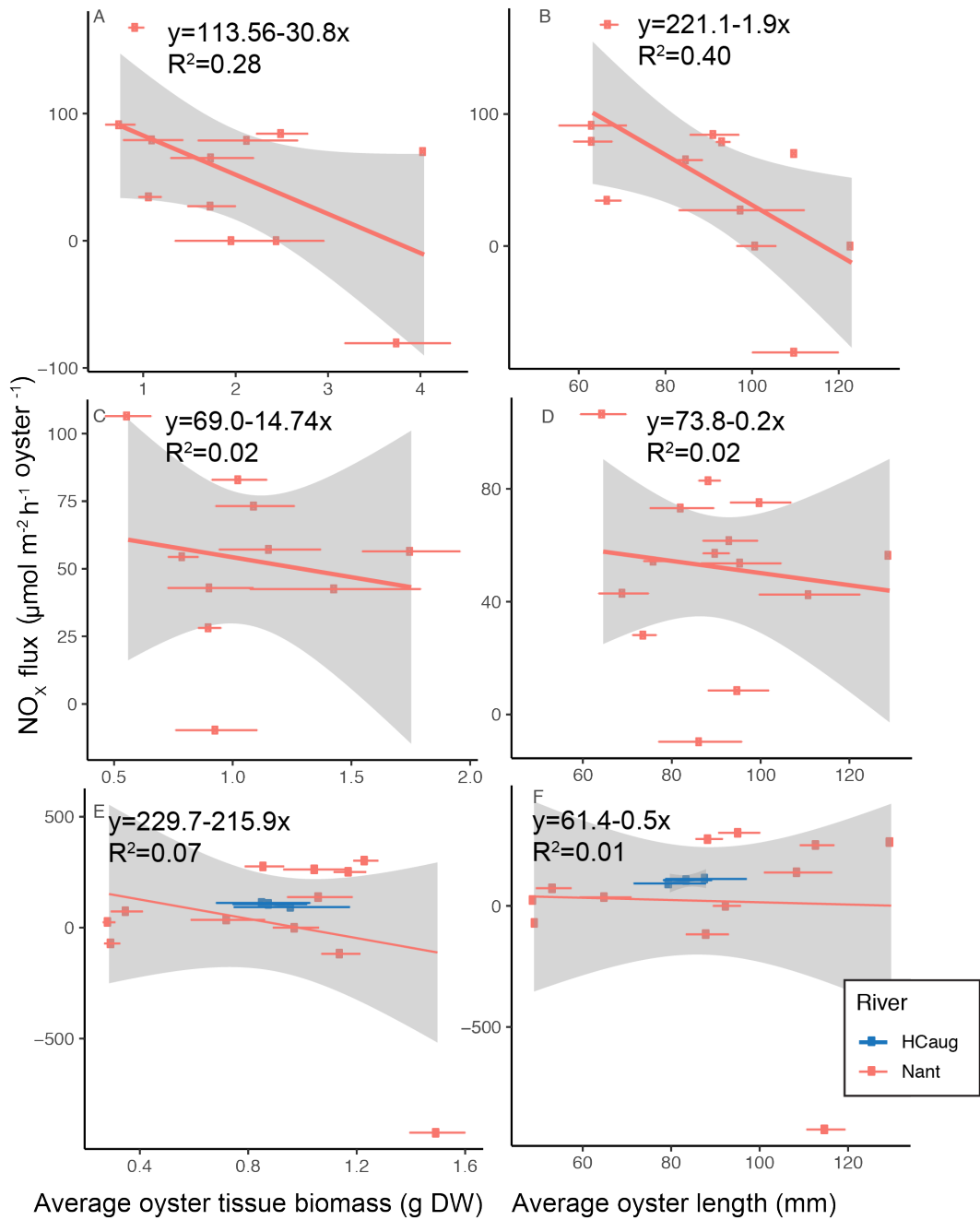


Fig. 5.7 Regressions of average oyster tissue biomass against NO_x fluxes during (a) May, (c) July, and (e) September. Regressions of average oyster length against NO_x fluxes during (b) May, (d) July, and (f) September. Blue dots represent oysters that were collected from a Harris Creek restoration site in 2017.

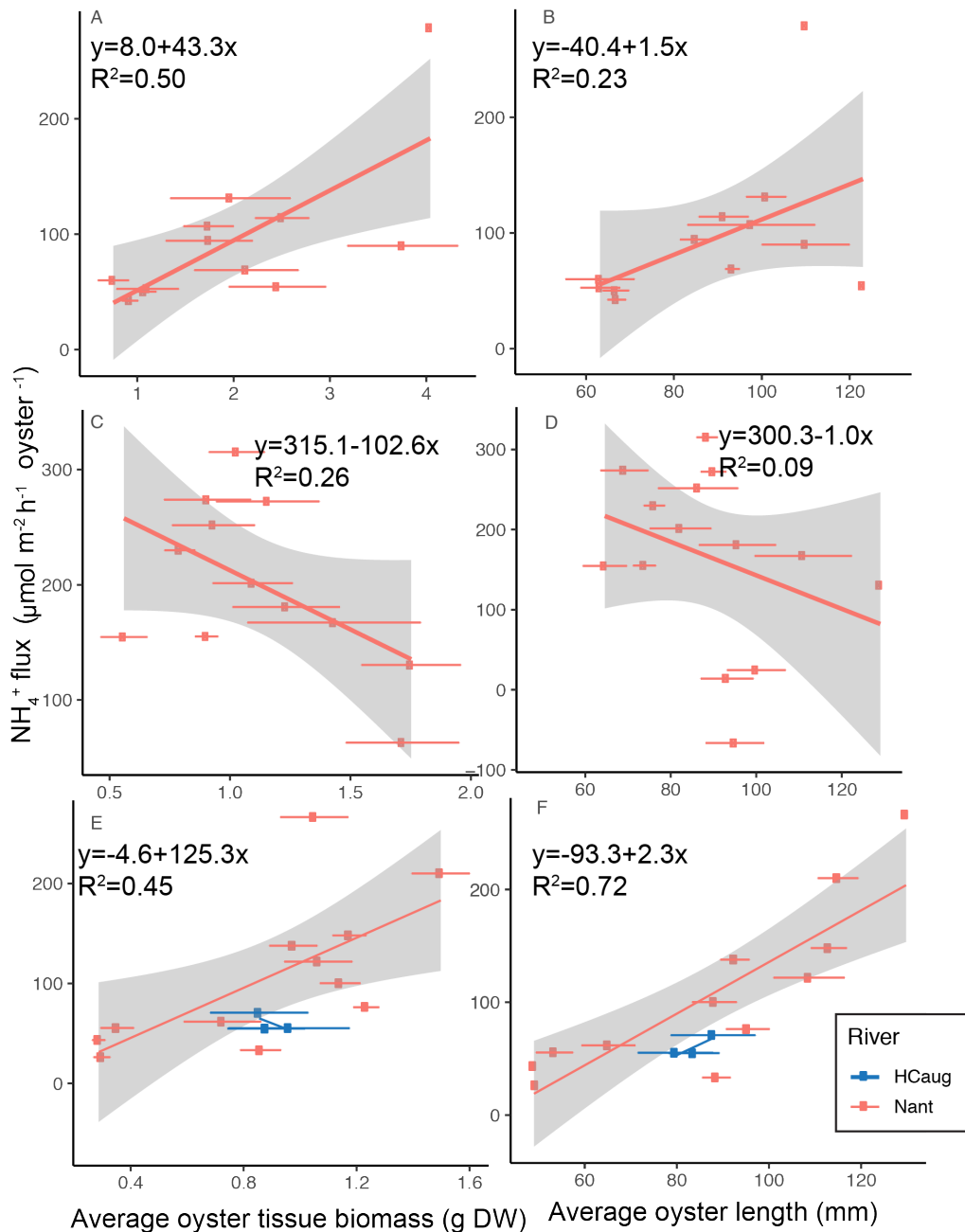


Fig. 5.8 Regressions of average oyster tissue biomass against NH_4^+ fluxes during (a) May, (c) July, and (e) September. Regressions of average oyster length against NH_4^+ fluxes during (b) May, (d) July, and (f) September. Blue dots represent oysters that were collected from a Harris Creek restoration site in 2017.

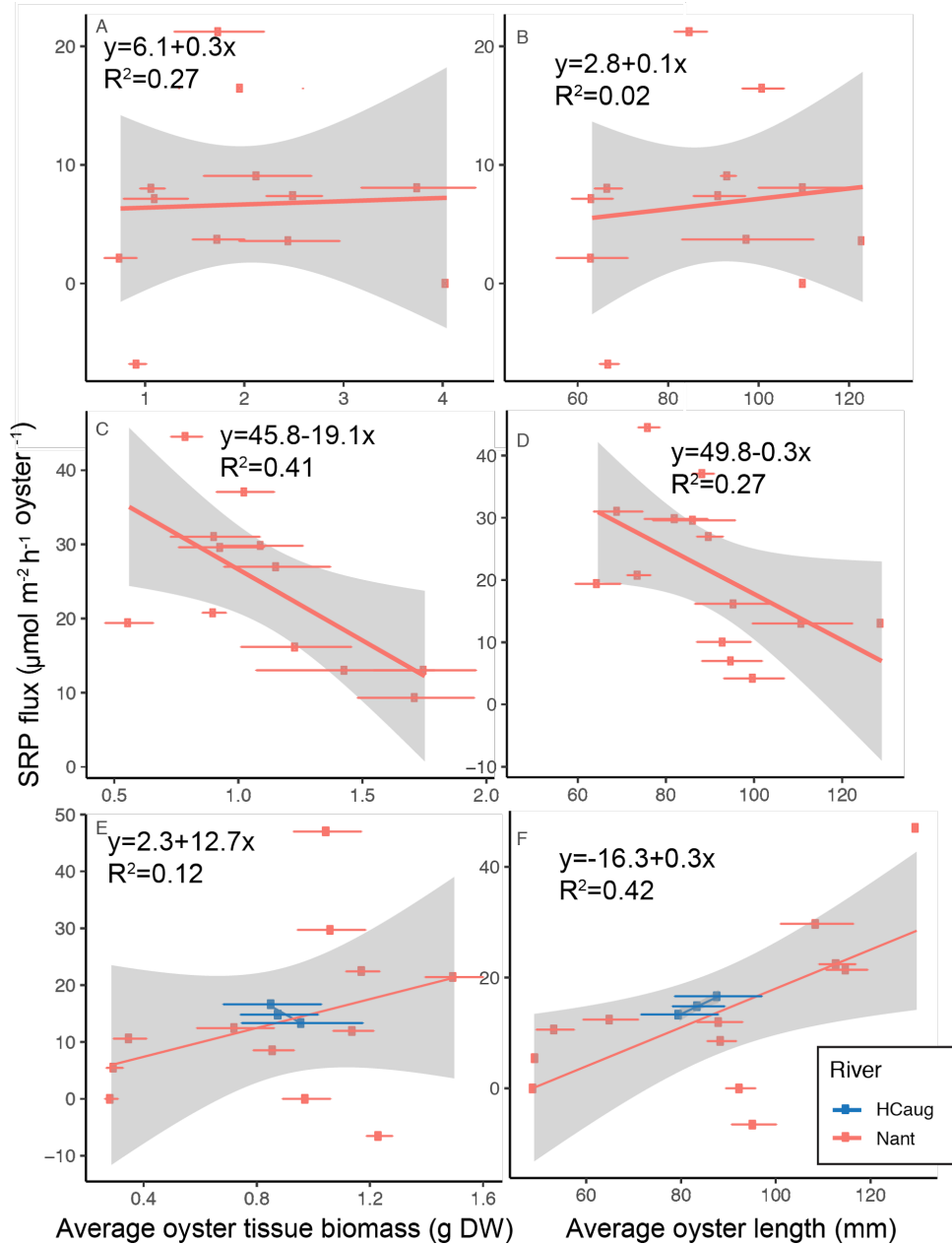


Fig. 5.9 Regressions of average oyster tissue biomass against SRP fluxes during (a) May, (c) July, and (e) September. Regressions of average oyster length against SRP fluxes during (b) May, (d) July, and (f) September. Blue dots represent oysters that were collected from a Harris Creek restoration site in 2017.

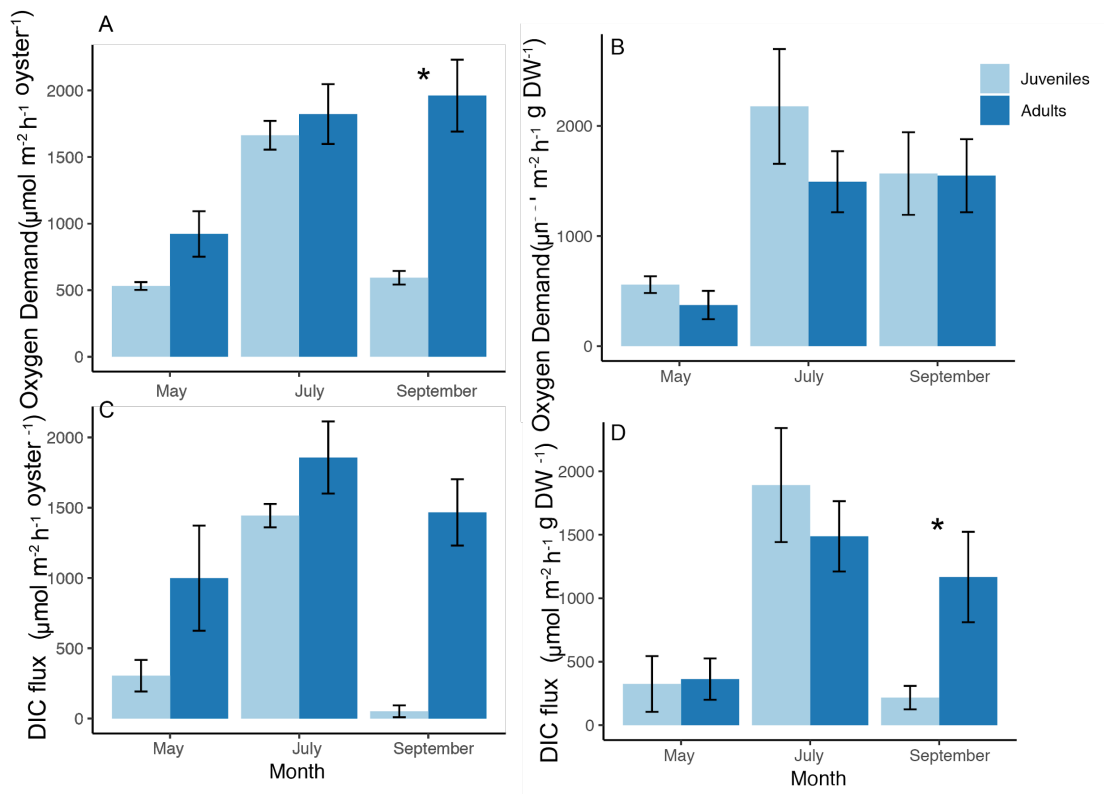


Fig. 5.10 Respiration-based oyster driven fluxes of oxygen demand normalized by (a) oyster and (b) oyster dry weight. Respiration-based oyster driven fluxes of DIC normalized by (c) oyster and (d) oyster dry weight. Mean \pm SE (n=4). Asterisks indicate significant differences between oyster sizes for each month (one-way ANOVA, $\alpha=0.05$).

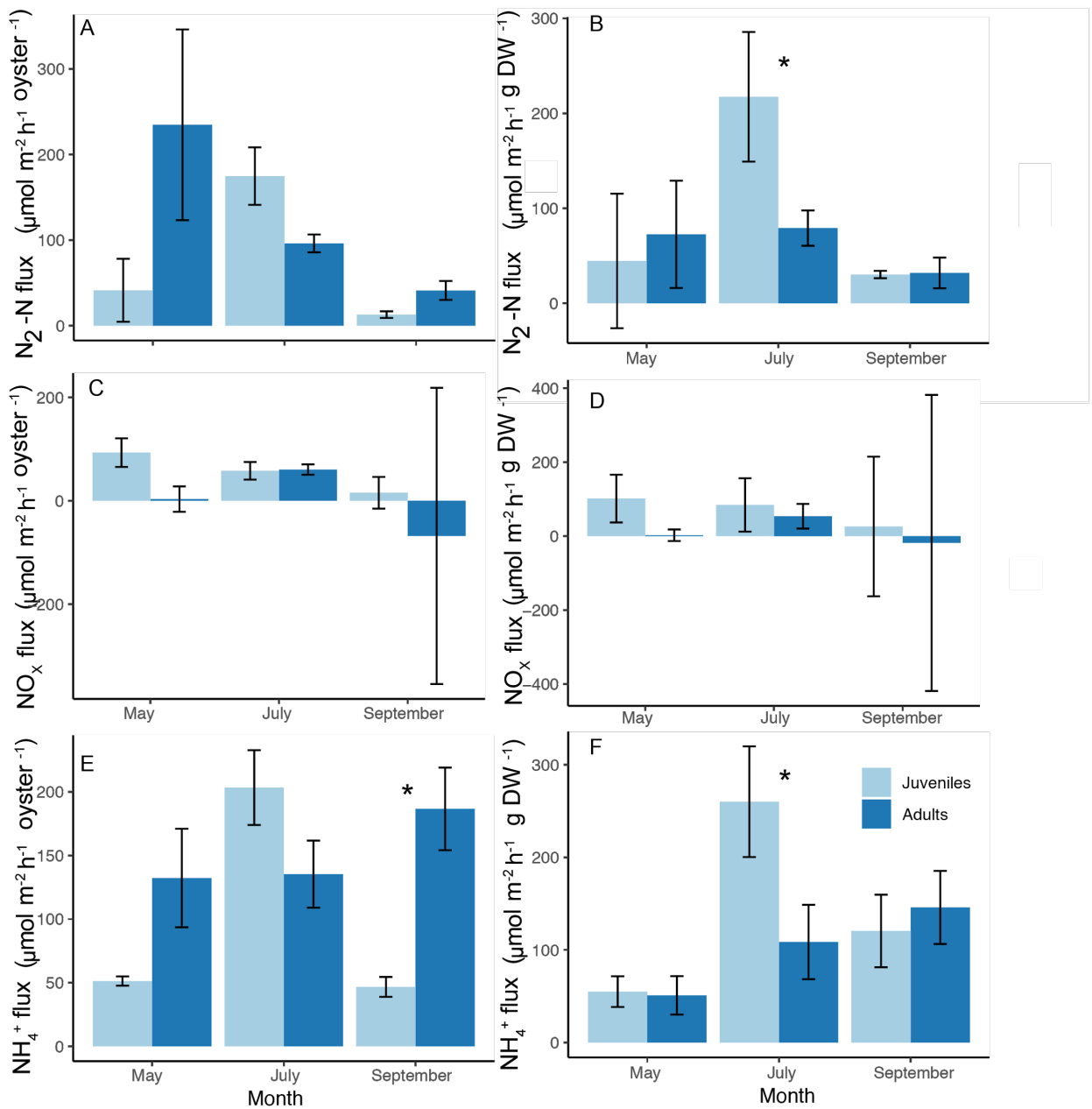


Fig. 5.11 Denitrification rates normalized by (a) oyster and (b) oyster dry weight. NO_x fluxes normalized by (c) oyster and (d) oyster dry weight. NH_4^+ fluxes normalized by (e) oyster and (f) oyster dry weight. Mean \pm SE (n=4). Asterisks indicate significant difference between oyster sizes for each month (one-way ANOVA, $\alpha=0.05$).

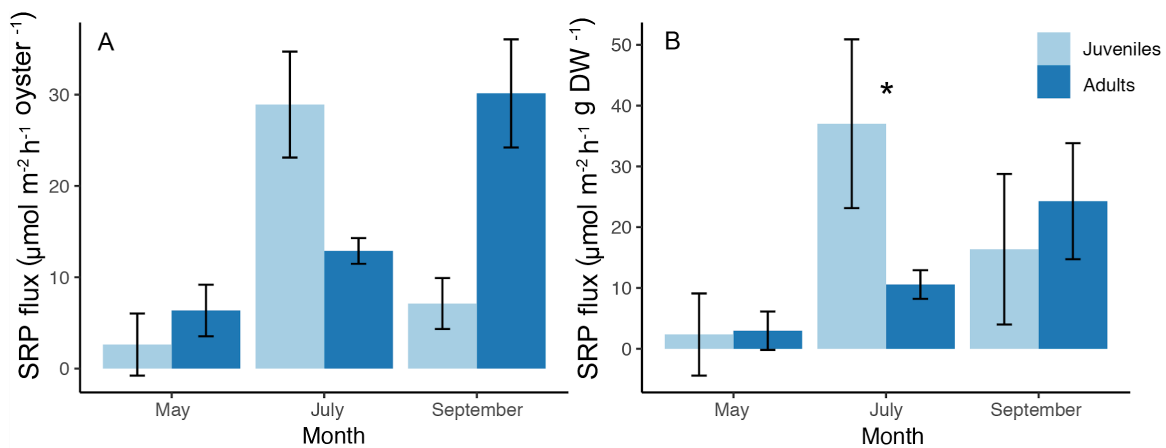


Fig. 5.12 SRP fluxes normalized by (a) oyster and (b) oyster dry weight. Mean \pm SE (n=4). Asterisks indicate significant difference between oyster sizes for each month (one-way ANOVA, $\alpha=0.05$).

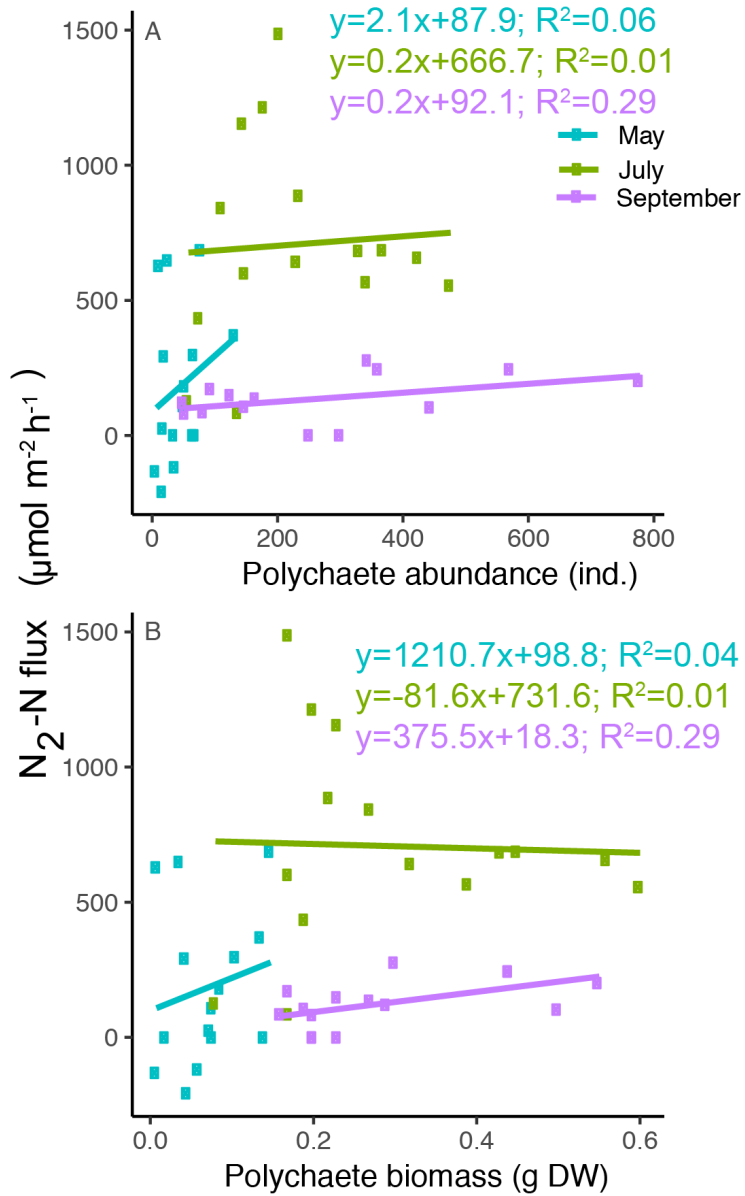


Fig. 5.13 Regressions of (a) polychaete abundance and (b) polychaete biomass against chamber denitrification rates.

Chapter 6: Conclusions

This research on oyster-associated biogeochemistry involved three different methods in two types of oyster sustainability efforts: oyster restoration in Harris Creek, a tributary to the Choptank River; and an on-bottom aquaculture lease in the Nanticoke River, a major tributary to the Chesapeake Bay. Growing interest in using oysters to extract nitrogen from eutrophic coastal waters, along with observations of differential oyster associated denitrification rates, lead to the following dissertation questions. Do current methods for measuring oyster-associated denitrification capture the natural variability and enough benthos to provide reliable estimates for assessment of nutrient benefits? If so, how does an oyster compare to other parts of the oyster habitat in terms of biogeochemical cycling? Finally, is it the oyster or the environment that determines the balance of denitrification enhancement versus remineralization? The overall goal of oyster restoration and aquaculture are the same: to seed the Bay with more oysters while providing ecosystem services, such as nitrogen removal. This work provided an opportunity to investigate whether sediment-based biogeochemical concepts hold true for oysters and learn about the influence of oysters and associated activities on overall biogeochemistry.

Combined, the chapters illustrate how important oysters are to the overall biogeochemistry of restoration reefs and aquaculture. A synthesis of my work and previous studies puts the oyster into context relative to sediments and an entire oyster reef (Table 6.1). Rates of denitrification associated with sediments from oyster aquaculture in my study are compatible with previous research on sediments adjacent to oyster reefs or

below floating aquaculture, such as estuarine environments in Maryland, North Carolina, Louisiana, and New York (Holyoke 2008; Piehler and Smyth 2011b; Smyth et al. 2013; Hoellein and Zarnoch 2014; Testa et al. 2015; Westbrook 2016). However, other than potentially muddy sediments or long residence times, which would concentrate the deposition of biodeposits in one area and ultimately reduce denitrification rates (Newell 2004), it is unclear why oyster-associated sediments had such low rates in Virginia (Lunstrum et al. 2017; Smyth et al. 2018). Meanwhile, this work has revealed that oysters can support rates of denitrification that are equivalent or higher than fluxes estimated from sediment cores. Likewise, Smyth et al. (2013) and Arfken et al. (2017) have observed denitrification rates from single oysters of approximately $400 \mu\text{mol m}^{-2} \text{h}^{-1}$. Incubations of oysters alone, by Caffrey et al. (2016) have produced estimates that are approximately ten-fold lower ($40.6 \mu\text{mol m}^{-2} \text{h}^{-1}$ for an abundance of 130 oysters). Denitrification rates ranging from $250\text{-}1590 \mu\text{mol m}^{-2} \text{h}^{-1}$ have been measured from total reef (oysters and sediments) incubations from previous work in Harris Creek, MD and Ninigret Pond, RI. Interestingly, in Chapter 2 I learned that separate rates from sediments and oysters are not additive. Overall, oysters alone provide conservative estimates of denitrification; however, this assumption requires an understanding of the ambient remineralization conditions without oysters.

In general, oysters may support just as much denitrification as sediments; however, it is evident that oyster biogeochemistry is controlled by many of the same factors that regulate sediment biogeochemistry. Sediment biogeochemistry is commonly regulated by water column concentrations of NO_x (Kemp et al. 1990). It has not been clear how oyster-associated denitrification is regulated by NO_x . This work has shown that

NO_x concentrations influence denitrification rates following aquaculture dredging and rates associated with the live oysters. Similar results of elevated denitrification fluxes following the addition of NO₃⁻ have been observed from clam aquaculture sediments (Smyth et al. 2018). Likewise, denitrification rates from oysters alone and sediment incubations show similar responses in denitrification rates with changes in seasonal temperatures. For example, denitrification rates decreased from May to July as temperatures increased, which reinforced my understanding that coupled nitrification/denitrification depends on temperature. In addition, temperature controlled oyster dry weight biomass, which may also regulate oyster-associated rates of denitrification. Incubations of oysters alone in Chapter 5 did not assess the role of phytoplankton availability in determining denitrification rates; however, decreased chlorophyll *a* in July sediment incubations likely provided little organic matter to be mineralized.

Depending on seasonal conditions, oyster grow-out methods play an important role in modulating benthic biogeochemistry. As demonstrated by the impact of aquaculture dredging on fluxes in May and September, understanding how aquaculture gear works on an aquaculture lease is necessary. Further work must take into consideration: the size of the oysters, oyster density, oyster location (i.e., surface floats, rack and bag, or on-bottom), and the residence time at the aquaculture lease. In addition to grow-out methods, it is known that oysters can grow in different tidal zones, salinities, and they can be genetically different (i.e., triploid vs. diploid). It is unknown how these factors may influence oyster-associated biogeochemistry. All of these factors have

potential consequences for determining whether denitrification or remineralization dominates in a system.

Oyster sustainability efforts are likely to continue to increase over time. In fact, from 2016 to 2017 global molluscan production has grown by 3% (FAO UN 2019). Therefore, provided that oysters are grown in favorable denitrification environmental conditions, this work adds to the growing consensus that oysters can play an important role in mitigating nitrogen in coastal areas. As established by the nonadditive nature of fluxes measured from sediments and oysters, oyster-associated biogeochemical interactions are complex, and require future research to tease apart the driving mechanisms.

Table 6.1 Summary of previous research on oyster-associated denitrification. Standard deviations are provided for denitrification rates if they were stated in the text. “~” denotes rates that were estimated from figures. SH stands for shell height. The units from the data for chapter 5 are $\mu\text{mol m}^{-2} \text{h}^{-1}$ per gram DW.

Location	Experiment	Denitrification rate ($\mu\text{mol m}^{-2} \text{h}^{-1}$)	Water Depth (m)	Oyster background info	Reference
La Trappe Creek, MD	Under floating aquaculture, La Trappe Creek	70.8±5.4	0.7-2	NA	Holyoke 2008
Bogue Sound, NC	Sediments adjacent to oyster reef	range from ~75-190	NA	NA	Piehler and Smyth 2011
Choptank River, MD	Restored reef (oysters+sediment)	250±60 to 1590±220	4	average SH 114 mm	Kellogg et al. 2013

Calico Creek, NC	live oyster, sediment, both	~400 (oyster), ~100 (sediment), ~200 (both)	NA	intertidal flat, outer shell scrubbed prior, average SH 93.3 mm	Smyth et al. 2013
Jamaica Bay, NY	incubated sandy sediments below oysters deployed 7 cm away from sandy sediment	~100 (PD)	1-1.5	Oyster densities 40-150 oysters m ⁻² , average SH 86.1 mm	Hoellein and Zarnoch 2014
Back Sound, NC	Sediments adjacent to oyster reef	~210 (mudflat), ~200 (marsh), ~200 (seagrass)	NA	restored oyster reefs in mudflat, marsh, and seagrass	Smyth et al. 2015
Choptank River, MD	Sediments below aquaculture	55.8±20.8	0.5-1.5	surface floats; 662 oysters per tray; average SH 54 mm	Testa et al. 2015
Pensacola Bay, FL	Oysters alone	40.6 (for an abundance of 130 oysters m ⁻²)	NA	SH >71.5 mm	Caffrey et al. 2016
Ninigret Pond, RI	restored reef (oysters+sediment); below aquaculture bags	581.9±164.2 (restored); 346.1±168.6 (aquaculture); 60.9±44.3 (cultch)	0.4-1.2	~54 oysters m ⁻² , SH 55mm (restored reef); 700 oysters m ⁻² (aquaculture)	Humphries et al. 2016
Atlantic Beach, NC	Oysters along, shell alone, sediment alone	364.4±23.5 (live oysters), 355.3±6.4 (shell), 270.5±20.1 (sediment)	NA	NA	Arfken et al. 2017

Cherrystone Inlet, VA	Sediments below aquaculture	9.6±2.0 to 19.2±1.4 (January-April)	1.1	rack and bag method; 300 oysters per bag or 70 harvested oysters m ⁻²	Lunstrum et al. 2017
Smith Island Bay, VA	sediments adjacent to restored oyster reef	~17	0.4		Smyth et al. 2018
Harris Creek, MD	restored Oysters+sediments, oysters alone	370±200 (oysters+sed); 310±140 (oysters)	~1.0		Jackson et al. 2018 (Chapter 2)
Sister Lake, LA	Sediments adjacent to oyster reef	562.5±208.4 (shallow); 649.2±165.5 (Deep)	shallow (<1), deep (>1)	shallow-water reef and deep-water reef with SH >75 mm	Westbrook et al. 2019
Nanticoke River, MD	sediments between oysters on-bottom aquaculture with and without harvest	74.9±313.7 (harvest), 72.9±150.8 (nonharvest)	1.5	~40 oysters m ⁻²	Chapter 4
Nanticoke River, MD	oysters alone	[-83.2±35.8 (shell); 134.4 per g in May, -70.7 per gram DW July, 31.04 per g DW September]	1.5	oysters were planted on the bottom	Chapter 5

References

- Allison, Stuart K., and Stephen D. Murphy. 2017. *Routledge Handbook of Ecological and Environmental Restoration*. Taylor & Francis.
- Arfken, Ann, Bongkeun Song, Jeff S. Bowman, and Michael Piehler. 2017. Denitrification Potential of the Eastern Oyster Microbiome Using a 16S rRNA Gene Based Metabolic Inference Approach. *PloS One* 12 (9): e0185071.
- Asmus, Ragnhild M., and Harald Asmus. 1991. Mussel Beds: Limiting or Promoting Phytoplankton? *Journal of Experimental Marine Biology and Ecology* 148 (2): 215–32.
- Bahr, Leonard M. 1974. Aspects of the Structure and Function of the Intertidal Oyster Reef Community in Georgia. University of Georgia.
- Barnes, Debra. 1991. *Final Policy and Generic Environmental Impact Statement on Management of Shellfish in Uncertified Areas Program*. New York State Department of Environmental Conservation.
- Bayne, B. L. 2009. Carbon and Nitrogen Relationships in the Feeding and Growth of the Pacific Oyster, *Crassostrea Gigas* (Thunberg). *Journal of Experimental Marine Biology and Ecology* 374 (1): 19–30.
- . 2017. Chapter 10 - Oysters and the Ecosystem. In *Developments in Aquaculture and Fisheries Science*, edited by Brian Bayne, 41:703–834. Elsevier.
- Bayne, B. L., and A. J. S. Hawkins. 1992. Ecological and Physiological Aspects of Herbivory in Benthic Suspension-Feeding Molluscs. *Plant-Animal Interactions in the Marine Benthos. Systematics Association Special Volume* 46: 265–88.
- Bayne, B. L., and R. C. Newell. 1983. 9 - Physiological Energetics of Marine Molluscs. In *The Mollusca*, edited by A. S. M. Saleuddin and Karl M. Wilbur, 407–515. Academic Press.
- Bayne, Brian Leicester. 2017. *Biology of Oysters*. Academic Press.
- Beck, Michael W., Robert D. Brumbaugh, Laura Airoidi, Alvar Carranza, Loren D. Coen, Christine Crawford, Omar Defeo, Graham J. Edgar, Boze Hancock, and Matthew C. Kay. 2011. Oyster Reefs at Risk and Recommendations for Conservation, Restoration, and Management. *Bioscience* 61 (2): 107–16.
- Beiras, R., A. Pérez Camacho, and M. Albentosa. 1995. Short-Term and Long-Term Alterations in the Energy Budget of Young Oyster *Ostrea Edulis* L. in Response to Temperature Change. *Journal of Experimental Marine Biology and Ecology* 186 (2): 221–36.

- Boucher, Guy, and Renata Boucher-Rodoni. 1988. In Situ Measurement of Respiratory Metabolism and Nitrogen Fluxes at the Interface of Oyster Beds. *Marine Ecology Progress Series. Oldendorf* 44 (3): 229–38.
- Breitburg, Denise, Lisa A. Levin, Andreas Oschlies, Marilaure Grégoire, Francisco P. Chavez, Daniel J. Conley, Véronique Garçon, et al. 2018. Declining Oxygen in the Global Ocean and Coastal Waters. *Science* 359 (6371). <https://doi.org/10.1126/science.aam7240>.
- Bricker, Suzanne B., Joao Gomes Ferreira, Changbo Zhu, Julie M. Rose, Eve Galimany, Gary Wikfors, Camille Saurel, et al. 2018. Role of Shellfish Aquaculture in the Reduction of Eutrophication in an Urban Estuary. *Environmental Science & Technology* 52 (1): 173–83.
- Burgin, Amy J., and Stephen K. Hamilton. 2007. Have We Overemphasized the Role of Denitrification in Aquatic Ecosystems? A Review of Nitrate Removal Pathways. *Frontiers in Ecology and the Environment* 5 (2): 89–96.
- Burkholder, Joann M., and Sandra E. Shumway. 2011. Bivalve Shellfish Aquaculture and Eutrophication. In *Shellfish Aquaculture and the Environment*, edited by Sandra E. Shumway, 58:155–215. Systematics Association, Special Volume No. Oxford, UK: Wiley-Blackwell.
- Caffrey, Jane M., James T. Hollibaugh, and Behzad Mortazavi. 2016. Living Oysters and Their Shells as Sites of Nitrification and Denitrification. *Marine Pollution Bulletin*.
- Cai, Wei-jun, and Yongchen Wang. 1998. The Chemistry, Fluxes, and Sources of Carbon Dioxide in the Estuarine Waters of the Satilla and Altamaha Rivers, Georgia. *Limnology and Oceanography* 43 (4): 657–68.
- Cerco, Carl F., and Mark R. Noel. 2005. Evaluating Ecosystem Effects of Oyster Restoration in Chesapeake Bay. *Report of US Army Engineer Research and Development Center, Vicksburg MS*. http://dnr.maryland.gov/fisheries/Documents/CercoandNoel_final.pdf.
- . 2007. Can Oyster Restoration Reverse Cultural Eutrophication in Chesapeake Bay? *Estuaries and Coasts* 30 (2): 331–43.
- Cline, Joel D. 1969. Spectrophotometric Determination of Hydrogen Sulfide in Natural Waters 1. *Limnology and Oceanography* 14 (3): 454–58.
- Cloern, James E. 2001. Our Evolving Conceptual Model of the Coastal Eutrophication Problem. *Marine Ecology Progress Series* 210 (2001): 223–53.
- Coen, Loren D., and Melanie J. Bishop. 2015. The Ecology, Evolution, Impacts and Management of Host–parasite Interactions of Marine Molluscs. *Journal of Invertebrate Pathology* 131

- (October): 177–211.
- Coen, Loren D., Robert D. Brumbaugh, David Bushek, Ray Grizzle, Mark W. Luckenbach, Martin H. Posey, Sean P. Powers, and Sgregory Tolley. 2007. Ecosystem Services Related to Oyster Restoration. *Marine Ecology Progress Series* 341: 303–7.
- Coen, Loren Dean. 1995. *A Review of the Potential Impacts of Mechanical Harvesting on Subtidal and Intertidal Shellfish Resources*. South Carolina Department of Natural Resources, Marine Resources Research Institute Charleston, SC.
- Coen, Loren D., and Austin T. Humphries. 2017. Oyster-Generated Marine Habitats: Their Services, Enhancement, Restoration and Monitoring. In *Routledge Handbook of Ecological and Environmental Restoration*, edited by Stuart K. Allison and Stephen D. Murphy, 274–94. Taylor & Francis.
- Cornwell, Jeffrey C., W. Michael Kemp, and Todd M. Kana. 1999. Denitrification in Coastal Ecosystems: Methods, Environmental Controls, and Ecosystem Level Controls, a Review. *Aquatic Ecology* 33 (1): 41–54.
- Cornwell, Jeffrey C., Michael S. Owens, and Lisa M. Kellogg. 2016. Integrated Assessment of Oyster Reef Ecosystem Services: Quantifying Denitrification Rates and Nutrient Fluxes. *Integrated Assessment* 3: 16–2016.
- Cornwell, Jeff, Julie Rose, Lisa Kellogg, Mark Luckenbach, Suzanne Bricker, Ken Paynter, Chris Moore, Matt Parker, Larry Sanford, and Bill Wolinski. 2016. Panel Recommendations on the Oyster BMP Nutrient and Suspended Sediment Reduction Effectiveness Determination Decision Framework and Nitrogen and Phosphorus Assimilation in Oyster Tissue Reduction Effectiveness for Oyster Aquaculture Practices.
- Cox, C., and R. Mann. 1992. Temporal and Spatial Changes in Fecundity of Eastern Oysters, *Crassostrea Virginica* (Gmelin, 1791) in the James River, Virginia. *Journal of Shellfish Research* 11: 49–54.
- Crawford, Christine M., Catriona K. A. Macleod, and Iona M. Mitchell. 2003. Effects of Shellfish Farming on the Benthic Environment. *Aquaculture* 224 (1): 117–40.
- Dame, Richard F. 2016. *Ecology of Marine Bivalves: An Ecosystem Approach*. CRC press.
- Dame, Richard F., John D. Spurrier, and Thomas G. Wolaver. 1989. Carbon, Nitrogen and Phosphorus Processing by an Oyster Reef. *Marine Ecology Progress Series* 54 (3): 249–56.
- Dame, Richard F., John D. Spurrier, and Richard G. Zingmark. 1992. In Situ Metabolism of an Oyster Reef. *Journal of Experimental Marine Biology and Ecology* 164 (2): 147–59.

- Dame, Richard F., Richard G. Zingmark, and Elizabeth Haskin. 1984. Oyster Reefs as Processors of Estuarine Materials. *Journal of Experimental Marine Biology and Ecology* 83 (3): 239–47.
- Dame, R., and S. Libes. 1993. Oyster Reefs and Nutrient Retention in Tidal Creeks. *Journal of Experimental Marine Biology and Ecology* 171 (2): 251–58.
- DeAlteris, Joseph, Brian D. Kilpatrick, and Robert B. Rheault. 2004. A Comparative Evaluation of the Habitat Value of Shellfish Aquaculture Gear, Submerged Aquatic Vegetation and a Non-Vegetated Seabed. Fisheries, Animal and Veterinary Sciences Faculty Publications, . https://digitalcommons.uri.edu/favs_facpubs/26/.
- Diaz, R. J., and R. Rosenberg. 1995. Marine Benthic Hypoxia: A Review of Its Ecological Effects and the Behavioural Responses of Benthic Macrofauna. *Oceanography and Marine Biology: An Annual Review*.
- D. Krom, Michael, and Robert A. Berner. 1981. The Diagenesis of Phosphorus in a Nearshore Marine Sediment. *Geochimica et Cosmochimica Acta* 45 (2): 207–16.
- Doane, Timothy A., and William R. Horwath. 2003. Spectrophotometric Determination of Nitrate with a Single Reagent. *Analytical Letters* 36 (12): 2713–22.
- Dumbauld, Brett R., Jennifer L. Ruesink, and Steven S. Rumrill. 2009. The Ecological Role of Bivalve Shellfish Aquaculture in the Estuarine Environment: A Review with Application to Oyster and Clam Culture in West Coast (USA) Estuaries. *Aquaculture* 290 (3): 196–223.
- Ehrich, Melinda K., and Lora A. Harris. 2015. A Review of Existing Eastern Oyster Filtration Rate Models. *Ecological Modelling* 297: 201–12.
- Eyre, Bradley D., Søren Rysgaard, Tage Dalsgaard, and Peter Bondo Christensen. 2002. Comparison of Isotope Pairing and N₂:Ar Methods for Measuring Sediment denitrification—Assumption, Modifications, and Implications. *Estuaries* 25 (6): 1077–87.
- Feinman, Sarah G., Yuna R. Farah, Jonathan M. Bauer, and Jennifer L. Bowen. 2017. The Influence of Oyster Farming on Sediment Bacterial Communities. *Estuaries and Coasts*, 1–15.
- Food and Agriculture Organization of the United Nations. 2018. *2018 The State of World Fisheries and Aquaculture: Meeting the Sustainable Development Goals*. Food & Agriculture Org.
- Frankignoulle, Michel, Christine Canon, and Jean-Pierre Gattuso. 1994. Marine Calcification as a

- Source of Carbon Dioxide: Positive Feedback of Increasing Atmospheric CO₂.
Limnology and Oceanography 39 (2): 458–62.
- Fulford, R. S., D. L. Breitburg, R. I. E. Newell, W. M. Kemp, and M. Luckenbach. 2007. Effects of Oyster Population Restoration Strategies on Phytoplankton Biomass in Chesapeake Bay: A Flexible Modeling Approach. *Marine Ecology Progress Series* 336 (April): 43–61.
- Giles, Hilke, Conrad A. Pilditch, and Dudley G. Bell. 2006. Sedimentation from Mussel (*Perna Canaliculus*) Culture in the Firth of Thames, New Zealand: Impacts on Sediment Oxygen and Nutrient Fluxes. *Aquaculture* 261 (1): 125–40.
- Glibert, Patricia M., Frances P. Wilkerson, Richard C. Dugdale, John A. Raven, Christopher L. Dupont, Peter R. Leavitt, Alexander E. Parker, Joann M. Burkholder, and Todd M. Kana. 2015. Pluses and Minuses of Ammonium and Nitrate Uptake and Assimilation by Phytoplankton and Implications for Productivity and Community Composition, with Emphasis on Nitrogen-enriched Conditions. *Limnology and Oceanography*.
- Green, Dannielle S., Bas Boots, and Tasman P. Crowe. 2012. Effects of Non-Indigenous Oysters on Microbial Diversity and Ecosystem Functioning. *PloS One* 7 (10): e48410.
- Grizzle, Raymond E., Jennifer K. Greene, and Loren D. Coen. 2008. Seston Removal by Natural and Constructed Intertidal Eastern Oyster (*Crassostrea Virginica*) Reefs: A Comparison with Previous Laboratory Studies, and the Value of in Situ Methods. *Estuaries and Coasts* 31 (6): 1208–20.
- Groffman, Peter M., Mark A. Altabet, J. K. Böhlke, Klaus Butterbach-Bahl, Mark B. David, Mary K. Firestone, Anne E. Giblin, Todd M. Kana, Lars Peter Nielsen, and Mary A. Voytek. 2006. Methods for Measuring Denitrification: Diverse Approaches to a Difficult Problem. *Ecological Applications: A Publication of the Ecological Society of America* 16 (6): 2091–2122.
- Gross, Thomas F., and Arthur R. M. Nowell. 1983. Mean Flow and Turbulence Scaling in a Tidal Boundary Layer. *Continental Shelf Research* 2 (2): 109–26.
- Hagy, James D., Walter R. Boynton, Carolyn W. Keefe, and Kathryn V. Wood. 2004. Hypoxia in Chesapeake Bay, 1950–2001: Long-Term Change in Relation to Nutrient Loading and River Flow. *Estuaries* 27 (4): 634–58.
- Hardison, Amber K., Christopher K. Algar, Anne E. Giblin, and Jeremy J. Rich. 2015. Influence of Organic Carbon and Nitrate Loading on Partitioning between Dissimilatory Nitrate Reduction to Ammonium (DNRA) and N₂ Production. *Geochimica et Cosmochimica*

- Acta* 164 (September): 146–60.
- Hargrave, Barry T. 1972. Aerobic Decomposition of Sediment and Detritus as a Function of Particle Surface Area and Organic Content. *Limnology and Oceanography*.
<https://doi.org/10.4319/lo.1972.17.4.0583>.
- Higgins, Colleen B., Kurt Stephenson, and Bonnie L. Brown. 2011. Nutrient Bioassimilation Capacity of Aquacultured Oysters: Quantification of an Ecosystem Service. *Journal of Environmental Quality* 40 (1): 271–77.
- Higgins, Colleen B., Craig Tobias, Michael F. Piehler, Ashley R. Smyth, Richard F. Dame, Kurt Stephenson, and Bonnie L. Brown. 2013. Effect of Aquacultured Oyster Biodeposition on Sediment N₂ Production in Chesapeake Bay. *Marine Ecology Progress Series* 473: 7–27.
- Hoellein, Timothy J., and Chester B. Zarnoch. 2014. Effect of Eastern Oysters (*Crassostrea Virginica*) on Sediment Carbon and Nitrogen Dynamics in an Urban Estuary. *Ecological Applications: A Publication of the Ecological Society of America* 24 (2): 271–86.
- Hoellein, Timothy J., Chester B. Zarnoch, and Raymond E. Grizzle. 2015. Eastern Oyster (*Crassostrea Virginica*) Filtration, Biodeposition, and Sediment Nitrogen Cycling at Two Oyster Reefs with Contrasting Water Quality in Great Bay Estuary (New Hampshire, USA). *Biogeochemistry* 122 (1): 113–29.
- Holyoke, Rebecca Rae. 2008. Biodeposition and Biogeochemical Processes in Shallow, Mesohaline Sediments of Chesapeake Bay. <https://drum.lib.umd.edu/handle/1903/8025>.
- Humphries, Austin T., Suzanne G. Ayvazian, Joanna C. Carey, Boze T. Hancock, Sinead Grabbert, Donald Cobb, Charles J. Strobel, and Robinson W. Fulweiler. 2016. Directly Measured Denitrification Reveals Oyster Aquaculture and Restored Oyster Reefs Remove Nitrogen at Comparable High Rates. *Frontiers in Marine Science* 3 (74).
<https://doi.org/10.3389/fmars.2016.00074>.
- Hutchinson, S., and L. E. Hawkins. 1992. Quantification of the Physiological Responses of the European Flat Oyster *Ostrea Edulis* to Temperature and Salinity. *The Journal of Molluscan Studies* 58 (2): 215–26.
- Jackson, Melanie, Michael S. Owens, Jeffrey C. Cornwell, and M. Lisa Kellogg. 2018. Comparison of Methods for Determining Biogeochemical Fluxes from a Restored Oyster Reef. *PloS One* 13 (12): e0209799.
- Jones, Nicole L., Janet K. Thompson, Kevin R. Arrigo, and Stephen G. Monismith. 2009. Hydrodynamic Control of Phytoplankton Loss to the Benthos in an Estuarine

- Environment. *Limnology and Oceanography* 54 (3): 952–69.
- Kaiser, M. J., I. Laing, and S. D. Utting. 1998. Environmental Impacts of Bivalve Mariculture. *Journal of Shellfish Research*.
https://www.researchgate.net/profile/Michel_Kaiser/publication/258998107_Environmental_impacts_of_bivalve_mariculture/links/5454c83b0cf2bccc490c8d51/Environmental-impacts-of-bivalve-mariculture.
- Kana, Todd M., Christina Darkangelo, M. Duane Hunt, James B. Oldham, George E. Bennett, and Jeffrey C. Cornwell. 1994. Membrane Inlet Mass Spectrometer for Rapid High-Precision Determination of N₂, O₂, and Ar in Environmental Water Samples. *Analytical Chemistry* 66 (23): 4166–70.
- Kaspar, H. F., P. A. Gillespie, I. C. Boyer, and A. L. MacKenzie. 1985. Effects of Mussel Aquaculture on the Nitrogen Cycle and Benthic Communities in Kenepuru Sound, Marlborough Sounds, New Zealand. *Marine Biology* 85 (2): 127–36.
- Kellogg, M. Lisa, Mark J. Brush, Lisa Kellogg, and Mark Brush. n.d. An Updated Model for Estimating the TMDL-Related Benefits of Oyster Reef Restoration.
https://www.conservationgateway.org/Documents/Harris_Creek_Model_and_Oyster_Reef_Restoration_Benefits.pdf.
- Kellogg, M. Lisa, Jeffrey C. Cornwell, Michael S. Owens, and Kennedy T. Paynter. 2013. Denitrification and Nutrient Assimilation on a Restored Oyster Reef. *Marine Ecology Progress Series* 480: 1–19.
- Kellogg, M. Lisa, Ashley R. Smyth, Mark W. Luckenbach, Ruth H. Carmichael, Bonnie L. Brown, Jeffrey C. Cornwell, Michael F. Piehler, Michael S. Owens, D. Joseph Dalrymple, and Colleen B. Higgins. 2014. Use of Oysters to Mitigate Eutrophication in Coastal Waters. *Estuarine, Coastal and Shelf Science* 151: 156–68.
- Kemp, W. M., W. R. Boynton, J. E. Adolf, D. F. Boesch, W. C. Boicourt, G. Brush, J. C. Cornwell, et al. 2005. Eutrophication of Chesapeake Bay: Historical Trends and Ecological Interactions. *Marine Ecology Progress Series* 303 (November): 1–29.
- Kemp, W. M., P. Sampou, J. Caffrey, M. Mayer, K. Henriksen, and W. R. Boynton. 1990. Ammonium Recycling versus Denitrification in Chesapeake Bay Sediments. *Limnology and Oceanography* 35 (7): 1545–63.
- Kennedy, Victor S., Roger I. E. Newell, and Albert F. Eble. 1996. *The Eastern Oyster: Crassostrea Virginica*. University of Maryland Sea Grant College.
- Kennedy, V. S. 1986. Expected Seasonal Presence of *Crassostrea Virginica* (Gmelin) Larval

- Populations, Emphasizing Chesapeake Bay. *American Malacological Bulletin* 3: 25–29.
- K Henriksen, W. M. Kemp. 1988. Nitrification in Estuarine and Coastal Marine Sediments. In *Nitrogen Cycling in Coastal Marine Environments*, edited by J. Sorensen TH Blackburn, 207–50. Wiley and Sons.
- Kirby, Michael Xavier. 2004. Fishing down the Coast: Historical Expansion and Collapse of Oyster Fisheries along Continental Margins. *Proceedings of the National Academy of Sciences of the United States of America* 101 (35): 13096–99.
- Kyte, Michael A., and Kenneth K. Chew. 1975. A Review of the Hydraulic Escalator Shellfish Harvester and Its Known Effects in Relation to the Soft-Shell Clam, *Mya Arenaria*. <https://repository.library.noaa.gov/view/noaa/14712>.
- Lejart, Morgane, Jacques Clavier, Laurent Chauvaud, and Christian Hily. 2012. Respiration and Calcification of *Crassostrea Gigas*: Contribution of an Intertidal Invasive Species to Coastal Ecosystem CO₂ Fluxes. *Estuaries and Coasts* 35 (2): 622–32.
- Lenihan, Hunter S., and Charles H. Peterson. 2004. Conserving Oyster Reef Habitat by Switching from Dredging and Tonging to Diver-Harvesting. *Fishery Bulletin* 102 (2): 298–305.
- Lorrai, Claudia, Daniel F. McGinnis, Peter Berg, Andreas Brand, and Alfred Wüest. 2010. Application of Oxygen Eddy Correlation in Aquatic Systems. *Journal of Atmospheric and Oceanic Technology* 27 (9): 1533–46.
- Lunstrum, Abby, and Lillian R. Aoki. 2016. Oxygen Interference with Membrane Inlet Mass Spectrometry May Overestimate Denitrification Rates Calculated with the Isotope Pairing Technique: O₂ Interference with MIMS and IPT. *Limnology and Oceanography, Methods / ASLO* 14 (7): 425–31.
- Lunstrum, Abby, Karen McGlathery, and Ashley Smyth. 2017. Oyster (*Crassostrea Virginica*) Aquaculture Shifts Sediment Nitrogen Processes toward Mineralization over Denitrification. *Estuaries and Coasts*, 1–17.
- Mann, Roger, Julia S. Rainer, and Reinaldo Morales-Alamo. 1994. Reproductive Activity of Oysters, *Crassostrea virginica*(Gmelin, 1791) in the James River, Virginia, during 1987-1988. *Journal of Shellfish Research* 13 (1): 157–64.
- Mao, Yuze, Yi Zhou, Hongsheng Yang, and Rucai Wang. 2006. Seasonal Variation in Metabolism of Cultured Pacific Oyster, *Crassostrea Gigas*, in Sanggou Bay, China. *Aquaculture* 253 (1): 322–33.
- Maryland Department of Natural Resources fishing and Boating Services and The University of Maryland Center for Environmental Science. 2018. A Stock Assessment of the Eastern

- Oyster, *Crassostrea Virginica*, in the Maryland Waters of Chesapeake Bay, November.
- McGillis, Wade R., Chris Langdon, Brice Loose, Kimberly K. Yates, and Jorge Corredor. 2011. Productivity of a Coral Reef Using Boundary Layer and Enclosure Methods. *Geophysical Research Letters* 38 (3). <https://onlinelibrary.wiley.com/doi/abs/10.1029/2010GL046179>.
- Meseck, Shannon L., Renée Mercaldo-Allen, Julie M. Rose, Paul Clark, Catherine Kuropat, Jose J. Pereira, and Ronald Goldberg. 2014. Effects of Hydraulic Dredging for *Mercenaria Mercenaria*, Northern Quahog, on Sediment Biogeochemistry. *Journal of the World Aquaculture Society* 45 (3): 301–11.
- Murphy, Anna E., Iris C. Anderson, Ashley R. Smyth, Bongkeun Song, and Mark W. Luckenbach. 2016. Microbial Nitrogen Processing in Hard Clam (*Mercenaria Mercenaria*) Aquaculture Sediments: The Relative Importance of Denitrification and Dissimilatory Nitrate Reduction to Ammonium (DNRA). *Limnology and Oceanography* 61 (5): 1589–1604.
- National Research Council (NRC). 1993. *Managing Wastewater in Coastal Urban Areas*. Edited by Committee on Wastewater Management for Coastal Urban Areas. Washington, DC: The National Academies Press.
- Nelson, Kimberly A., Lynn A. Leonard, Martin H. Posey, Troy D. Alphin, and Michael A. Mallin. 2004. Using Transplanted Oyster (*Crassostrea Virginica*) Beds to Improve Water Quality in Small Tidal Creeks: A Pilot Study. *Journal of Experimental Marine Biology and Ecology* 298 (2): 347–68.
- Newell, Roger I. E. 1988. Ecological Changes in Chesapeake Bay: Are They the Result of Overharvesting the American Oyster, *Crassostrea Virginica*. *Understanding the Estuary: Advances in Chesapeake Bay Research* 129: 536–46.
- . 2004. Ecosystem Influences of Natural and Cultivated Populations of Suspension-Feeding Bivalve Molluscs: A Review. *Journal of Shellfish Research* 23 (1): 51–62.
- Newell, Roger I. E., Jeffrey C. Cornwell, and Michael S. Owens. 2002. Influence of Simulated Bivalve Biodeposition and Microphytobenthos on Sediment Nitrogen Dynamics: A Laboratory Study. *Limnology and Oceanography* 47 (5): 1367–79.
- Newell, Roger I. E., T. R. Fisher, R. R. Holyoke, and J. C. Cornwell. 2005. Influence of Eastern Oysters on Nitrogen and Phosphorus Regeneration in Chesapeake Bay, USA. In *The Comparative Roles of Suspension-Feeders in Ecosystems*, 93–120. Springer.
- Newell, Roger I. E., and Stephen J. Jordan. 1983. Preferential Ingestion of Organic Material by the American Oyster *Crassostrea Virginica*. *Marine Ecology Progress Series*. Oldendorf

- 13 (1): 47–53.
- Nielsen, Lars Peter. 1992. Denitrification in Sediment Determined from Nitrogen Isotope Pairing. *FEMS Microbiology Ecology* 9 (4): 357–61.
- Nixon, Scott W. 1995. Coastal Marine Eutrophication: A Definition, Social Causes, and Future Concerns. *Ophelia* 41 (1): 199–219.
- Nizzoli, Daniele, Marco Bartoli, Martin Cooper, David T. Welsh, Graham J. C. Underwood, and Pierluigi Viaroli. 2007. Implications for Oxygen, Nutrient Fluxes and Denitrification Rates during the Early Stage of Sediment Colonisation by the Polychaete *Nereis* Spp. in Four Estuaries. *Estuarine, Coastal and Shelf Science* 75 (1): 125–34.
- Nizzoli, D., D. T. Welsh, E. A. Fano, and P. Viaroli. 2006. Impact of Clam and Mussel Farming on Benthic Metabolism and Nitrogen Cycling, with Emphasis on Nitrate Reduction Pathways. *Marine Ecology Progress Series* 315 (June): 151–65.
- National Oceanic and Atmospheric Administration (NOAA). 2016. Analysis of Monitoring Data from Harris Creek Sanctuary Oyster Reefs: Data on the First 102 Acres/12 Reefs Restored.
<https://chesapeakebay.noaa.gov/images/stories/habitats/hc3ydcheckinJuly2016.pdf>.
- Orth, R. J., W. C. Dennison, J. S. Lefcheck, and C. Gurbisz. 2017. Submersed Aquatic Vegetation in Chesapeake Bay: Sentinel Species in a Changing World. *Bioscience*.
<https://academic.oup.com/bioscience/article-abstract/67/8/698/3861062>.
- Owens, Michael S., and Jeffrey C. Cornwell. 2016. The Benthic Exchange of O₂, N₂ and Dissolved Nutrients Using Small Core Incubations. *Journal of Visualized Experiments: JoVE*, no. 114.
- Paerl, Hans W., Timothy G. Otten, and Raphael Kudela. 2018. Mitigating the Expansion of Harmful Algal Blooms Across the Freshwater-to-Marine Continuum. *Environmental Science & Technology* 52 (10): 5519–29.
- Paola, Chris. 1985. A Method for Spatially Averaging Small-Scale Bottom Roughness. *Marine Geology*. [https://doi.org/10.1016/0025-3227\(85\)90035-0](https://doi.org/10.1016/0025-3227(85)90035-0).
- Parsons, Timothy R. 2013. *A Manual of Chemical & Biological Methods for Seawater Analysis*. Elsevier.
- Petersen, Jens Kjerulf, Berit Hasler, Karen Timmermann, Pernille Nielsen, Ditte Bruunshøj Tørring, Martin Mørk Larsen, and Marianne Holmer. 2014. Mussels as a Tool for Mitigation of Nutrients in the Marine Environment. *Marine Pollution Bulletin* 82 (1-2): 137–43.

- Peterson, C. H., J. H. Grabowski, and S. P. Powers. 2003. Estimated Enhancement of Fish Production Resulting from Restoring Oyster Reef Habitat: Quantitative Valuation. *Marine Ecology Progress Series* 264: 249–64.
- Peters, Robert Henry. 1983. Temperature and Metabolic Rate. In *The Ecological Implications of Body Size*, 54–78. Cambridge University Press.
- Piazza, Bryan P., Patrick D. Banks, and Megan K. La Peyre. 2005. The Potential for Created Oyster Shell Reefs as a Sustainable Shoreline Protection Strategy in Louisiana. *Restoration Ecology* 13 (3): 499–506.
- Piehler, M. F., and A. R. Smyth. 2011a. Habitat-specific Distinctions in Estuarine Denitrification Affect Both Ecosystem Function and Services. *Ecosphere* 2 (1): 1–17.
- . 2011b. Habitat-Specific Distinctions in Estuarine Denitrification Affect Both Ecosystem Function and Services. *Ecosphere* 2 (1): 1–17.
- Pietros, Jennifer Mugg, and Michael A. Rice. 2003. The Impacts of Aquacultured Oysters, *Crassostrea Virginica* (Gmelin, 1791) on Water Column Nitrogen and Sedimentation: Results of a Mesocosm Study. *Aquaculture* 220 (1): 407–22.
- Reidenbach, Matthew A., Peter Berg, Andrew Hume, Jennifer C. R. Hansen, and Elizabeth R. Whitman. 2013a. Hydrodynamics of Intertidal Oyster Reefs: The Influence of Boundary Layer Flow Processes on Sediment and Oxygen Exchange. *Limnology and Oceanography: Fluids and Environments* 3 (1): 225–39.
- . 2013b. Hydrodynamics of Intertidal Oyster Reefs: The Influence of Boundary Layer Flow Processes on Sediment and Oxygen Exchange: Oyster Reef Sediment and Oxygen Exchange. *Limnology and Oceanography* 3 (1): 225–39.
- Risgaard-Petersen, Nils, Suren Rysgaard, Lars Peter Nielsen, and Niels Peter Revsbech. 1994. Diurnal Variation of Denitrification and Nitrification in Sediments Colonized by Benthic Microphytes. *Limnology and Oceanography* 39 (3): 573–79.
- Risgaard-Petersen, N., and S. Rysgaard. 1995. Nitrate Reduction in Sediments and Waterlogged Soil Measured by ¹⁵N Techniques. In *Methods in Applied Soil Microbiology and Biochemistry*, 287–95. Academic Press.
- Rodney, William S., and Kennedy T. Paynter. 2006. Comparisons of Macrofaunal Assemblages on Restored and Non-Restored Oyster Reefs in Mesohaline Regions of Chesapeake Bay in Maryland. *Journal of Experimental Marine Biology and Ecology* 335 (1): 39–51.
- Rose, Julie M., Suzanne B. Bricker, Mark A. Tedesco, and Gary H. Wikfors. 2014. A Role for Shellfish Aquaculture in Coastal Nitrogen Management. *Environmental Science &*

- Technology* 48 (5): 2519–25.
- Rysgaard, Søren, Nils Risgaard-Petersen, Sloth Niels Peter, Jensen Kim, and Nielsen Lars Peter. 1994. Oxygen Regulation of Nitrification and Denitrification in Sediments. *Limnology and Oceanography* 39 (7): 1643–52.
- Schatte Olivier, Andrew van der, Laurence Jones, Lewis Le Vay, Michael Christie, James Wilson, and Shelagh K. Malham. 2018. A Global Review of the Ecosystem Services Provided by Bivalve Aquaculture. *Reviews in Aquaculture* 7 (November): 109.
- Secor, David H., Edward D. Houde, and Loren L. Kellogg. 2017. Estuarine Retention and Production of Striped Bass Larvae: A Mark-Recapture Experiment. *ICES Journal of Marine Science: Journal Du Conseil* 74 (6): 1735–48.
- Seitzinger, Sybil P. 1988. Denitrification in Freshwater and Coastal Marine Ecosystems: Ecological and Geochemical Significance. *Limnology and Oceanography* 33 (4part2): 702–24.
- Shumway, Sandra E. 2011. *Shellfish Aquaculture and the Environment*. John Wiley & Sons.
- Shumway, Sandra E., Chris Davis, Robin Downey, Rick Karney, John Kraeuter, Jay Parsons, Robert Rheault, Gary Wikfors, and Others. 2003. Shellfish Aquaculture--in Praise of Sustainable Economies and Environments. *World Aquaculture* 34 (4): 8–10.
- Shumway, Sandra E., and Richard K. Koehn. 1982. Oxygen Consumption in the American Oyster *Crassostrea Virginica*. *Marine Ecology Progress Series. Oldendorf* 9 (1): 59–68.
- Sidwell, Virginia D., Audrey L. Loomis, and Robert M. Grodner. 1979. Geographic and Monthly Variation in Composition of Oysters *Crassostrea virginica*. *Marine Fisheries Review* 41: 13–17.
- Smyth, Ashley R., Nathan R. Gerald, and Michael F. Piehler. 2013. Oyster-Mediated Benthic-Pelagic Coupling Modifies Nitrogen Pools and Processes. *Marine Ecology Progress Series* 493: 23–30.
- Smyth, Ashley R., Anna E. Murphy, Iris C. Anderson, and Bongkeun Song. 2018. Differential Effects of Bivalves on Sediment Nitrogen Cycling in a Shallow Coastal Bay. *Estuaries and Coasts*, 1–17.
- Smyth, Ashley R., Michael F. Piehler, and Jonathan H. Grabowski. 2015. Habitat Context Influences Nitrogen Removal by Restored Oyster Reefs. *The Journal of Applied Ecology* 52 (3): 716–25.
- Steingruber, S. M., J. Friedrich, R. Gächter, and B. Wehrli. 2001. Measurement of Denitrification in Sediments with the ¹⁵N Isotope Pairing Technique. *Applied and Environmental*

- Microbiology* 67 (9): 3771–78.
- Stief, P. 2013. Stimulation of Microbial Nitrogen Cycling in Aquatic Ecosystems by Benthic Macrofauna: Mechanisms and Environmental Implications. *Biogeosciences* 10 (12): 7829–46.
- Stokesbury, Kevin D. E., Edward P. Baker, Bradley P. Harris, and Robert B. Rheault. 2011. Environmental Impacts Related to Mechanical Harvest of Cultured Shellfish. In *Shellfish Aquaculture and the Environment*, edited by Sandra E. Shumway, 6:319–38. American Fisheries Society Symposium. Oxford, UK: Wiley-Blackwell.
- Takeshita, Yuichiro, Wade McGillis, Ellen M. Briggs, Amanda L. Carter, Emily M. Donham, Todd R. Martz, Nichole N. Price, and Jennifer E. Smith. 2016. Assessment of Net Community Production and Calcification of a Coral Reef Using a Boundary Layer Approach. *Journal of Geophysical Research, C: Oceans* 121 (8): 5655–71.
- R Development Core Team. 2013. R Development Core Team. *RA Lang Environ Stat Comput* 55: 275–86.
- Testa, Jeremy M., Damian C. Brady, Jeffrey C. Cornwell, Michael S. Owens, Lawrence P. Sanford, Carter R. Newell, Steven E. Suttles, and Roger I. E. Newell. 2015. Modeling the Impact of Floating Oyster (*Crassostrea Virginica*) Aquaculture on Sediment-Water Nutrient and Oxygen Fluxes. *Aquaculture Environment Interactions* 7 (3): 205–22.
- The European Union Water Framework Directive 2000/60/EC*. 2000. *European Parliament*. <https://www.gpo.gov/fdsys/pkg/STATUTE-86/pdf/STATUTE-86-Pg816.pdf>.
- The Nature Conservancy. 1994. Nanticoke-Blackwater River Bioserve Strategic Plan. Draft 6--10--94. Maryland Nature Conservancy, Chevy Chase, MD.
- Tiedje, James M. 1988. Ecology of Denitrification and Dissimilatory Nitrate Reduction to Ammonium. *Biology of Anaerobic Microorganisms* 717: 179–244.
- Tran, Damien, Jean-Charles Massabuau, and Catherine Vercelli. 2008. Influence of Sex and Spawning Status on Oxygen Consumption and Blood Oxygenation Status in Oysters *Crassostrea Gigas* Cultured in a Mediterranean Lagoon (Thau, France). *Aquaculture* 277 (1): 58–65.
- United States Clean Water Act. 1972. *Public Law 92-500, Economic and Social Aspects, Technical Volume*. <https://www.gpo.gov/fdsys/pkg/STATUTE-86/pdf/STATUTE-86-Pg816.pdf>.
- University of Maryland, and College Park. Natural Resources Institute. 1953. *Educational Series*. Chesapeake Biological Laboratory.

- US Environmental Protection Agency. 2010. Chesapeake Bay Total Maximum Daily Load for Nitrogen, Phosphorus and Sediment. US Environmental Protection Agency, et al. www.epa.gov/reg3wapd/tmdl/ChesapeakeBay/tmdlexec.html.
- Vieillard, Amanda Marie. 2017. Impacts of New England Oyster Aquaculture on Sediment Nitrogen Cycling: Implications for Nitrogen Removal and Retention. https://opencommons.uconn.edu/cgi/viewcontent.cgi?article=2239&context=gs_theses.
- Volaric, M. P., P. Berg, and M. A. Reidenbach. 2018. Oxygen Metabolism of Intertidal Oyster Reefs Measured by Aquatic Eddy Covariance. *Marine Ecology Progress Series* 599 (July): 75–91.
- Waldbusser, George G., Erin P. Voigt, Heather Bergschneider, Mark A. Green, and Roger I. E. Newell. 2011. Biocalcification in the Eastern Oyster (*Crassostrea Virginica*) in Relation to Long-Term Trends in Chesapeake Bay pH. *Estuaries and Coasts* 34 (2): 221–31.
- Ward, J. E., R. I. E. Newell, R. J. Thompson, and B. A. Macdonald. 1994. In Vivo Studies of Suspension-Feeding Processes in the Eastern Oyster, *Crassostrea Virginica* (Gmelin). *The Biological Bulletin* 186 (2): 221–40.
- Welsh, D. T., and G. Castadelli. 2004. Bacterial Nitrification Activity Directly Associated with Isolated Benthic Marine Animals. *Marine Biology* 144 (5): 1029–37.
- Westbrook, Phillip Thomas. 2016. Bioassimilation, Burial, and Sediment Denitrification at Shallow-Water and Deep-Water Oyster Reefs in Two Louisiana Estuaries. Louisiana State University. https://digitalcommons.lsu.edu/gradschool_theses/4584/.
- Wilber, Dara H., and Douglas G. Clarke. 2001. Biological Effects of Suspended Sediments: A Review of Suspended Sediment Impacts on Fish and Shellfish with Relation to Dredging Activities in Estuaries. *North American Journal of Fisheries Management* 21 (4): 855–75.
- Wilberg, Michael J., Maude E. Livings, Jennifer S. Barkman, Brian T. Morris, and Jason M. Robinson. 2011. Overfishing, Disease, Habitat Loss, and Potential Extirpation of Oysters in Upper Chesapeake Bay. *Marine Ecology Progress Series* 436: 131–44.
- Yin, Guoyu, Lijun Hou, Min Liu, Zhanfei Liu, and Wayne S. Gardner. 2014. A Novel Membrane Inlet Mass Spectrometer Method to Measure $^{15}\text{NH}_4^+$ for Isotope Enrichment Experiments in Aquatic Ecosystems. *Environmental Science & Technology*.